THE ASTROPHYSICAL JOURNAL SUPPLEMENT SERIES, 58:661–710, 1985 August

ON THE EVOLUTION OF CLOSE BINARIES WITH COMPONENTS OF INITIAL MASS BETWEEN 3 $M_\odot$ AND 12 $M_\odot$[1]

ICKO IBEN, JR., AND ALEXANDER V. TUTUKOV[2]
University of Illinois at Urbana-Champaign
Received 1984 July 31; accepted 1985 February 6

CONTENTS

ABSTRACT

The evolution of components of close binary systems of intermediate mass (component masses in the range 3–12 $M_\odot$) and of Population I composition ($X = 0.7$, $Z = 0.02$) is studied numerically. We assume that a model star first fills its Roche lobe after it has developed a helium core and becomes a giant and that mass loss from the model continues until model radius decreases below a predetermined limit. How much of the matter that is lost from the Roche-lobe–filling model is transferred to its companion and how much is lost from the system are left undetermined. In the mass loss/exchange process, a model of initial mass in the 3–10 $M_\odot$ range is transformed into a compact "helium" star (which, nevertheless, retains some hydrogen-rich matter in its envelope). In our experiments, models of initial mass 3, 4, 5, 6.95, and 9.85 $M_\odot$ produce remnants of mass 0.378, 0.523, 0.765, 1.11, and 1.95 $M_\odot$, respectively. The lifetime of the core helium-burning phase of each remnant ranges from 200% (0.378 $M_\odot$ remnant) to 20% (1.95 $M_\odot$ remnant) of the main-sequence lifetime of its progenitor, and the possibility arises that the primordial secondary, if it is initially massive enough or if it has accreted sufficient matter during the first mass-transfer episode, will expand and transfer matter back to the primary remnant while this remnant is still relatively compact. We show that, then, most of the matter outside the helium core of the secondary will be ejected from the system.

Following the exhaustion of helium at its center, the remnant of each component develops a growing core composed of carbon and oxygen. In the case of the most massive remnants, the envelope expands during core growth, and the Roche lobe is filled again. As a consequence of the ensuing mass loss/exchange event, the remnants of mass 1.11 $M_\odot$ and 1.95 $M_\odot$ lose all of the hydrogen remaining at their surfaces and ultimately evolve into non-DA degenerate dwarfs of mass 0.89 $M_\odot$ and 1.06 $M_\odot$, respectively; their envelopes are now composed predominantly of helium. The remnant of mass 0.76 $M_\odot$ loses an additional 0.013 $M_\odot$ of hydrogen-rich matter from its surface by Roche-lobe overflow and, during a final hydrogen-burning "flash," reduces the amount of hydrogen-rich matter in surface layers to about 8×10^{-5} $M_\odot$. If, while passing through a planetary nebula nucleus stage, the remnant experiences a stellar wind that is strong enough to blow off this thin envelope, it may ultimately become a non-DA white dwarf with a surface composed predominantly of helium. Otherwise it becomes a DA white dwarf.

[1]Supported in part by the USA National Science Foundation grant AST 81-15325.
[2]On leave from the Astronomical Council of the USSR Academy of Sciences, Moscow.

The 0.523 $M_\odot$ remnant remains compact, losing no further matter by Roche-lobe overflow, but experiences final hydrogen shell flashes that reduce the mass of the hydrogen-rich envelope to less than 10^{-5} $M_\odot$. It too may become a non-DA white dwarf in consequence of a stellar wind operating during a planetary nebula nucleus stage. Neither the 0.378 $M_\odot$ remnant nor the 0.523 $M_\odot$ remnant burns helium into carbon and oxygen over the entire interior. After all nuclear burning has ceased in the 0.523 $M_\odot$ remnant, a layer of unburned helium of mass 0.046 $M_\odot$ remains near the surface. After central helium is exhausted in the 0.378 $M_\odot$ remnant, a series of helium shell flashes occurs, followed by a phase of quiescent helium burning; after all nuclear burning has ceased, the masses of carbon and oxygen, of helium, and of hydrogen are, respectively, 0.263, 0.115, and 0.00018 $M_\odot$.

In our experiments, we assume that each mass-loss/mass-transfer event is nonconservative of the orbital angular momentum and total mass of the system, usually in such a way that the Roche lobe of the mass-losing star either remains constant or decreases in size. In so doing, we assume implicitly that the binary system passes through a common-envelope phase during some portion of each mass-transfer event. However, it is possible to generalize the results to accommodate hypothetical situations in which mass transfer is predominantly conservative of both system mass and orbital angular momentum. We conclude that, in binary systems composed initially of intermediate-mass stars (primary masses in the range 3–10 $M_\odot$) close enough that the primary has the potential to substantially overflow its Roche lobe before or while beginning core helium burning, the first mass-loss/mass-transfer event will in most instances be followed by three additional mass-loss/mass-transfer events. In many instances, especially when initial stellar masses are comparable, the two component stars will alternate as mass donors. This last result is a consequence of the fact that the core helium-burning lifetime $\tau_{\rm He}$ of the first compact remnant of the primary can be a substantial fraction of the main-sequence lifetime $\tau_{\rm H}$ of the primary and, therefore, can often be larger than that portion of the main-sequence lifetime of the secondary remaining after the first mass-transfer event. We find $\tau_{\rm He}/\tau_{\rm H} \approx 2$, 1, 1/2, 1/3, and 1/5 for initial primary masses of 3, 4, 5, 6.95, and 9.85 $M_\odot$.

The location in the H-R diagram of a single 12 $M_\odot$ model at the start and during most of the core helium-burning phase is to the blue of the main giant branch. We therefore assume that, except in a very close binary, a component of initial mass 12 $M_\odot$ does not fill its Roche lobe until it has almost exhausted helium at its center. Assuming that mass is lost on the thermal time scale of the envelope as long as stellar radius exceeds 300 $R_\odot$, a remnant of mass about 4.5 $M_\odot$ results. If common-envelope action reduces the Roche-lobe radius to less than 100 $R_\odot$, then the mass of the shell helium-burning remnant will continue to decrease to about 3.5 $M_\odot$ before carbon is ignited at the center. When carbon ignites, the mass of the CO core is about 2.0 $M_\odot$, and the core composition will be converted predominantly into oxygen and neon, with substantial traces of sodium and magnesium (an "ONe" core). This model must ultimately experience a supernova event triggered by electron capture. If Roche-lobe filling occurs just before or at the beginning of the core helium-burning phase, the fate of the 12 $M_\odot$ component is much the same; the only difference is that the mass of the remnant when carbon ignition occurs is about 2.4 $M_\odot$ instead of 3.5 $M_\odot$. A component of initial mass 11 $M_\odot$ becomes a giant before igniting helium at its center, forms a remnant of mass 2.3 $M_\odot$ during a first mass-loss episode, but then ignites carbon at the center during the second mass-loss episode, when stellar mass has been reduced to about 2.2 $M_\odot$. This model will develop an ONe core of mass 1.4 $M_\odot$ and experience a supernova event. A component of initial mass 10.5 $M_\odot$ produces a first remnant of mass about 2.1 $M_\odot$, and, assuming that Roche-lobe overflow continues as long as stellar radius is greater than 100 $R_\odot$, model mass decreases to about 1.1 $M_\odot$ before carbon is ignited at the model center. Further evolution will convert this model into an ONe white dwarf.

Whether or not a binary component can avoid a supernova event and become a degenerate dwarf of the ONe variety depends very sensitively on the initial orbital parameters of the binary system and on the assumed efficacy of common-envelope action. For the Population I composition we have chosen, our experiments show definitely only that initial mass must be larger than 8.8 $M_\odot$ and smaller than 11 $M_\odot$. However, they also show that, for appropriate initial conditions, CO degenerate dwarfs may arise from progenitors initially as massive as 10.3 $M_\odot$ and that an electron-capture supernova may arise from a progenitor as light as 10.6 $M_\odot$. Thus, only progenitors of mass in the narrow range 10.3–10.6 $M_\odot$ are assured of producing ONe degenerate dwarfs.

Our models provide a numerical framework for the development of scenarios for various possible outcomes of binary evolution. As examples, we discuss the relevance of our models to an understanding of the formation of the following: double cores of planetary nebulae; R CrB stars and nonvariable hydrogen-deficient stars; barium stars; He, CO, and ONe white dwarfs in cataclysmic variables; immediate binary precursors of both Type I and Type II supernovae; and millisecond and binary pulsars. One major result is that the formation frequency of binary systems consisting of two helium degenerate dwarfs which, by the emission of gravitational waves, are brought close enough to merge within a Hubble time and which, at the same time, are massive enough to explode on merging may be far too small to account for the observed formation frequency of Type I supernovae.

Subject headings: stars: abundances — stars: binaries — stars: evolution — stars: white dwarfs

I. INTRODUCTION

Our objective in this paper is to contribute to the understanding of the evolution of close binary systems in which at least one of the components has a mass in the range 3–12 $M_\odot$. There are several reasons why binaries with component masses in this range are especially attractive for study. Each component may fill its Roche lobe twice, losing hydrogen-rich matter during the first Roche-lobe–filling phase and helium-rich matter during the second lobe-filling phase. For initial stellar masses in the range 6–10 $M_\odot$, the final product of a component can be a carbon-oxygen (CO) dwarf with a helium-rich envelope which is completely devoid of hydrogen. For an initial component mass in the 2.3–6 $M_\odot$ range, a thin "topping" of hydrogen-rich matter may remain above the CO core when the final model remnant evolves into a white dwarf configuration. However, if a sufficiently strong stellar wind operates during the planetary nebula nucleus (PNN) phase, even this thin topping may disappear to reveal the underlying CO core. Stars of initial mass less than about 2.3 $M_\odot$ may ultimately evolve into helium white dwarfs capped by a hydrogen-rich surface.

The evolution of some close binaries in which the initial mass of a component is somewhere in the range ~ 9–11 $M_\odot$ can lead to the formation of "ONe" degenerate dwarfs composed of oxygen, neon, sodium, and magnesium (e.g., Nomoto 1980; van den Heuvel 1981*a*, *b*; Law and Ritter 1983; Iben and Tutukov 1984*b*), and it is of great interest to find more precisely the conditions for the formation of such dwarfs.

Over the past few years it has been found that the nuclei of several planetary nebulae are double stars with rather short orbital periods (Grauer and Bond 1982, 1983, 1984; Bond 1985). Studies of the evolution of binaries with primary masses in the 3–12 $M_\odot$ range can provide new and relevant information concerning the formation of such systems. The penultimate configuration of an initially close binary with primary mass in the studied range is, in many instances, an exceedingly close pair of degenerate dwarfs composed primarily of carbon and oxygen or of oxygen and neon. It is quite possible that some, if not most, supernovae of Type I are due to the merging of a close pair of degenerate CO dwarfs after they have been drawn into Roche-lobe contact by the loss of orbital angular momentum attending the radiation of gravitational waves (Iben and Tutukov 1984*a*, *b*; see also Webbink 1984*a*).

If the mass of the remnant of a primary whose initial mass is in the range, say, 10–12 $M_\odot$ exceeds the Chandrasekhar mass (~ 1.4 $M_\odot$), the inner ~ 1.4 $M_\odot$ of this remnant (an ONe core) may implode to form a neutron star before its companion can evolve into a degenerate dwarf. The likelihood of implosion follows from the fact that ^{24}Mg and ^{23}Na are also present in the ONe core and the collapse initiated by electron capture on ^{24}Mg (Barkat, Reiss, and Rakavy 1974; Barkat *et al.* 1975; Barkat 1975) or on ^{23}Na and ^{20}Ne cannot be halted by oxygen burning (Miyaji *et al.* 1980; Nomoto 1982). If the system can survive such an event as a binary (which is probable, since the mass of the companion exceeds the mass of the immediate neutron star progenitor and the mass of the envelope ejected from this progenitor is small compared with the total mass of each remnant binary component), and if mass transfer later occurs from the companion to the neutron star, the system may appear for a time as a bright low-mass X-ray binary.

If the mass of the ONe remnant is less than the Chandrasekhar mass (progenitor main-sequence mass somewhere in the range 9–11 $M_\odot$), the remnant will cool to become an electron-degenerate dwarf. Mass transfer onto this degenerate dwarf may occur twice, once after the initial secondary has developed a helium core and, next, after the secondary has developed a CO core. During these mass-transfer events, the system may appear briefly as a symbiotic star, interrupted by perhaps one or more nova outbursts displaying considerable oxygen and neon in the spectrum. Either as a result of the formation of a common envelope or as a result of nova ejection, very little mass will be permanently transferred to the degenerate dwarf remnant of the primary. However, after the secondary ultimately evolves into a degenerate dwarf (of either the CO or ONe variety), and if the orbital separation (after the last transfer of hydrogen- and helium-rich matter) is less than about 3 $R_\odot$, gravitational-wave radiation will force Roche-lobe contact of the two remnant degenerate dwarfs within a Hubble time. The secondary will dissolve into a thick disk (Tutukov and Yungelson 1979*b*) about the ONe primary, and, by accretion from this disk, the primary will achieve the Chandrasekhar mass and then implode to become an isolated pulsar. During the formation of the thick disk and during the subsequent phase of accretion from this disk, the ONe dwarf will have been spun up to a high rotation rate, and, therefore, the final pulsar may have a frequency in the millisecond range. It may be estimated that this scenario will be played out at a frequency of about 4% of the Type II supernova formation rate (Iben and Tutukov 1984*b*).

Another important problem which a study of close binary evolution can help resolve is that of the origin of the peculiar compositions seen at the surfaces of some stars. Nuclear reactions change the composition of the matter deep inside a star. Convective mixing and mass loss, as it occurs in members of binaries, can lead to an exposure of processed matter at the stellar surface, where it is accessible to observational scrutiny. Observations have revealed several different types of chemical composition anomalies such as helium-rich stars, R-CrB stars, planetary nebula nuclei with pure helium envelopes, barium stars, and high-temperature accretion regions in Algol-type systems, some of which can perhaps be understood in terms of the evolution of close binaries with components of initial mass in the interval 3–12 $M_\odot$.

In order to pursue a concrete calculational program, we have been forced to make rather drastic, but it is hoped not completely unrealistic, simplifying assumptions as to what occurs in extremely complicated situations for which the physics remains to be fully explored (see, e.g., Plavec, Ulrich, and Polidan 1973; Sparks and Stecher 1974; Ritter 1975, 1976; Paczyński 1976; Webbink 1976; Thomas 1977; Meyer and Meyer-Hofmeister 1979; Taam, Bodenheimer, and Ostriker 1978; Tutukov and Yungelson 1979*a*; Webbink 1979*a*, *b*; Tutukov and Yungelson 1981; Law and Ritter 1983;

Plavec 1983*a*, *b*; Bodenheimer and Taam 1984; Taam 1984). The presence of another component defines a Roche-lobe structure and limits the expansion of the potential mass donor, forcing the loss from this component of all matter outside its Roche lobe. In zeroth approximation, one may assume that the rate of mass exchange is determined by the formal condition of precise Roche-lobe filling by the mass-losing star and by the assumption that both the total mass and the total orbital angular momentum are conserved during the mass-transfer event. But, if the companion cannot accrete all of the matter provided by the Roche-lobe–filling star, it expands. If an equilibrium between transfer and accretion cannot be reached until the companion fills its Roche lobe, the system becomes a contact one, with two stellar cores experiencing drag forces inside a common envelope, and mass is lost from the system. This can occur if the thermal time scale of the mass-losing component at the moment of Roche-lobe filling is much shorter than the thermal time scale of the accreting component. The second well-established case in which a common envelope must form is realized if the component filling its Roche lobe has a deep convective envelope and its mass exceeds about 60% of the mass of the accreting star (e.g., Iben and Tutukov 1984*b*). In this case the donor expands more rapidly than its Roche lobe, and mass is lost from the system on a time scale more rapid than the thermal time scale of either component. Frictional drag forces cause the two stellar cores to drift together during the common-envelope episode.

We may estimate the final parameters of a system after the loss of the common envelope by way of the recipe (Tutukov and Yungelson 1979*a*)

$$\frac{M_1^2}{A} = \alpha \frac{M_{1R} M_2}{A_f}, \tag{1}$$

where A and A_f are initial and final semimajor axes, respectively, M_1 and M_{1R} are initial and final masses of the Roche-lobe–filling component, M_2 is the mass of the companion, and α is a measure of the efficiency of transformation of orbital energy into the energy required to drive mass from the system. The mass-loss rate during the common-envelope stage is not easy to estimate. Mass loss probably occurs initially on the thermal time scale of the extended envelope of the primary and finishes on the dynamical time scale of this envelope when the secondary encounters the densest part of the envelope.

In the absence of a quantitative theory of mass loss during the common-envelope stage, we suppose in the numerical exercises undertaken here that mass loss begins when the star becomes larger than some limit and continues at a constant rate until the radius of the model becomes somewhat smaller than this limit. The assumed mass-loss rate $\dot{M}$ has been chosen initially to be of the order of $M/\tau_{\rm KH}$, where M is the mass of the Roche-lobe–filling star and $\tau_{\rm KH}$ is the "thermal time scale" of this star defined by

$$\tau_{\rm KH} \sim 3 \times 10^7 \frac{M^2}{RL} \text{ yr}, \tag{2}$$

where mass M, radius R, and luminosity L are all in solar units. In all instances, the mass-losing model has a deep convective envelope during most of the mass-loss phase, and model radius exceeds the radius of its Roche lobe until the very end of the phase when the base of the convective envelope reaches its maximum inward extent and continued mass loss begins to expose matter which has been highly processed by hydrogen burning during the prior main-sequence phase. The reduction in opacity and the increased average molecular weight in the envelope (defined as all matter between the hydrogen-burning shell and the surface) cause the model star to shrink, and the mass-loss rate is rapidly diminished and then terminated. The total amount of mass which can be lost by the initial primary during the shrinking stage is, in all instances, very small compared with the total amount of mass lost during the first, large-$\dot{M}$ phase.

After core helium burning is completed in a model of initial mass larger than about 4.5 $M_\odot$, the model swells again. The swelling can continue until the radius of the model is as large as the radius of the progenitor at the point when the first mass-loss phase is terminated; then mass is once again abstracted from the model until a second shrinkage sets in. If the remnant mass is large enough (in the present study, remnant masses from 1.1 $M_\odot$ to 2.3 $M_\odot$), most of the helium-rich matter outside the helium-burning shell expands and ultimately reaches the Roche-lobe radius, where it is lost from the star. If the remnant mass is too small (in the present study, remnant mass less than about 0.7 $M_\odot$), expansion is minimal and a second phase of Roche-lobe overflow does not occur; however, most of the hydrogen remaining in the remnant is burned up in a series of hydrogen shell flashes. If the mass of the remnant of the first mass-loss episode is in an intermediate range between about 0.7 $M_\odot$ and about 0.8 $M_\odot$ (we have computed only one model in this range), matter in the helium-rich portion of the remnant does not expand, but matter in the hydrogen-rich envelope expands to such an extent that a second episode of Roche-lobe overflow will occur. During this second episode, most of the hydrogen-rich envelope is lost from the star and a large fraction of the hydrogen remaining after the cessation of mass loss is converted into helium in a final hydrogen shell flash and its aftermath of quiescent hydrogen burning.

A model of initial mass 12 $M_\odot$ does not develop a deep convective envelope until after having nearly completed the core helium-burning phase. Mass loss is assumed to first occur when stellar radius exceeds 300 $R_\odot$ and is continued during the subsequent growth of a helium-exhausted core, as long as stellar radius exceeds ~ 100 $R_\odot$. Carbon is ignited at the center when the mass of the growing CO core reaches $M_{\rm He} \sim 2.0$ $M_\odot$, and the total remnant mass is then $M_{R1} \sim 3.5$ $M_\odot$. If mass loss is begun just as the 12 $M_\odot$ model is entering the core helium-burning phase (stellar radius about 135 $R_\odot$), a remnant of mass $M_{R1} \sim 2.5$ $M_\odot$ results. After core helium burning, this remnant expands again, but carbon is ignited again when $M_{\rm He} \sim 2.0$ $M_\odot$ and $M_{R2} \sim 2.3$ $M_\odot$. Models of initial mass 10.5 and 11 $M_\odot$ both develop deep convective envelopes before helium is ignited at the center and, losing mass according to the algorithms just described, become core helium-burning remnants of mass $M_{R1} = 2.0$ $M_\odot$ and $M_{R1} = 2.32$ $M_\odot$, respectively. Both models experience a second mass-loss episode after helium is exhausted at the center, but

carbon is ignited at the center of the initially more massive remnant after it has lost only an additional 0.14 $M_\odot$. At the point of carbon ignition, the center of the helium-burning shell is at a mass 1.9 $M_\odot$ from the model center, and it is clear that the model will develop an ONe core of mass of the order of 1.4 $M_\odot$ before losing much more mass; electron capture on trace amounts of ^{24}Mg and ^{23}Na will cause core collapse and neutron star formation. The remnant of mass $M_{R1} = 2.0\ M_\odot$ loses an additional 0.8 $M_\odot$ before igniting carbon at the center, and it will develop into an ONe degenerate dwarf of mass about $M_{R2} \sim 1.2\ M_\odot$.

In summary, before first overflowing their Roche lobes, binary components which have masses in the range 2.3 $M_\odot$ to about 4.8 $M_\odot$ experience just one episode of mass loss while burning nuclear fuel and ultimately become degenerate dwarfs of mass in the range 0.32 $M_\odot$ to about 0.7 $M_\odot$; the composition of these dwarfs is primarily carbon and oxygen; however, with decreasing dwarf mass, the mass of helium in an outer layer increases relative to the mass of the CO core, reaching a substantial fraction of the remnant below 0.4–0.5 $M_\odot$. Binary components of initial mass in the range 4.8–5.2 $M_\odot$ lose hydrogen-rich matter in two episodes of Roche-lobe overflow and become CO degenerate dwarfs of mass in the range 0.7–0.8 $M_\odot$. Components of initial mass in the range 5.2–10.3 $M_\odot$ lose most of their hydrogen-rich material during a first episode of Roche-lobe overflow to form compact helium-burning remnants of mass in the range 0.8–2.05 $M_\odot$; during a second stage of Roche-lobe overflow, they lose the remainder of their hydrogen-rich material and some helium-rich matter as well to become CO degenerate dwarfs of mass in the range 0.8–1.08 $M_\odot$. Components of initial mass in the range 10.3–10.6 $M_\odot$ can become ONe degenerate dwarfs after two episodes of Roche-lobe overflow, and such degenerate dwarfs may also be formed under special circumstances from progenitors of initial mass in the range 8.8–10.3 $M_\odot$. In spite of one or more phases of mass loss by Roche-lobe overflow, components of initial mass larger than about 10.6 $M_\odot$ form ONe cores of mass close to the Chandrasekhar limit and experience core collapse triggered by electron capture on ^{24}Mg, ^{23}Na, and ^{20}Ne.

In all studies of the long-term evolution of binary systems, there is a potential for confusion in the use of the words primary and secondary. In this paper, that component which is primordially more massive than its companion will be called the primary, regardless of whether (as a consequence of mass transfer) it is more or less massive than its companion, the secondary, and regardless of whether it is losing or gaining mass. Quantities such as mass, luminosity, and radius are in all cases given in solar units, whether or not this is noted explicitly.

The computational program used to follow the evolution of all models is an evolved version of a program first described in 1965 (Iben 1965*a*, *b*). Several subsequent modifications of the input physics are discussed by Iben (1975, 1976), Lamb, Iben, and Howard (1976), and Becker and Iben (1979). Every model is spherically symmetric, the gravitational potential due to the companion is neglected, the effects of rotation are ignored, and the surface boundary condition is that appropriate to a single, isolated star. Initial abundances by mass of hydrogen, helium, and heavier elements are, in all instances, $X = 0.70$, $Y = 0.28$, and $Z = 0.02$.

The remainder of the paper is divided into nine sections. In § II we discuss the evolution of components (of initial mass in the 5–10 $M_\odot$ range) which experience two phases of Roche-lobe overflow and become CO degenerate dwarfs. In § III we examine the evolution of components of initial mass 10.5, 11, and 12 $M_\odot$ and attempt to find the conditions necessary for the formation of ONe degenerate dwarfs. In § IV we explore the evolution of models of 3 and 4 $M_\odot$ that experience only one phase of Roche-lobe overflow and become degenerate dwarfs which, although composed predominantly of carbon and oxygen, also contain substantial amounts of helium. We may call these hybrids HeCO degenerate dwarfs. In § V we summarize the results for all cases considered and provide a mapping that relates the mass and composition of a degenerate remnant to the mass and status (single star or Roche-lobe–filling component of an interacting binary) of its progenitor. In § VI we explore the response to accretion of the nuclear-burning companion of a Roche-lobe–filling component, and in § VII we examine the response of a cold CO degenerate dwarf to accretion. In § VIII we comment on the formation of pulsars in binary systems and make extensive comparisons with the observations with regard to core helium-burning stars and non-DA white dwarfs, nonvariable helium-rich stars and R CrB stars, shell and Be stars, nuclei of planetary nebulae, and Ba and CH stars. Finally in § IX we summarize our results.

II. ON THE EVOLUTION OF COMPONENTS WHICH DEVELOP A CARBON-OXYGEN REMNANT AFTER TWO EPISODES OF ROCHE-LOBE OVERFLOW

In this section, we describe conjectural evolutionary sequences for components of close binaries with initial masses of 5, 6.95, and 9.85 $M_\odot$. We have assumed that no mass is transferred onto the component which is being studied. Evolutionary tracks in the H-R diagram are shown in Figures 1–3, and the main parameters of several selected models are presented in Tables 1–3. The evolution with time of several interior characteristics is shown in Figures 4–6. Each evolutionary sequence can be thought of as describing a primordially more massive component which attempts to transfer mass to a main-sequence companion or as describing a primordially less massive component which attempts to transfer mass to its companion after this companion has already evolved either into a compact core helium-burning star or into a white dwarf configuration.

Hydrogen burning leads to the formation of a helium core, the mass of which at point C of each evolutionary track is given approximately by

$$M_{\rm He} = 0.058 M_{\rm MS}^{1.57}, \qquad (3)$$

where $M_{\rm MS}$ is the initial mass of the donor. Both $M_{\rm He}$ and $M_{\rm MS}$ are given in solar units. The quantity $M_{\rm He}$ defined by equation (3) is not the same as the quantity specified by the same symbol in the tables. In the tables, $M_{\rm He}$ is the mass at a point near the base of the hydrogen profile where the rate of

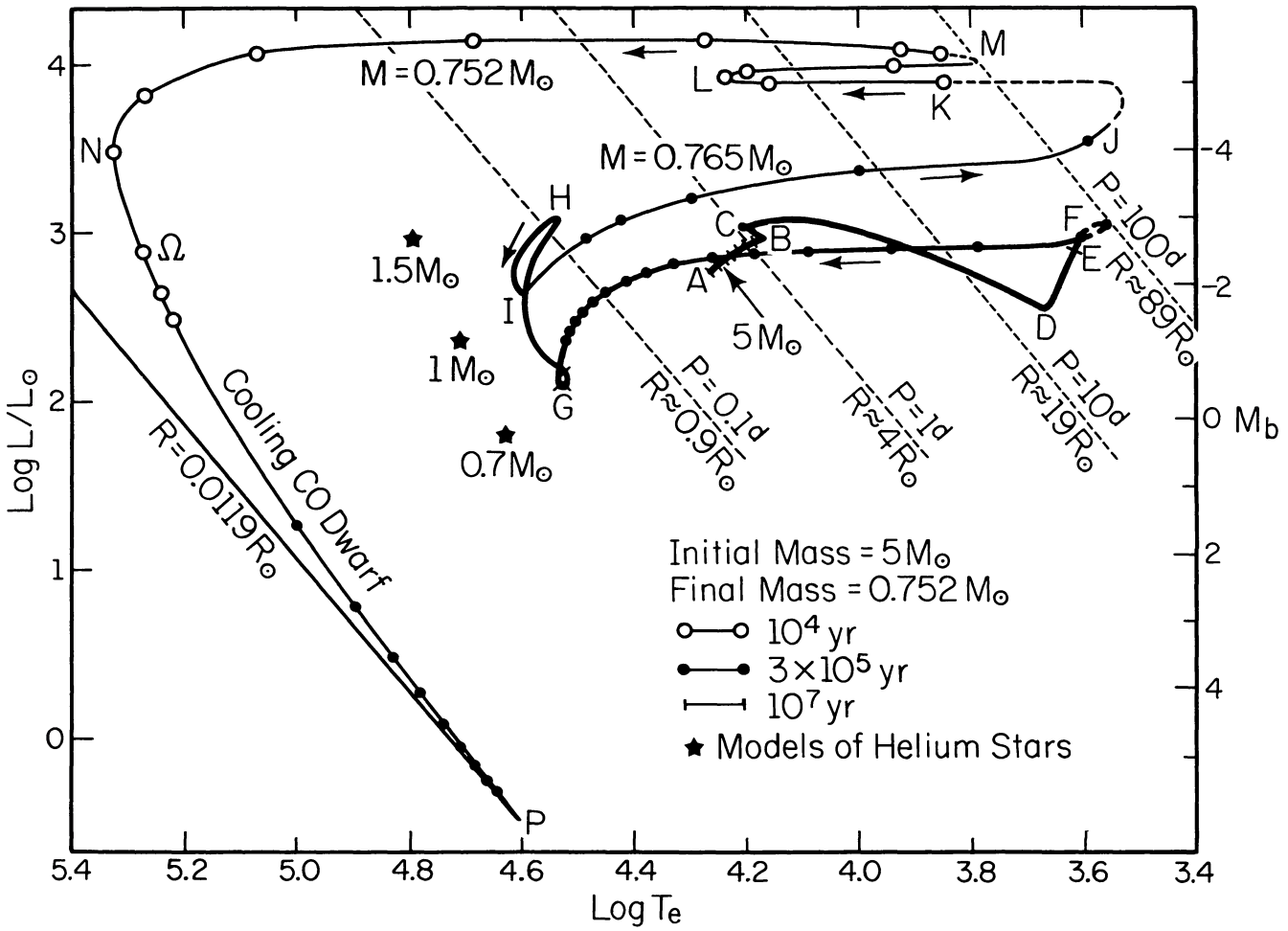

FIG. 1.—Evolution in the H-R diagram of a binary component of initial mass 5 $M_\odot$. Initial composition parameters are $X = 0.7$, $Z = 0.02$. The positions of helium model stars are given by the filled, five-pointed "stars" (Paczyński 1971). Lines of constant orbital period and Roche-lobe radius for a system consisting of two 5 $M_\odot$ unevolved stars are also shown. The temperature of the CO shell reaches a maximum at the point Ω along the track. The main parameters of the stellar model at other labeled points (A, B, ...) are presented in Table 1. Mass loss occurs along dashed portions of the track (E to F; J to K). Time evolution is measured by tick marks (10^7 yr), filled circles (3×10^5 yr), and open circles (10^4 yr).

nuclear energy generation is a maximum. The value of M_{He} defined by equation (3) is the mass coordinate at a point approximately midway through the hydrogen profile which separates the hydrogen-exhausted core and the outer, unburned layers of hydrogen. The meanings of the two values of M_{He} so defined may be illustrated by reference to the dashed curve in Figure 7. This curve gives the abundance of hydrogen versus mass at the end of the main-sequence phase (just as hydrogen is exhausted at the center) in the model of mass 9.85 $M_\odot$. The value $M_{He} = 1.52$ given in Table 3 corresponds to a point where the hydrogen abundance X_H is about 0.1. The value of $M_{He} = 2.1$ given by equation (3) corresponds to a point where $X_H \sim 0.35$, which is half of the surface value of X_H.

After the exhaustion of central hydrogen, the peak in the nuclear energy generation rate moves outward through the hydrogen profile. The helium core contracts and the envelope simultaneously expands until, by assumption, the stellar surface makes contact with the Roche lobe at point E. Mass is then abstracted until the radius of the model again drops below that defined by point E. We would obtain essentially the same final remnant mass by initiating mass loss at any point between C and E. At the moment of detachment (point F), almost all of the initial hydrogen-rich envelope has been removed. The mass of the remnant is given in rough approximation by equation (3). Thanks to convective dredge-up during the giant phase, the mass of the helium core is reduced to

$$M_{He} = 0.043 M_{MS}^{1.67}. \quad (4)$$

The solid and dotted curves in Figure 7 give the distribution of hydrogen in the interior of the model of initial mass $M_{MS} = 9.85\ M_\odot$ at the moment of the deepest inward penetration of envelope convection during the first giant phase. Recall that M_{He} given by equation (3), $M_{He} \sim 2.1\ M_\odot$, actually defines the mass point at which the hydrogen abundance is one-half of its surface value when central hydrogen is ex-

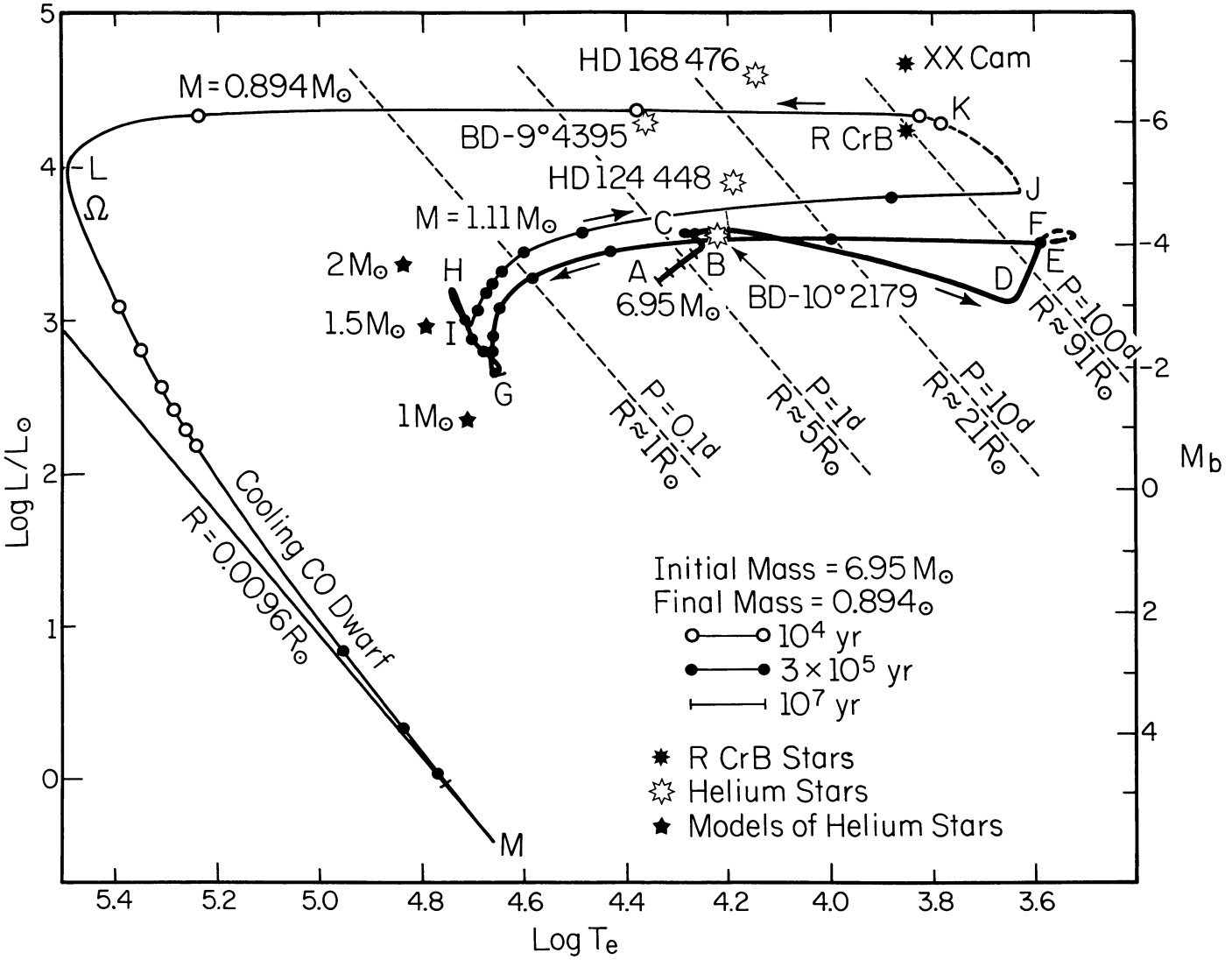

FIG. 2.—Same as Fig. 1, but for a component of initial mass 6.95 $M_\odot$. Lines of constant orbital period and Roche-lobe radius for a system consisting of two unevolved stars of mass 6.95 $M_\odot$ are displayed. The main parameters of the model at labeled points (A,B,...) are presented in Table 2. Filled, eight-pointed "stars" give the estimated location of R CrB stars, and open, eight-pointed "stars" give the estimated location of helium stars.

hausted. Equation (4) defines the mass reached by the base of the convective envelope at its maximum inward extent, marked by the discontinuity in the hydrogen profile at 1.95 $M_\odot$. The second discontinuity in the hydrogen profile (at 1.90 $M_\odot$) is created during a brief episode of complex mixing which occurs at the end of the core hydrogen-burning phase. The first portion of this mixing episode exhibits some of the characteristics of semiconvection (see, e.g., Simpson 1971; Varshavskij and Tutukov 1972*a*, *b*, 1975). In our treatment, which allows only complete mixing when the Schwarzschild criterion for convective stability is violated, mixing occurs in a sequence of fully mixed zones which alternate with radiative zones and which shift about in mass fraction (see Iben 1966*a*, *b*; Lamb, Iben, and Howard 1976). The "semiconvective" region is soon replaced by one or more truly convective layers (see Simpson 1971 and Lamb, Iben, and Howard 1976 for discussions) which effectively destroy the composition profiles established by semiconvective-like mixing and replace them by another set of profiles.

In the particular case of the model of initial mass 9.85 $M_\odot$, mass loss is initiated at a rate $\dot{M} = -3\times10^{-3}$ $M_\odot$ yr^{-1} when the radius of the model star first reaches $R = 300$ $R_\odot$. The radius of the model remains between 300 $R_\odot$ and 350 $R_\odot$ until the outer mass zone approaches the first discontinuity in the hydrogen abundance at $M \approx 1.95$ $M_\odot$, whereupon model radius decreases abruptly to about 200 $R_\odot$. For how much longer mass should be abstracted from the model depends on the extent to which the real counterparts of the interacting model stars have been brought together during the preceding common-envelope phase. For example, if mass continues to be abstracted at a modest rate ($\sim 10^{-5}$ $M_\odot$ yr^{-1}) as the model mass drops below 1.95 $M_\odot$, model radius remains fixed at about 200 $R_\odot$ until the outer mass zone approaches the second discontinuity in the hydrogen abundance at $M \approx 1.90$

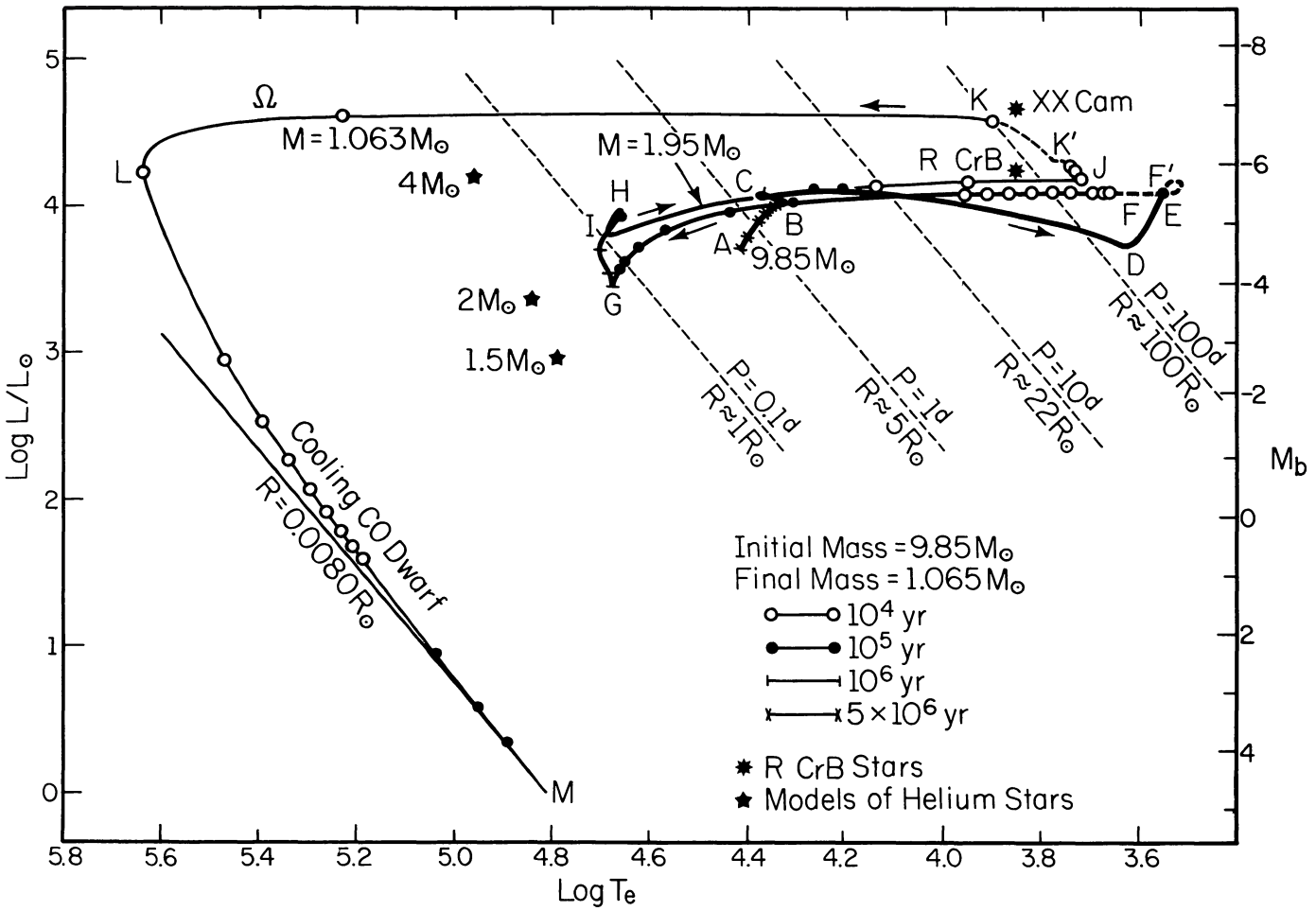

FIG. 3.—Same as Figs. 1 and 2, but for a component of initial mass 9.85 $M_\odot$. Lines of constant orbital period and Roche-lobe radius for a system consisting of two point masses, each of mass 9.85 $M_\odot$, are shown. The main parameters of the model at labeled points (A, B, ...) are presented in Table 3. The time for evolution between points indicated by open circles is 10^4 yr, by filled circles is 10^5 yr, by tick marks is 10^6 yr, and by crosses is 5×10^6 yr.

TABLE 1

SOME PARAMETERS OF A CLOSE BINARY COMPONENT WITH INITIAL MASS 5 $M_\odot$

Stage	Age ($\times10^{15}$ s)	$M_*/M_\odot$	log $L/L_\odot$	log $R/R_\odot$	log T_e	log T_c	log ρ_c	$M_{He}/M_\odot$	$M_{CO}/M_\odot$	X	Y	X_{12} ($\times10^{-3}$)	X_{14} ($\times10^{-3}$)	X_{16} ($\times10^{-3}$)
A	0.0	5.000	2.79	0.40	4.26	7.44	1.35	...	...	0.70	0.28	2.82	0.92	8.40
B	2.056581	5.000	2.97	0.66	4.17	7.51	1.48	...	...	0.70	0.28	2.82	0.92	8.40
C	2.123886	5.000	3.04	0.62	4.21	7.58	1.93	0.624	...	0.70	0.28	2.82	0.92	8.40
D ...	2.208651	5.000	2.56	1.46	3.67	7.96	4.09	0.624	...	0.70	0.28	2.82	0.92	8.40
E	2.308960	5.000	2.98	1.80	3.61	8.03	4.28	0.624	...	0.69	0.29	1.65	2.75	7.86
F	2.322347	0.765	3.00	1.82	3.60	8.10	4.15	0.628	...	0.36	0.62	0.10	11.1	0.60
G ...	2.651283	0.765	2.08	−0.49	4.53	8.13	4.02	0.724	...	0.36	0.62	0.10	11.0	0.60
H ...	3.333460	0.765	3.09	−0.00	4.53	8.33	4.82	0.732	0.344	0.36	0.62	0.10	11.0	0.60
I	3.345335	0.765	2.63	−0.36	4.60	8.27	5.02	0.735	0.345	0.36	0.62	0.10	11.0	0.60
J	3.467145	0.765	3.72	2.27	3.55	8.17	6.18	0.736	0.614	0.36	0.62	0.10	11.0	0.60
K ...	3.468126	0.756	3.76	1.71	3.85	8.16	6.20	0.734	0.626	0.18	0.80	0.09	11.3	0.27
L	3.472806	0.755	3.93	1.02	4.23	8.13	6.40	0.734	0.692	0.13	0.85	0.09	11.3	0.27
M ...	3.473946	0.75229	4.09	1.81	3.88	8.12	6.48	0.739	0.714	0.13	0.85	0.09	11.3	0.27
N ...	3.475594	0.75229	3.44	−1.42	5.33	8.10	6.59	0.75202	0.742	0.13	0.85	0.08	11.3	0.27
P	3.594200	0.75229	−0.51	−1.92	4.60	7.75	6.83	0.75224	0.743	0.13	0.85	0.08	11.3	0.27

TABLE 2

SOME PARAMETERS OF A CLOSE BINARY COMPONENT WITH INITIAL MASS 6.95 $M_\odot$

Stage	Age ($\times 10^{15}$ s)	$M_*/M_\odot$	$\log L/L_\odot$	$\log R/R_\odot$	$\log T_e$	$\log T_c$	$\log \rho_c$	$M_{He}/M_\odot$	$M_{CO}/M_\odot$	X	Y	X_{12} ($\times 10^{-3}$)	X_{14} ($\times 10^{-3}$)	X_{16} ($\times 10^{-3}$)
A	0.0	6.947	3.28	0.49	4.34	7.48	1.18	...	...	0.70	0.28	2.82	0.92	8.40
B	1.073949	6.947	3.50	0.77	4.25	7.55	1.30	...	...	0.70	0.28	2.82	0.92	8.40
C	1.108949	6.947	3.56	0.72	4.29	7.64	1.74	...	...	0.70	0.28	2.82	0.92	8.40
D ...	1.129107	6.947	3.16	1.81	3.65	8.04	3.93	...	...	0.70	0.28	2.82	0.92	8.40
E	1.129680	6.947	3.52	2.09	3.59	8.07	4.01	...	...	0.70	0.28	2.01	1.86	8.39
F	1.130852	1.109	3.46	2.09	3.59	8.13	3.95	0.95	...	0.16	0.82	0.12	11.2	0.33
G ...	1.258117	1.109	2.64	−0.46	4.65	8.16	3.78	1.052	...	0.26	0.72	0.09	11.2	0.33
H ...	1.468572	1.109	3.20	−0.36	4.74	8.34	4.29	1.053	0.359	0.26	0.72	0.09	11.2	0.33
I	1.470736	1.109	2.95	−0.43	4.72	8.28	4.53	1.065	0.359	0.26	0.72	0.08	11.2	0.33
J	1.538204	1.109	3.87	2.19	3.64	8.40	6.05	1.065	0.699	0.26	0.72	0.08	11.2	0.33
K ...	1.543329	0.894	4.31	2.10	3.80	8.19	6.75	...	0.878	0.0	0.98	0.22	11.2	0.18
L	1.544380	0.894	3.92	−1.49	5.49	8.14	6.95	...	0.890	0.0	0.98	0.24	11.2	0.18
M ...	1.609851	0.894	−0.41	−2.00	4.66	7.80	7.17	...	0.890	0.0	0.98	0.24	11.2	0.18

TABLE 3

SOME PARAMETERS OF A CLOSE BINARY COMPONENT WITH INITIAL MASS 9.85 $M_\odot$

Stage	Age ($\times 10^{14}$ s)	$M_*/M_\odot$	$\log L/L_\odot$	$\log R/R_\odot$	$\log T_e$	$\log T_c$	$\log \rho_c$	$M_{He}/M_\odot$	$M_{CO}/M_\odot$	X	Y	X_{12} ($\times 10^{-3}$)	X_{14} ($\times 10^{-3}$)	X_{16} ($\times 10^{-3}$)
A	0.0	9.852	3.76	0.57	4.42	7.51	0.98	...	...	0.708	0.28	2.82	0.92	8.40
B	5.883507	9.852	4.03	0.87	4.33	7.59	1.16	...	...	0.708	0.28	2.82	0.92	8.40
C	6.010057	9.852	4.08	0.82	4.37	7.70	1.60	1.52	...	0.708	0.28	2.82	0.92	8.40
D ...	6.060533	9.852	3.72	2.15	3.62	8.16	3.60	1.52	...	0.708	0.28	2.82	0.92	8.40
E	6.062730	9.852	4.11	2.48	3.55	8.16	3.56	1.52	...	0.680	0.30	1.73	2.88	7.55
F′ ...	6.067112	1.989	4.12	2.48	3.55	8.16	3.53	1.54	...	0.647	0.34	1.51	4.01	6.63
F	6.067124	1.951	4.08	2.34	3.61	8.16	3.53	1.54	...	0.472	0.52	0.11	9.93	1.77
G ...	6.529839	1.951	3.45	−0.10	4.68	8.21	3.47	1.82	...	0.472	0.52	0.11	9.93	1.77
H ...	7.241783	1.951	3.93	0.16	4.66	8.43	4.09	1.85	0.729	0.472	0.52	0.11	9.93	1.77
I	7.290012	1.951	4.09	0.96	4.30	8.54	5.31	1.86	0.955	0.472	0.52	0.11	9.93	1.77
J	7.302422	1.951	4.19	2.19	3.71	8.61	5.79	1.86	0.985	0.472	0.52	0.11	9.93	1.77
K′ ...	7.311913	1.238	4.30	2.13	3.77	8.60	6.66	...	1.023	0.0	0.99	0.22	11.2	0.19
K ...	7.316132	1.063	4.60	1.97	3.92	8.32	7.28	...	1.050	0.0	0.97	12.8	0.03	0.28
L	7.317475	1.063	4.23	−1.63	5.63	8.26	7.39	...	1.061	0.0	0.97	12.8	0.03	0.28
M ...	7.509881	1.063	0.00	−1.10	4.81	7.91	7.60	...	1.062	0.0	0.97	12.8	0.03	0.29

NOTE.—In models K, L, and M, $X_{18} = 5.03 \times 10^{-3}$, $X_{22} = 11.3 \times 10^{-3}$, and $X_{25} \approx 0$. In all other models, $X_{18} = X_{22} = X_{25} = 0$.

$M_\odot$, whereupon model radius drops to about 100 $R_\odot$. A very rapid decrease in radius to about 20 $R_\odot$ occurs when mass is decreased only slightly further. We infer that Roche-lobe detachment occurs when the model mass reaches a value somewhere in the neighborhood of $M_{R1} = 1.90$–1.95 $M_\odot$. The subsequent evolution has been followed for both extremes $M_{R1} = 1.95$ $M_\odot$ (case A) and $M_{R1} = 1.90$ $M_\odot$ (case B).

After the first mass-loss episode is completed, the remnant contracts toward the region where sequences of pure helium models reside (the five-pointed star symbols in Figs. 1–3 mark the location of pure "helium main-sequence" models [Paczyński 1971]). The rate of hydrogen burning decreases rapidly during the initial stages of core helium burning (see Figs. 4–6). Because of the larger opacity and smaller molecular weight of hydrogen-rich matter, the minimum radii of our core helium-burning remnants (at point G) are somewhat larger than those of pure helium stars of the same mass. This is illustrated directly in Figure 8, where the two evolutionary models (for cases A and B) differ by only 0.05 $M_\odot$ in the amount of hydrogen-rich matter in the envelope.

The most remarkable property of the helium-burning remnants of lowest mass is their long lifetime compared with the lifetime of their single-star counterparts during the core helium-burning phase. In fair approximation,

$$(\tau_{He}/\tau_{MS})_{binary} \sim 4.8 M_{MS}^{-1.34}, \quad (5)$$

where τ_{He} is the core helium-burning lifetime of the remnant and τ_{MS} is the main-sequence lifetime of its progenitor of mass M_{MS}. The analogous relationship for single stars (Iben 1967) is

$$(\tau_{He}/\tau_{MS})_{single} \sim 0.56 M_{MS}^{-0.52}. \quad (6)$$

Relationship (5) is derived from

$$\tau_{MS} \sim 1.32 \times 10^9 M_{MS}^{-1.86} \text{ yr}, \quad (7)$$

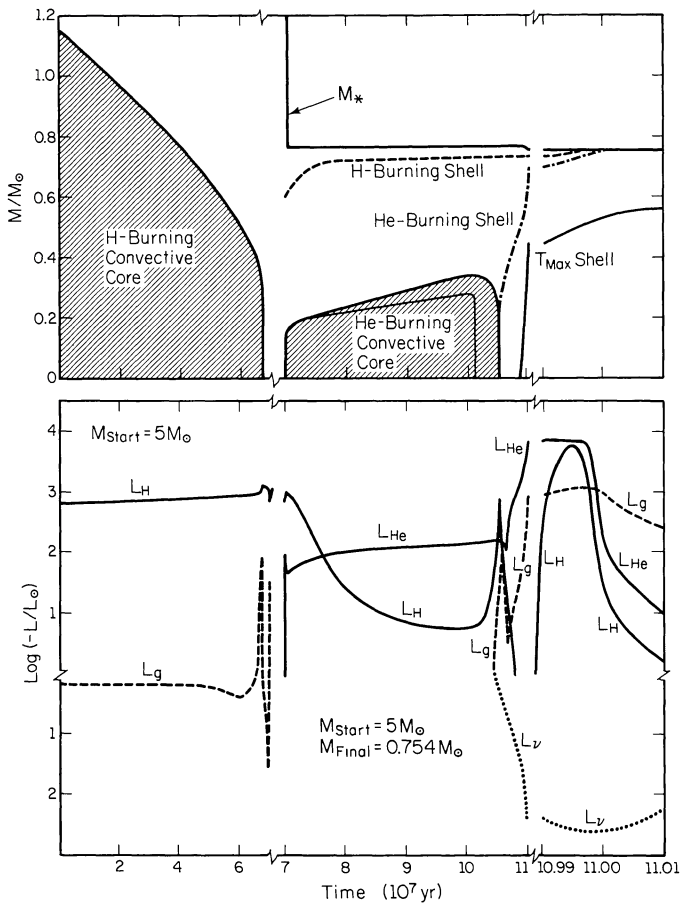

FIG. 4.—The structural evolution of a binary component of initial mass 5 $M_\odot$. In the upper panel are shown core convective regions, stellar mass, locations of the hydrogen-burning and of the helium-burning shells, and the location of the off-center point (labeled T_{max} Shell) at which $L = 0$ and T is at a relative maximum in the carbon-oxygen core. In the lower panel are shown rates of hydrogen burning (L_H), helium burning (L_{He}), "gravitational energy" production [$L_g = \int(P\rho^{-1}\, d\rho/dt - dU/dt)\, dM = \int \varepsilon_g\, dM$], and neutrino loss ($L_\nu$).

and

$$\tau_{He} \sim 6.3 \times 10^9 M_{MS}^{-3.2} \text{ yr}. \quad (8)$$

The major reason for the large values of τ_{He} for remnant binary components of lowest M_{MS} is the absence of a large reservoir of hydrogen fuel to burn and the consequent approximate constancy of the mass of the hydrogen-exhausted core. In single stars, shell hydrogen burning produces energy at roughly 5–10 times the rate at which core helium burning produces energy, and therefore, the rates at which the two burning modes simultaneously process matter are roughly the same. For example, during core helium burning in a 5 $M_\odot$ single star, approximately 0.3 $M_\odot$ of hydrogen-rich matter is converted into helium at the same time that about 0.3 $M_\odot$ of helium is converted into carbon and oxygen (Iben 1966*a*). The average temperatures and densities in the helium-burning core thus increase from those appropriate for a hydrogen-exhausted core of mass $\sim 0.77\ M_\odot$ to those appropriate for one of mass $\sim 1.1\ M_\odot$, and the value of τ_{He}/τ_{MS} is only about 0.25 (as opposed to about 0.50 when the mass of the hydrogen-exhausted core of a binary remnant remains nearly constant at about 0.75 $M_\odot$). As the mass of a single star increases, the amount of matter added to the hydrogen-exhausted core during the core helium-burning phase becomes a smaller and smaller fraction of the core mass. It is for this reason that the values for τ_{He}/τ_{MS} given by the two expressions (5) and (6) approach one another as $M_{MS} \to 10\ M_\odot$.

In the case of the 0.765 $M_\odot$ remnant, we have explored the effect of convective overshoot at the edge of the convective core. The thin solid line within the hatched region labeled "He-Burning Convective Core" in Figure 4 gives the mass in the convective core as a function of time when overshoot is neglected. To test the effect of overshoot, we have repeated the calculation, this time increasing the mass of the formally mixed central region beyond that given by employing the Schwarzschild criterion to matter in each mass zone. After each time step, we first determine the central region within which matter is formally unstable to convection according to the Schwarzschild criterion and then mix homogeneously matter in this region with matter in the shell immediately adjacent to but just outside the region that is formally unsta-

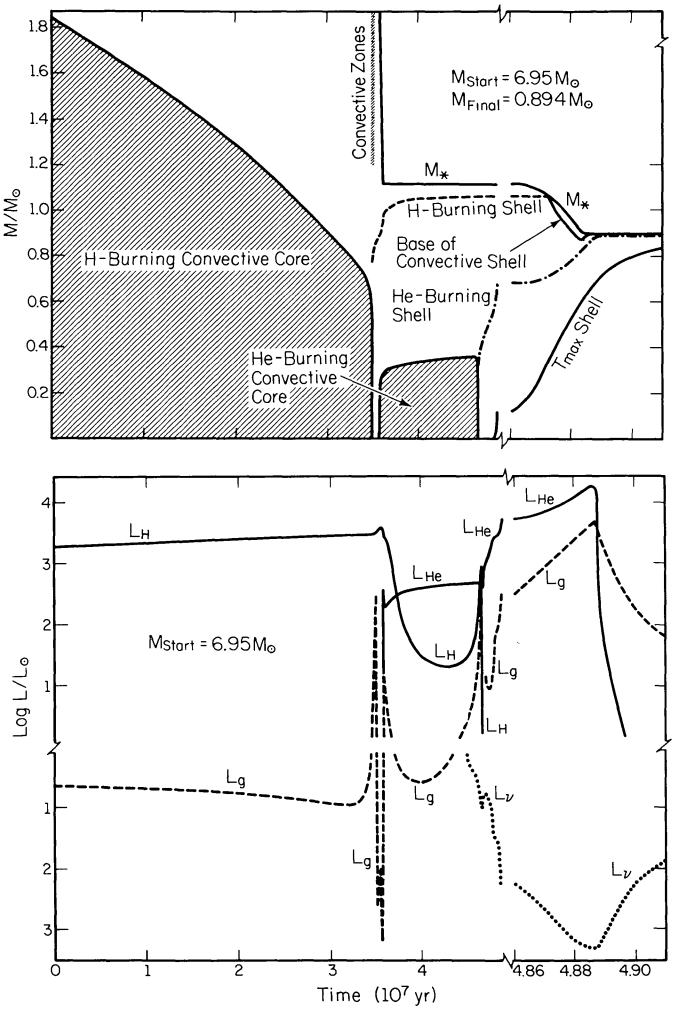

FIG. 5.—Same as Fig. 4, but for a component of initial mass 6.95 $M_\odot$

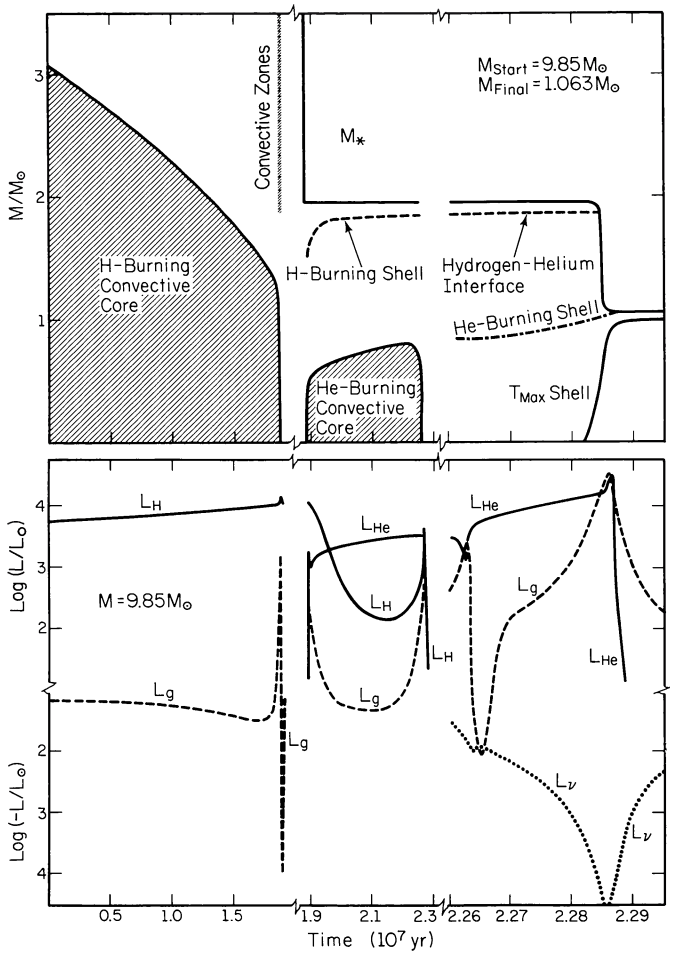

FIG. 6.—Same as Figs. 4 and 5, but for a component of initial mass 9.85 $M_\odot$.

ble. The time steps are chosen short enough and the zoning is fine enough that the size of the formally mixed region is essentially independent of the zoning details. This procedure leads to near identity of the adiabatic and radiative gradients at the edge of the mixed region. The thick solid curve that bounds the hatched region in Figure 4 is the result. As expected, the inclusion of overshoot increases the maximum mass of the convective core (by about 20%) and the duration of the core helium-burning phase (by about 10%). Since, in any case, the final mass of the CO core after the shell helium-burning phase is considerably larger than the maximum mass of the convective core during helium burning, whether or not one includes overshoot has no influence on the final mass of the CO core. We have not included overshoot in following the evolution of the 1.11 $M_\odot$ remnant of the 6.95 $M_\odot$ model, but we have included it in following the evolution of all other core helium-burning remnants described in this paper.

After it has exhausted helium at its center, the primary remnant develops a CO core (points H in Figs. 1–3), and, since core temperatures are too low to ignite carbon and since core matter is initially nondegenerate, the core contracts rapidly. The star now consists of a large CO core surrounded by an almost pure helium envelope which is burning helium at its base. A thin "topping" of hydrogen-rich matter is still present. For example, in the case $M_{MS}=9.85\ M_\odot$, $M_{R1}=1.95\ M_\odot$, hydrogen is effectively exhausted over the inner 1.85 $M_\odot$ of the remnant at this stage (see Fig. 7).

Matter in the contracting CO core becomes electron degenerate between points H and I (see Figs. 1–3 and Fig. 9), and the luminosity of the star eventually approaches within a factor of 2 or 3 that given by the standard relationship for single asymptotic giant-branch (AGB) stars, $L/L_\odot \sim 6\times 10^4\ (M_{CO}/M_\odot - 0.5)$, even though helium burning supplies all of the energy appearing at the surface, in contrast to the situation in AGB models from which the relationship is de-

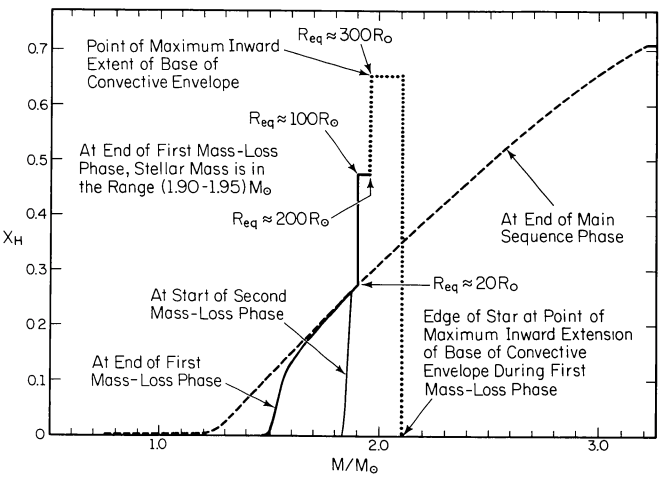

FIG. 7.—Hydrogen profiles in the model of initial mass 9.85 $M_\odot$ before, during, and after the first mass-loss phase and just before the second mass-loss phase.

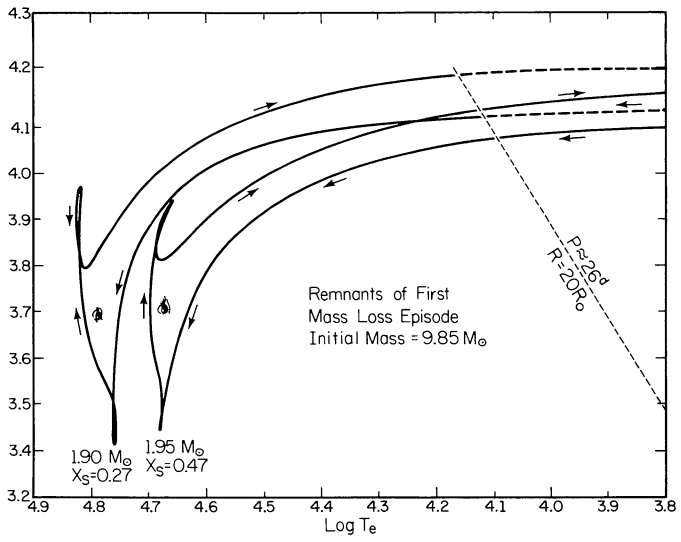

FIG. 8.—Comparison of tracks in the H-R diagram of possible core helium-burning remnants of the model of initial mass 9.85 $M_\odot$. Remnant masses are 1.95 $M_\odot$ (case A) and 1.90 $M_\odot$ (case B).

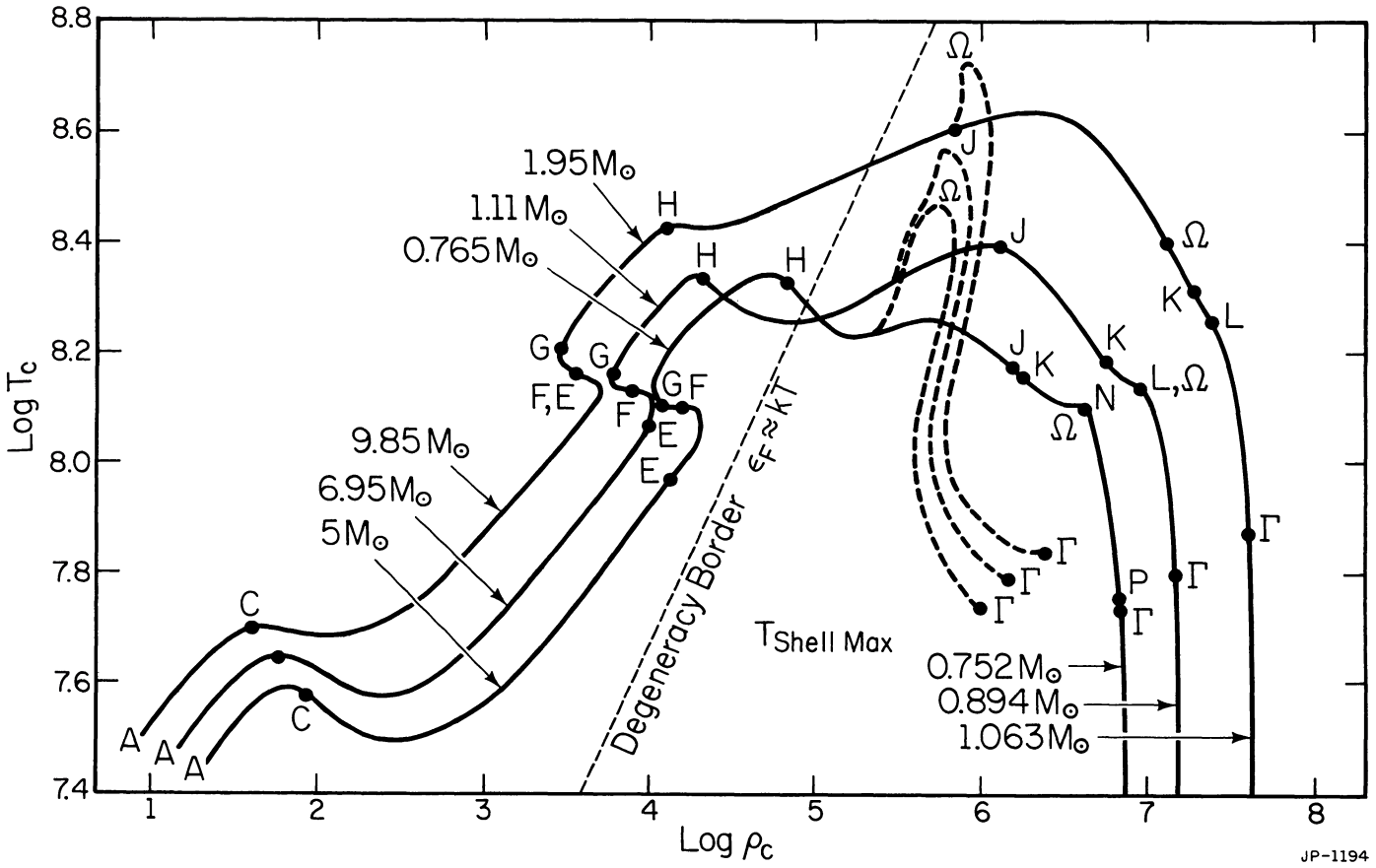

FIG. 9.—Evolution in the ρ-T plane of the centers of binary components of initial masses 5, 6.95, and 9.85 $M_\odot$. The ρ-T evolution of the off-center points in the carbon-oxygen core where temperature is at a relative maximum (and where the carbon-burning rate is largest and luminosity is zero) is shown by the heavy dashed lines. The position along which electron Fermi energy ϵ_F approximately equals kT is given by the light dashed curve.

rived and in which hydrogen burning supplies most of the energy appearing at the surface (Paczyński 1971; Uus 1970). However, even though the nuclear energy released by 1 g of pure helium is only about one-fifth of the nuclear energy liberated by 1 g of hydrogen-rich matter, because of the smaller average hydrogen-exhausted core masses and hence lower average luminosities, the shell helium-burning lifetimes of our stars are comparable to those of low-mass AGB stars, namely, $1-2\times10^6$ yr.

The CO cores plus helium-burning shells in our models behave quite similarly to models made initially of pure helium. Divine (1965) shows that a helium star of solar mass expands to giant dimensions during shell helium burning and that this is not true for helium stars more massive than 6 $M_\odot$ or less massive than 0.5 $M_\odot$. Consistent with this, the matter in and below the hydrogen-burning shell in the 0.77 $M_\odot$ remnant of the binary component of initial mass $M_{MS} = 5$ $M_\odot$ also does not expand. It is only matter in the hydrogen-rich envelope that is included in the expansion. And it is only this hydrogen-rich matter that is lost through Roche-lobe overflow after the Roche lobe is again filled (during the J–K stage of Fig. 1). The hydrogen-helium "discontinuity" remains at a distance of about 0.2 $R_\odot$ from the stellar center. When the mass of the hydrogen-rich envelope decreases to about 0.01 $M_\odot$, the envelope begins to contract, interrupted briefly by one weak hydrogen-burning thermal flash (see points L–M in Fig. 1 and L_H in Fig. 4).

Paczyński (1971) shows that the upper mass boundary between those helium stars which expand during the helium shell-burning stage and those which do not lies between 2 $M_\odot$ and 2.5 $M_\odot$ (see also Delgado and Thomas 1981; Law 1982; Law and Ritter 1983; Nomoto 1984*a*). As expected, the 1.11 $M_\odot$ remnant of our 6.95 $M_\odot$ binary star component and the 1.90 $M_\odot$ and 1.95 $M_\odot$ remnants of our 9.85 $M_\odot$ binary star component expand after CO core formation. Not only does the thin topping of hydrogen-rich matter expand outward but so too does matter for some distance below the hydrogen-helium interface. Therefore, during the second Roche-lobe–filling stage (J–K in Figs. 2 and 3), not only do the model stars lose all of their hydrogen-rich envelopes but they also lose part of their helium-rich envelopes. The resulting CO dwarfs have pure helium envelopes. In this way, some fraction of all non-DA white dwarfs may be formed.

There is a parallel between the behavior of initially pure helium stars or helium-burning remnants formed in close binaries and the "helium stars" formed in the interiors of single stars of intermediate mass. Detailed numerical calculations of single-star evolution show clearly (see, e.g., Figs.

6*a*–6*c* in Becker and Iben 1979) that only if the mass of the helium core formed in such stars exceeds some limit (which depends on composition) will the outer helium-rich layers expand during shell helium burning. For a Population I composition this limit is about 0.85 $M_\odot$, and the mass of the parent star which develops a core of this limiting mass is about 5 $M_\odot$. It is only stars in which helium layers expand that experience the so-called second dredge-up phenomenon. The increase in opacity in the expanding helium layers and at the inner edge of the hydrogen-rich envelope beyond them, coupled with an increase in luminosity through this region of variable composition, leads to the penetration of the base of the convective envelope into the helium-rich region.

An important question related to the formation of the final CO white dwarf is the duration of the second mass-exchange phase involving mass loss from the original primary. The thermal time scale of the envelope of a supergiant of mass ~ 1 $M_\odot$, radius about ~ 100 $R_\odot$, and luminosity of the order of 6000 $L_\odot$ is only about 50 yr. The rate of helium burning in the helium-burning shell surrounding the CO core is about

$$\dot{M}_{\rm CO}(M_\odot\ {\rm yr}^{-1}) \sim {\rm few}\times 10^{-6}\,(M_{\rm CO}/M_\odot - 0.5). \quad (9)$$

Therefore, over a thermal time scale, the mass of the CO core can be increased by only $\sim {\rm few}\times 10^{-4}$ $M_\odot$, and the assumption that the duration of the Roche-lobe–filling stage coincides with the thermal time scale of the envelope is equivalent to the statement that Roche-lobe overflow "freezes" the mass of the CO core of a helium star remnant whose mass satisfies $M_{\rm He} \gtrsim M_\odot$. This "freezing" argument does not apply to the evolution of a helium remnant of initial mass smaller than ~ 1 $M_\odot$; such a remnant will lose only its hydrogen-rich envelope during the common-envelope stage (see Fig. 1 and Table 1). On the other hand, one might anticipate that a helium remnant of initial mass larger than ~ 1 $M_\odot$ may develop a CO core whose final mass is close to that obtaining when the Roche lobe is filled for a second time. However, in practice (see, in particular, the curve of stellar mass versus time in Fig. 5), the rate of mass loss which will permit a model to maintain a radius larger than a predetermined value is much smaller than that given by $M/\tau_{\rm KH}$. Hence the "freezing" argument is of only very approximate validity. Further, in a real situation, the result will also depend on the orbital separation and on the mass ratio of the two binary components at the moment of Roche-lobe overflow. If, for example, the secondary is still on the main sequence and, as a consequence of accretion from the primary, has become considerably more massive than the primary remnant, mass transfer is likely to be conservative of total system mass; the orbital separation may therefore increase in response to mass transfer, the mass-transfer rate may be smaller than we have assumed, and the final remnant mass of the primary may be larger. Given the uncertainty in the orbital shrinkage (or enlargement) occurring during any mass loss/transfer episode (we have assumed essentially no shrinkage in the 5 $M_\odot$ and 6.95 $M_\odot$ cases), it is conceivable that the final CO remnant mass can depend on the initial component mass in a nonmonotonic way, with, for example, the mass of the remnant of the 6.95 $M_\odot$ component in a given binary being smaller than that of the remnant of the 5 $M_\odot$ component in another binary.

In our experiments, final remnants are of masses 0.752, 0.894, and 1.063 $M_\odot$ (case A) or 1.048 $M_\odot$ (case B), respectively, for the primaries of primordial mass 5, 6.95, and 9.85 $M_\odot$. The difference between final remnant masses in the case A and case B scenarios which begin with a 9.85 $M_\odot$ progenitor is due to implicit assumptions regarding the nature of the companion and to assumptions regarding model radius when Roche-lobe detachment terminates each phase of mass loss. In case A, we have assumed that orbital separation, Roche-lobe radius, and model radius decrease during both the first and the second mass-loss episodes. In so doing, we have made the implicit assumption that a common envelope is formed or/and that the mass of the secondary is initially less or remains less than that of the primary mass donor. Case A is therefore appropriate to a situation in which the current (potential) accretor was the primordially more massive star and has already evolved into a white dwarf or neutron star; mass transferred onto the compact component will almost certainly be ejected into a common envelope and lost from the system, with a concomitant decrease in the orbital separation of the two components. In case B, we have assumed that a common envelope formed during the first phase of mass transfer is extremely effective and forces orbital shrinkage to such an extent that Roche-lobe detachment does not occur until the radius of the donor decreases below ~ 20 $R_\odot$. The second phase of mass loss is begun when model radius again reaches 20 $R_\odot$, and the mass-loss rate is chosen in such a way that model radius increases slowly to ~ 100 $R_\odot$, at which point mass loss is again terminated. The case B mass-loss algorithm is qualitatively appropriate for a binary system in which the primary is primordially distinctly more massive (by, say, a factor of 2) than its companion, so that a common envelope is formed during the first phase of mass transfer, whereas it is distinctly less massive than its main-sequence companion during the second phase of mass transfer, so that system mass and orbital angular momentum are likely to be preserved to some extent during mass flow.

The central portion of the CO core in all three model remnants is maintained at relatively low temperatures by neutrino cooling. But, heating due to the compression of matter accreted by the core through the helium shell source produces a maximum temperature at some distance from the center. The evolution in the ρ-T plane of this maximum core temperature, as shown in Figure 9, displays a roughly convergent character, which is a consequence of the fact that the behavior of a contracting core is a nearly unique function of core mass and of the fact that stars of different total mass may develop cores of the same mass during their evolution.

For the same progenitor main-sequence mass, the mass of the hydrogen-exhausted portion of a star at the end of the core helium-burning phase is smaller in the close binary star case than in the single-star case. Thus, during the shell helium-burning phase, when the stellar envelope swells to giant dimensions, the contracting CO core is smaller in a close binary component than in a single star. Accordingly, when the binary component fills its Roche lobe for the second time, the mass of its CO core, whose further growth is then attenuated, is smaller than the CO core of a single star (of the same progenitor mass) when it evolves onto the asymptotic giant

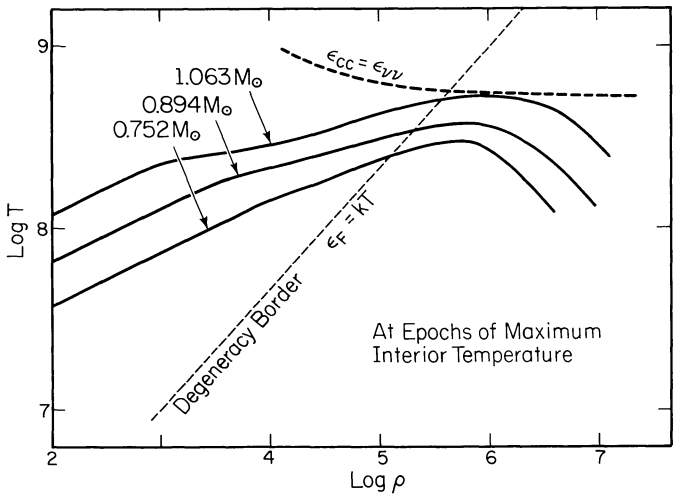

FIG. 10.—Distribution of density and temperature in the models located at points Ω in the H-R diagrams of Figs. 1–3. The locus of points where the carbon-burning rate and the neutrino loss rate are equal is given by the heavy dashed curve, and the locus of points where $\epsilon_F \approx kT$ is given by the light dashed curve.

branch, and the maximum interior temperature is, therefore, also smaller. This means that the minimum initial mass above which the primary in a close binary experiences a carbon shell flash can be larger than the minimum initial mass of a single star which experiences such a flash to terminate the further growth of its CO core. For single stars of Population I composition, the minimum stellar mass is approximately 8.8 $M_\odot$ and the final CO core mass is ~ 1.08 $M_\odot$ (Becker and Iben 1979); in a close binary, the minimum mass can be, as we see here, in excess of 9.8 $M_\odot$.

Figure 10 gives the density-temperature distributions in model CO cores of components of close binaries when the maximum off-center temperature is reached. The locus of points where the neutrino loss rate equals the rate of energy generation by carbon-burning reactions is also shown. It is clear that none of the three final remnants ignites carbon. We estimate, on the basis of the information in Figures 9 and 10 (see also the discussion in § III) that, in a close binary, the maximum initial mass of a primary component which does not ignite carbon at high temperature is about 10.3 $M_\odot$. For initial masses somewhat larger than this, carbon burning will continue until a degenerate ONe core is formed. We emphasize that the maximum mass of a degenerate CO core that can be formed by mass loss in a close binary is ~ 1.08 $M_\odot$ (see also Nomoto 1984*a*, *b*) and not 1.4 $M_\odot$, as has been suggested elsewhere (Law and Ritter 1983). Single stars also do not form CO degenerate dwarfs more massive than about 1.1 $M_\odot$ (see § V), and, since it appears likely that more mass is lost in a nova explosion than has been accreted prior to the nova explosion, any degenerate dwarf that is found to be more massive than 1.1 $M_\odot$ is likely to be composed of oxygen and neon.

In agreement with results found in many previous calculations, we find that helium burns stably in all remnants more massive than 0.5 $M_\odot$ (see § IV for the behavior of a less massive remnant). It may be argued that helium remnants avoid the "accumulation" instability that occurs in AGB stars because the effective "accretion" rate (of matter from the envelope) in a helium remnant is much larger than is the effective "accretion" rate (of matter processed by the hydrogen-burning shell) in an AGB star of comparable core mass and luminosity. The difference in "accretion" rates arises from the fact that, for a given CO core mass, stellar luminosities are comparable, but the energy content of a gram of hydrogen is an order of magnitude larger than that of a gram of helium.

The absence in all of our models of a thermal instability of the sort that occurs in AGB models (and leads to a change in envelope composition) has observational consequences. Many planetary nebula nuclei of the Wolf-Rayet type belong to the subclass WC (e.g., Heap 1982); that is, their envelopes are enriched in carbon. This can be easily understood if their progenitors have experienced a series of helium shell flashes that mix into the envelope some of the carbon produced in the shell (see, e.g., Iben and Renzini 1983). Nitrogen is destroyed by alpha-capture reactions in the convective shell during such flashes and cannot be reconstructed by CN cycling of fresh carbon at the base of the convective envelope between flashes except in the initially most massive AGB stars. A quite different envelope chemistry will arise if, as in our experiments involving close binaries, a helium shell flash phase does not precede the transformation into a compact star and the reservoir of initially unprocessed envelope material which is enriched by dredge-up is small. Under these circumstances, dredge-up carries to the surface only products of complete hydrogen burning and not products of helium burning. Further, the amount of dredged-up material may be comparable in mass to the amount of unprocessed matter which dilutes it. Therefore, surface nitrogen can become nearly as abundant as the sum of the initial CNO abundances in the star. An example of this possibility is shown in Figure 11, where surface abundance is given as a function of time for the case of the binary component of initial mass 5 $M_\odot$. Quite similar variations of surface composition occur in the other two cases except that, in them, the final surface abundances are the

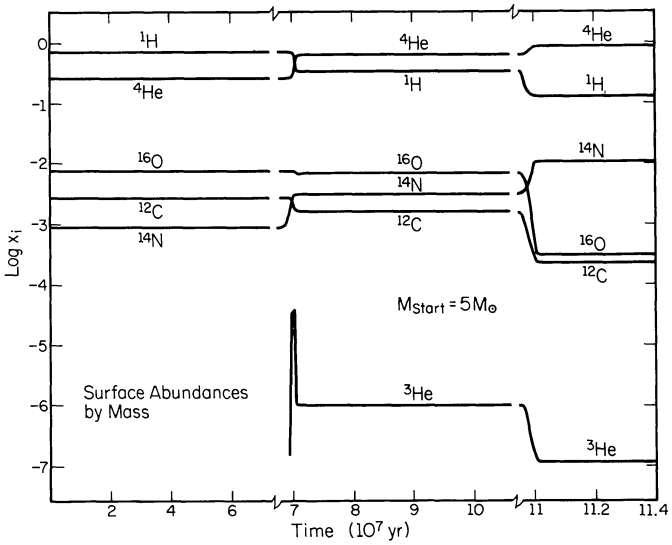

FIG. 11.—Variation with time of the surface composition of the model of initial mass 5 $M_\odot$. Abundances are by mass.

consequence of the direct exposure of matter that has experienced complete hydrogen burning, rather than the consequence of the exposure of material enriched by the dredge-up of material that has experienced only partial hydrogen burning.

PNNi with unusually large nitrogen abundances do exist. For example, the helium-rich nuclei of Abell 30 and Abell 78 have powerful P Cygni profiles of [N v] in their spectra (Hazard *et al.* 1980; Jacoby and Ford 1983). The formation of such nearly pure helium envelopes (with all CNO elements in the form of N) can be understood naturally in the framework of the binary scenario we have described.

As a caveat, however, we note that there is also a rough correlation between the nitrogen and helium abundances in extended nebular shells (e.g., Kaler, Iben, and Becker 1978), and this may be primarily a consequence of the fact that, for single AGB stars of sufficient mass to experience the second dredge-up phase (which can significantly enhance surface nitrogen and helium if the progenitor has an initial mass in excess of 5 $M_\odot$), the thermally pulsing lifetime is so short that dredge-up following thermal flashes does not significantly alter the abundances produced in the preceding second dredge-up phase (see Iben 1984*b*). The point to be made is that the existence of a large overabundance of nitrogen in a PN does not necessarily, or even usually, imply a close binary star origin for the PN. However, if hydrogen is absent at the same time that nitrogen is overabundant, then an explanation in terms of a binary origin becomes very attractive.

We return to a description of the evolution of the primary remnant. The mass of the CO core increases as the remnant evolves from I to K in Figures 1–3. After the completion of the second mass-loss phase, the burning of nuclear fuel remaining in the envelope above the CO core controls the rate of evolution of the remnant toward the degenerate dwarf state. The thermal time scale of an envelope of mass $\sim 0.01\ M_\odot$ and radius $\sim 10^2\ R_\odot$ through which $10^4\ L_\odot$ of radiant energy flows is only ~ 1 yr. The actual computed time scale of a few tens of thousands of years is due to the burning of helium (and, in the lowest-mass case, also hydrogen) in the envelope.

It is during the final contraction phase that the maximum off-center temperature is reached in the remnant core. The maximum temperature is achieved as each remnant reaches point Ω along the evolutionary tracks of Figures 1–3. Further evolution consists only of cooling by neutrino and radiative losses. Because of the large temperatures achieved in the relatively large helium-burning zone during the previous helium-burning phase, the remnant only slowly and asymptotically achieves a fixed radius.

For some problems, such as the evolution of cataclysmic binaries in which shear mixing dredges up matter from the dwarf interior into the accreted envelope and such as the supernova explosion which arises from the merging of two CO degenerate dwarfs of total mass larger than 1.4 $M_\odot$, it is of interest to know the distribution of nuclear species within a cooling degenerate dwarf. Abundance distributions within our model dwarfs of mass 0.752, 0.894, and 1.048 $M_\odot$ are displayed in Figures 12–14. For comparison we show in Figures 15 and 16 the distributions formed in degenerate dwarfs produced by single stars (models from Iben 1975 and Iben and Tutukov 1984*c*). It must be cautioned that these distributions, especially near the surface, will be considerably modified by gravitational and chemical diffusion in the course of evolution (see, e.g., Iben and MacDonald 1985). Furthermore, the ratio of ^{12}C to ^{16}O in the deep interior is a strong function of the rate of the $^{12}C(\alpha,\gamma)^{16}O$ reaction, and there are indications (Kettner *et al.* 1982) that this rate is perhaps several times larger than the rate which we have chosen which is

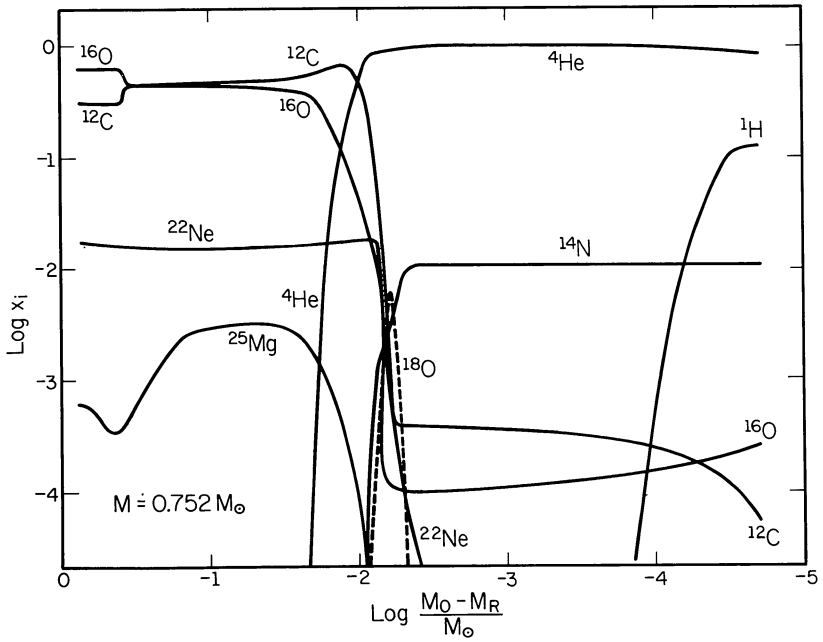

FIG. 12.—Abundances by mass of several nuclear species as a function of mass $M_0 - M_R$ inward from the surface within the 0.752 $M_\odot$ final remnant of the model of initial mass 5 $M_\odot$.

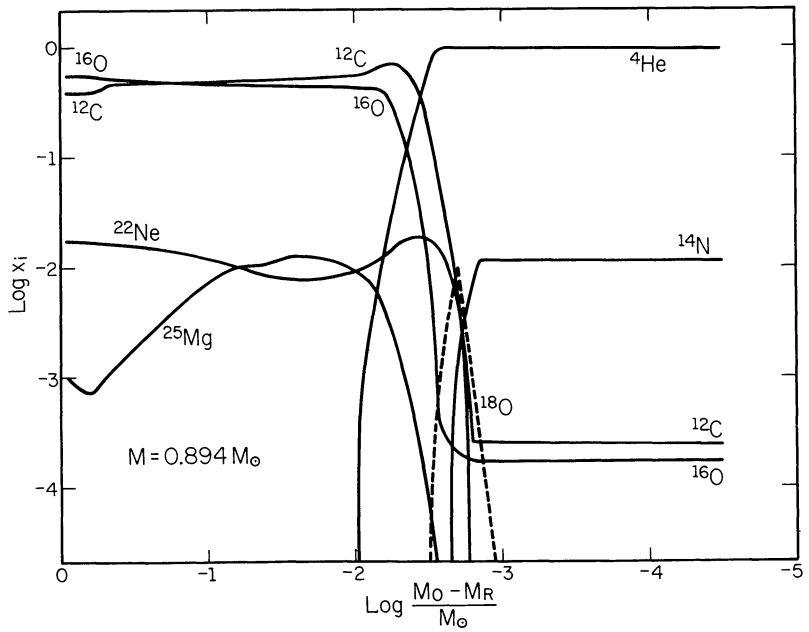

FIG. 13.—Same as Fig. 12 for nuclear species within the 0.894 $M_\odot$ final remnant of the model of initial mass 6.95 $M_\odot$

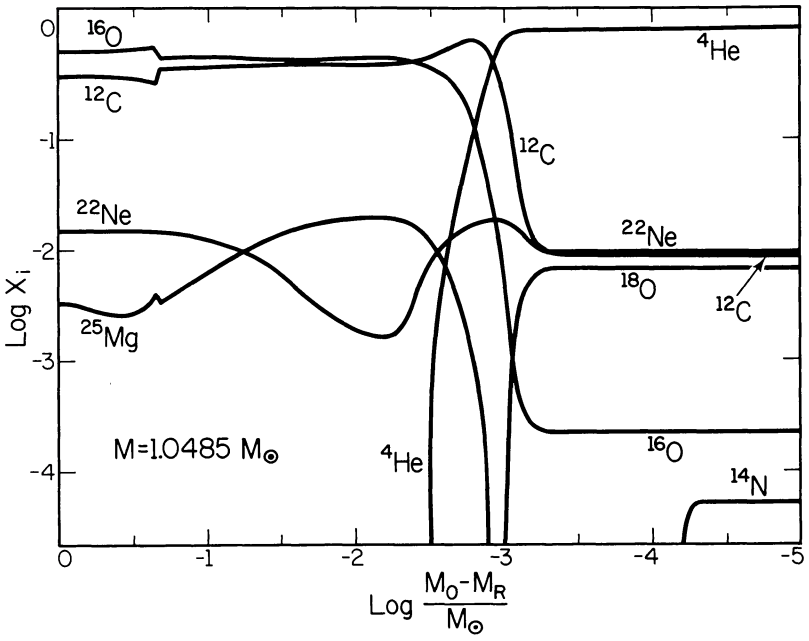

FIG. 14.—Same as Fig. 12 for nuclear species within the 1.048 $M_\odot$ final remnant of the model of initial mass 9.85 $M_\odot$ (case B)

approximately twice the rate given by Fowler, Caughlan, and Zimmerman (1975). A rate of only 2.5 times larger than the one which we have chosen will produce a CO core which contains very little ^{12}C (Iben 1972).

Of particular interest for the double degenerate scenario for R Coronae Borealis stars to be discussed in § VIII*c* is the mass of the helium-rich "buffer" layer that floats atop the CO core. For remnant masses between 0.75 $M_\odot$ and 1.05 $M_\odot$, the mass between the surface and the point where the helium abundance by mass is reduced to $Y = 0.1$ is given in good approximation by

$$\Delta M_{Y=0.1} = 10^{-2}\, M_\odot\, (M_{\rm remnant}/0.8\, M_\odot)^{-6.6}. \quad (10)$$

The mass below the surface where $Y = 0.9$ is given approximately by $\Delta M_{Y=0.9} \sim \Delta M_{Y=0.1}/1.6$.

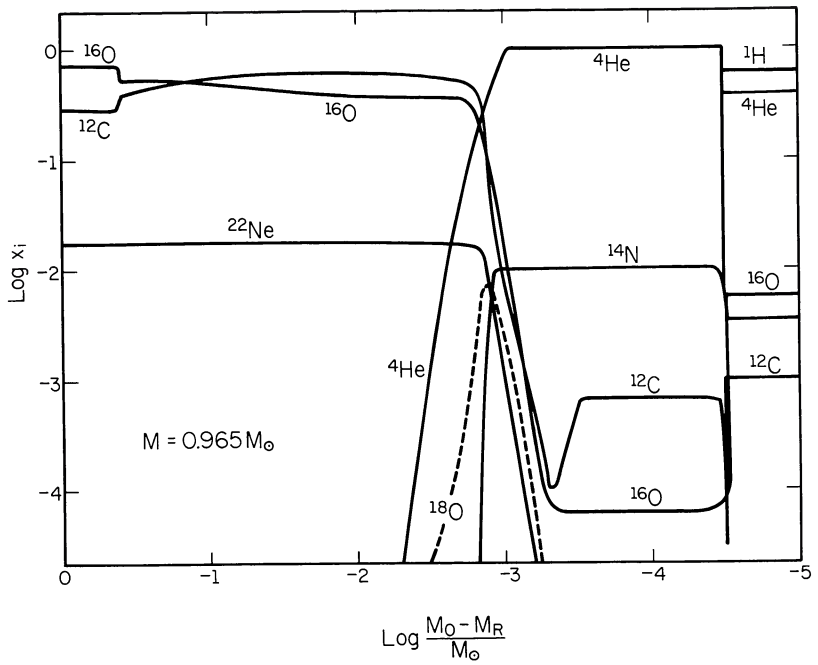

FIG. 15.—Same as Fig. 12 for nuclear species within the 0.965 $M_\odot$ core of a single AGB model star of mass 7 $M_\odot$ (Iben 1976). ^{22}Ne burning has been neglected, and the opacity parameter is $Z = 0.02$.

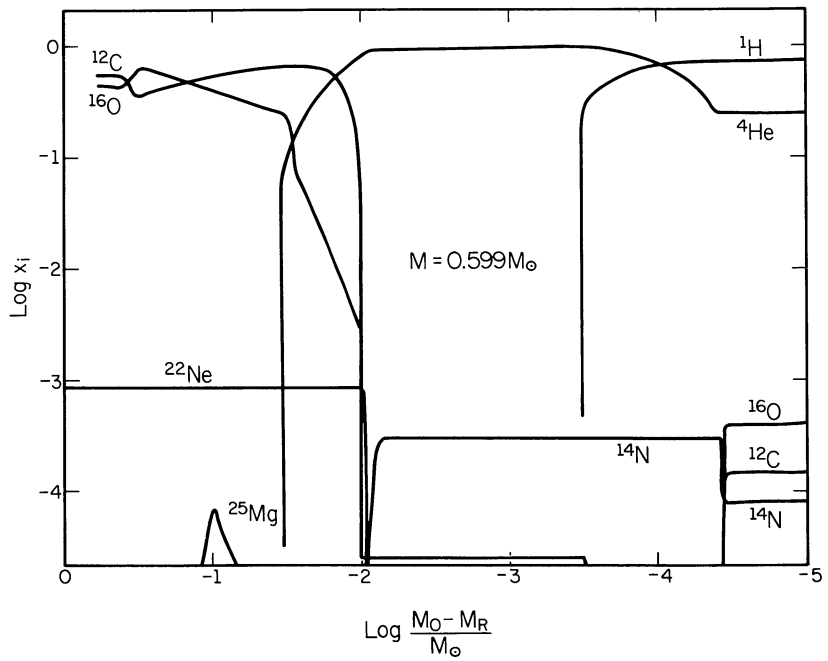

FIG. 16.—Same as Fig. 12 for nuclear species within a white dwarf model of mass 0.599 $M_\odot$ which derives from the evolution of a horizontal-branch model of approximately the same mass (Iben 1982). The opacity parameter is $Z = 0.001$, and all initial CNO abundances and the abundances of species derived from them are 20 times smaller than in the previous cases.

III. ON THE EVOLUTION OF COMPONENTS WHICH FORM AN OXYGEN-NEON CORE

The two descendants of our model of initial mass 9.85 $M_\odot$ evolve into CO degenerate dwarfs only because it has been assumed that the second phase of mass loss by Roche-lobe overflow continues while the model radius is smaller than it is at the start of the first phase (R decreases to ~ 100 $R_\odot$ for the case A model, and R increases from 20 $R_\odot$ to 100 $R_\odot$ for the case B model). This is probably legitimate (see eq. [1]) if the primordial masses of the two components are sufficiently different that the first episode of mass loss from the primary leads to a common envelope and very little mass is permanently accreted by the secondary.

However, if the two components are of comparable mass, the final portion of the first mass-transfer episode is likely to be conservative of both system mass and orbital angular momentum, resulting in an increase in orbital separation above that suggested by equation (1) (see § V). In this situation, a second phase of mass loss/transfer may not occur until, and/or terminate before, the primary has already developed such a large CO core that carbon is ignited at the center.

If its mass has been reduced to less than 1.4 $M_\odot$, either prior to or during carbon ignition, the carbon-burning star will go on to become an electron-degenerate object composed primarily of oxygen and neon. We shall call this object a "bare" ONe degenerate dwarf. If its mass remains larger than 1.4 $M_\odot$, an electron-degenerate ONe core of mass about 1.4 $M_\odot$ will form, and electron capture on the ^{24}Mg and ^{23}Na that is also present in the core will initiate core collapse. The final outcome will be a neutron star of baryonic mass about 1.4 $M_\odot$ and an ejected envelope of relatively small mass (e.g., Nomoto 1984*a*).

The minimum mass of a bare ONe degenerate dwarf is identical with the maximum mass of a "bare" CO degenerate dwarf, namely, about 1.08 $M_\odot$, and the minimum main-sequence mass of the progenitor of an ONe degenerate dwarf is 8.8 $M_\odot$ (for the composition chosen), or the same as the maximum mass of a single-star progenitor of a CO degenerate dwarf. Whether or not a binary component of mass somewhat larger than 8.8 $M_\odot$ will produce an ONe degenerate dwarf is a sensitive function of initial binary masses and of initial orbital parameters. Given our ignorance of the details of common-envelope evolution (and even of the details of evolution during mass-transfer phases when a common envelope is not formed), it is impossible to determine what this function is. We must content ourselves with plausible guesses.

For example, if the second phase of mass transfer from the 1.95 $M_\odot$ (case A) remnant of the 9.85 $M_\odot$ binary component in our experiments is delayed until this remnant expands to about 200 $R_\odot$, and if mass loss proceeds only as long as stellar radius is between, say, 200 $R_\odot$ and 250 $R_\odot$, the mass of the final remnant remaining after the second mass-loss episode is about 1.3 $M_\odot$. When the remnant has contracted to a radius of about 50 $R_\odot$, carbon is ignited under only mildly degenerate conditions at the model center. Although we do not follow the subsequent evolution in this paper, we can surmise from other studies in the literature that our 1.3 $M_\odot$ remnant will ultimately evolve into an ONe degenerate dwarf of this same mass.

In an effort to pin down the upper limit to the mass range of stars which can potentially evolve into bare ONe cores, we have evolved models of initial mass 12, 11, and 10.5 $M_\odot$. Evolution in the H-R diagram is presented in Figures 17–19, the time evolution of interior characteristics is shown in Figures 20–22, and evolution in the ρ-T plane is shown in Figure 23. Tables 4–6 contain information about the models at points labeled in the figures.

In all three instances, we have assumed that the first mass-loss episode begins when model radius exceeds about 300 $R_\odot$. The 10.5 $M_\odot$ and 11 $M_\odot$ models achieve this radius before the beginning of the core helium-burning phase, whereas (see Figs. 17 and 20) the 12 $M_\odot$ model ignites helium when model radius reaches about 135 $R_\odot$ and thereupon evolves back to the blue, where it remains for most of the rest of its core helium-burning phase. Only toward the end of the core-burning phase does the radius of the 12 $M_\odot$ model exceed 300 $R_\odot$. Then, even when mass is abstracted at a rate in excess of 10^{-3} $M_\odot$ yr^{-1}, the propensity for maintaining the envelope at a radius larger than 300 $R_\odot$ cannot be overcome until stellar mass is reduced to about 4.5 $M_\odot$. Further mass loss exposes layers containing matter which has been within the convective core during the main-sequence phase, and the model evolves to the blue at a rate and to an extent determined by the assumed rate of mass transfer and by the assumed duration of the mass-loss episode. This rate and this duration are, in a real situation, determined by the (unknown) efficacy of common-envelope action, and we content ourselves with simply presenting two conceivable outcomes: a case in which rate and duration are chosen in such a way that evolution to the blue is halted once stellar mass M_* is reduced to 3.89 $M_\odot$ (case $\overline{\text{A}}$) and one in which blueward evolution ceases when $M_* = 4.08$ $M_\odot$ (case $\overline{\text{B}}$). Obviously, the masses 4.08 $M_\odot$ and 3.89 $M_\odot$ (or any others) can be achieved in an infinite variety of ways. In our case $\overline{\text{A}}$ experiment, mass loss is allowed to proceed at the rate $\dot{M} = -10^{-5}$ $M_\odot$ yr^{-1} as stellar mass decreases from 4.50 $M_\odot$ to 3.89 $M_\odot$; when mass loss is terminated, and model radius is about 50 $R_\odot$, and the model continues to shrink of its own accord until its radius reaches about 15 $R_\odot$. In our case $\overline{\text{B}}$ experiment, mass loss is continued at an arbitrarily chosen, but continuously decreasing, rate until model radius again begins to increase in spite of mass loss; the turnaround occurs when model radius reaches about 70 $R_\odot$. The tendency for the model to evolve to the blue on its own accord appears to have its origin in the shrinkage in mass of the convective helium-burning core, and the turnaround occurs after convection ceases in the core and as the helium-burning shell begins to narrow.

In a real situation, the common envelope will force the binary components closer together, and the primary, whose radius will be considerably larger than the radius of its rapidly shrinking Roche lobe, will lose mass at rates much larger than those we have assumed until its mass is reduced to, say, about 5–6 $M_\odot$. Then, during the next portion of the mass-loss phase, when primary radius is very sensitive to stellar mass and mass-loss rate, conditions are not favorable for maintaining a common envelope; continued mass transfer is likely to be conservative of both system mass and orbital angular momentum. As long as mass loss continues and if the binary companion is the more massive component, the orbital sep-

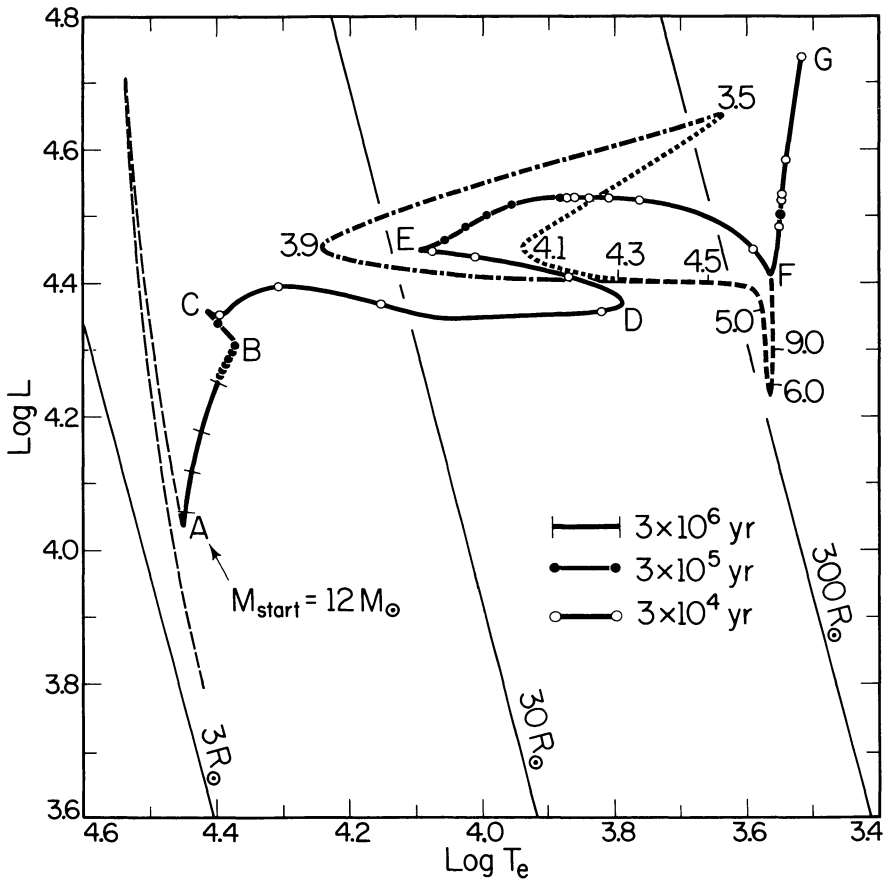

FIG. 17.—Evolution in the H-R diagram of a single star and of a binary component of initial mass 12 $M_\odot$. The main parameters of the model at labeled points (A, B, C, etc.) are given in Table 4. The initial main-sequence model has been obtained by adding 7 $M_\odot$ to a zero-age main-sequence model of mass 5 $M_\odot$ at a rate of 10^{-2} $M_\odot$ yr^{-1} (see the thin dashed curve to the left).

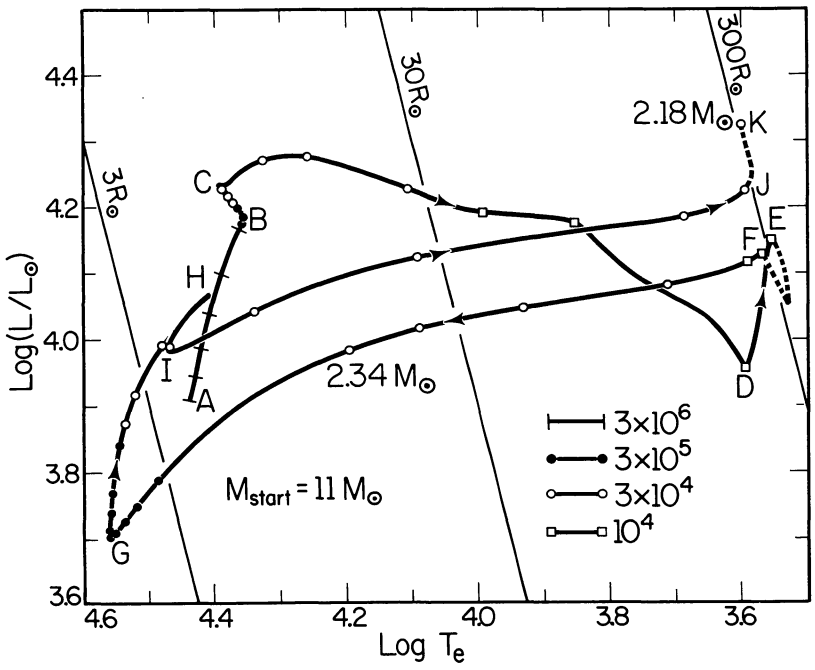

FIG. 18.—Evolution in the H-R diagram of a binary component of initial mass 11 $M_\odot$. The main parameters of the model at labeled points (A, B, C, etc.) are given in Table 5.

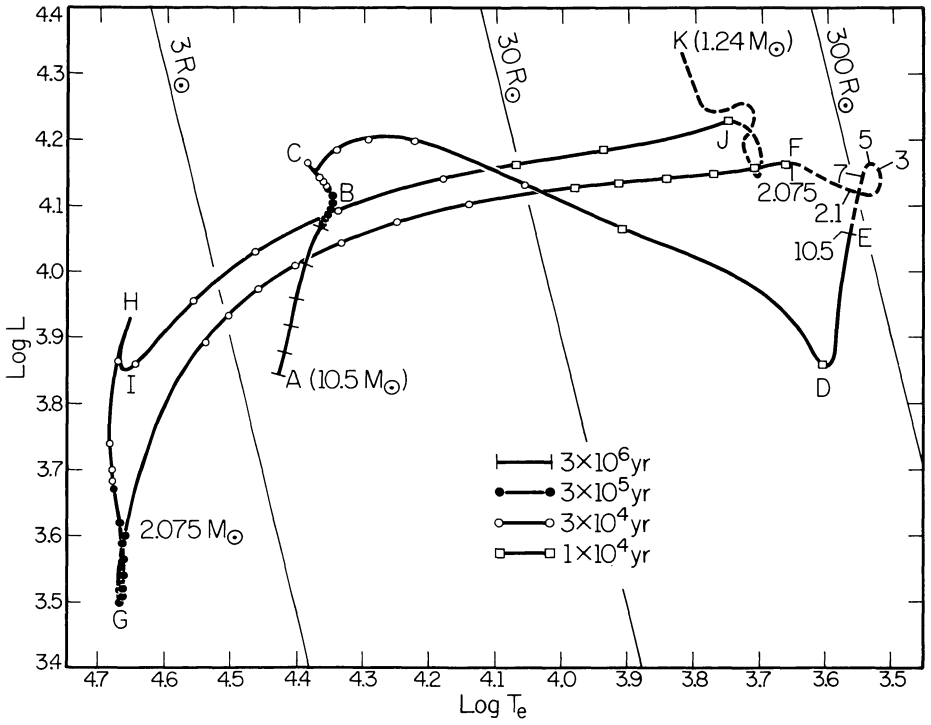

FIG. 19.—Evolution in the H-R diagram of a binary component of initial mass 10.5 $M_\odot$. The main parameters at labeled points are given in Table 6.

aration will increase, and our guess is that either temporary Roche-lobe detachment will occur (if primary mass is reduced below $\sim 3.9\ M_\odot$, case $\bar{A}$) or mass loss/transfer will become temporarily insignificant (if primary mass is reduced below $\sim 4.1\ M_\odot$, case $\bar{B}$). If the secondary is less massive than the primary, orbital separation and the radius of the primary's Roche lobe will continue to decrease, and, although mass transfer will continue uninterrupted, it will do so at a modest rate; primary mass will be reduced to something slightly less than 4 $M_\odot$ before turnaround in the H-R diagram occurs.

Mass transfer will resume or continue at an accelerated pace when the primary again expands in response to internal changes and either (as in case $\bar{A}$) once again fills its Roche lobe or (as in case $\bar{B}$) attempts to overflow at a more rapid rate the Roche lobe it already fills. In both cases $\bar{A}$ and $\bar{B}$, model radius continues to increase as long as the assumed rate of mass loss ($|\dot{M}|$) is less than $\dot{M}_{\rm crit} \sim (1\text{–}2)\times 10^{-5}\ M_\odot\ {\rm yr}^{-1}$; if it is much larger than $\dot{M}_{\rm crit}$, then model radius decreases in response to mass loss. If the secondary is more massive than the primary at this stage, then orbital radius is likely to increase and the mass-transfer rate will be determined by the condition of Roche-lobe filling, i.e., be less than or on the order of $\dot{M}_{\rm crit}$. If the accretor is less massive than the donor, then the Roche-lobe–filling condition will lead to an $|\dot{M}|$ larger than $\dot{M}_{\rm crit}$. In either case, carbon is ignited at the stellar center before model mass is reduced much below 3.5 $M_\odot$. Since subsequent nuclear-burning phases occur over a time span that is only a small fraction of the lifetime of the core helium-burning phase, the mass donor will experience a supernova instability.

We have also evolved a model of initial mass 12 $M_\odot$ which fills its Roche lobe just before the ignition of helium at the center. At this point, stellar radius is about 135 $R_\odot$. With $\dot{M} = -6\times 10^{-3}\ M_\odot\ {\rm yr}^{-1}$, stellar radius increases to a maximum of about 350 $R_\odot$, and not until stellar mass is reduced to $M_{R1} = 2.44\ M_\odot$ does the radius decrease to less than 135 $R_\odot$. The second stage of Roche-lobe overflow results in a further reduction to $M_{R2} \sim 2.42\ M_\odot$ before carbon is ignited at the stellar center.

Mass loss from the model of initial mass 11 $M_\odot$ (Figs. 18 and 21) follows algorithms similar to but slightly different from those used in exploring the evolution of the components described in § II. Roche-lobe filling is assumed to begin just after the onset of core helium burning, and the mass loss rate ($\dot{M} \sim -6\times 10^{-3}\ M_\odot\ {\rm yr}^{-1}$) has been chosen in such a way that stellar radius remains fixed at about 300 $R_\odot$. Roche-lobe detachment is assumed to occur when stellar radius decreases steadily, even for $\dot{M} = 0$. The remnant mass achieved in this way is $M_{R1} = 2.31\ M_\odot$. Core hydrogen-burning and core helium-burning lifetimes are, respectively, $t_{\rm H} \sim 1.6\times 10^7$ yr and $t_{\rm He} \sim 3\times 10^6$ yr, so that $t_{\rm He}/t_{\rm H} \sim 0.19$ is almost the same as in the case of the component of initial mass 9.85 $M_\odot$.

The second phase of Roche-lobe filling is assumed to begin when, during shell helium burning, stellar radius again reaches 300 $R_\odot$. This time, a mass-loss rate larger than $\dot{M}_{\rm crit} \approx -2.3\times 10^{-6}\ M_\odot\ {\rm yr}^{-1}$ would cause stellar radius to shrink, and, with $\dot{M} \sim \dot{M}_{\rm crit}$, only 0.13 $M_\odot$ of helium-rich matter is lost from the model before carbon is ignited off-center (see Fig. 23). Thus, the final remnant mass at carbon ignition is $M_{R2} \sim 2.18\ M_\odot$, and further evolution will result in the formation of an ONe core, core collapse caused by electron capture on ^{24}Mg and ^{23}Na, and formation of a neutron star.

Exactly the same algorithms are used in following the evolution of a component of initial mass 10.5 $M_\odot$ (see Figs. 19 and 22). This time, $M_{R1} \sim 2.08\ M_\odot$ and $M_{R2} \sim 1.2\ M_\odot$. The final remnant is considerably less massive than the Chandra-

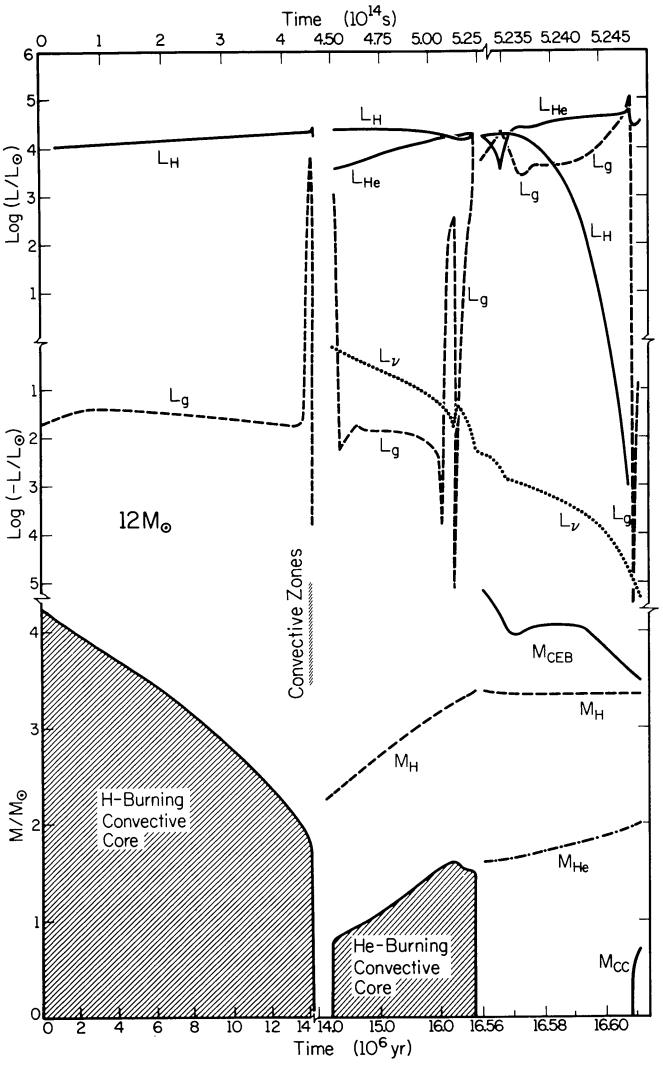

FIG. 20.—The variation with time of interior characteristics of the model of a single star of mass 12 $M_\odot$. Shown in the upper half are rates of hydrogen burning (L_H), helium burning (L_{He}), "gravitational energy" production (L_g), and neutrino loss (L_ν). In the lower half are shown masses of convective cores, total stellar mass, and the locations of the hydrogen-burning and helium-burning shells.

sekhar limit, and it will become a bare ONe degenerate dwarf. Interpolating between the results for the 11, 10.5, and 9.85 $M_\odot$ components, we guess that a model of initial mass larger than about 10.6 $M_\odot$ will go on to form a neutron star, whereas models in the mass range 10.3–10.6 $M_\odot$ will produce ONe degenerate dwarfs (see also § V).

IV. ON THE EVOLUTION OF CLOSE COMPONENTS WHICH EXPERIENCE ONLY ONE EPISODE OF ROCHE-LOBE OVERFLOW AND BECOME HELIUM-CARBON-OXYGEN DEGENERATE DWARFS

We have seen that, for initial masses in the range 5–11 $M_\odot$, the amount of mass lost by a binary component in a second phase of Roche-lobe overflow ($\Delta M_2 = M_{R1} - M_{R2}$) is a strong function of the initial mass of that component. The quantity ΔM_2 is finite but very small for initial mass as small as 5 $M_\odot$,

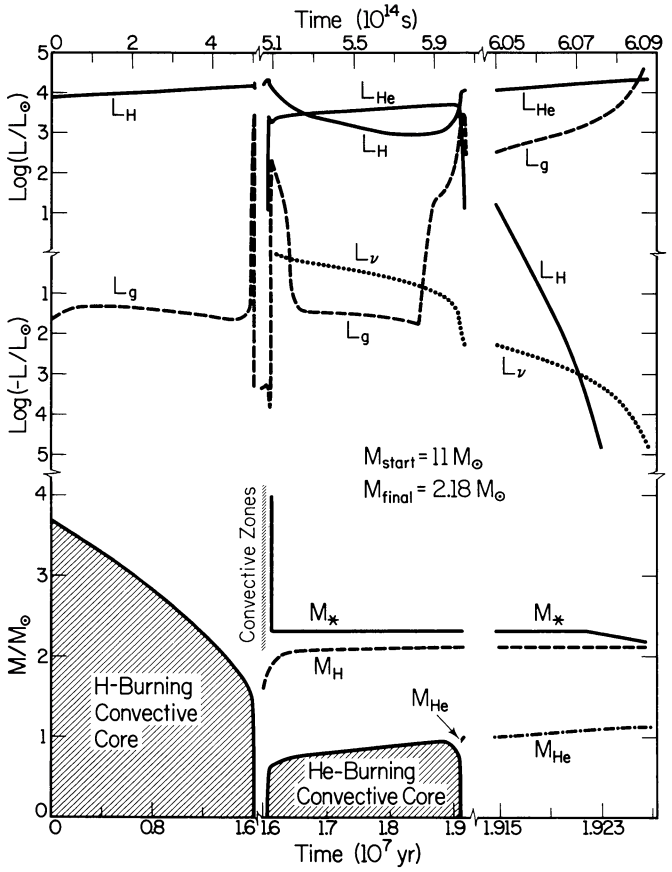

FIG. 21.—Same as Fig. 20, but for a binary component of initial mass 11 $M_\odot$.

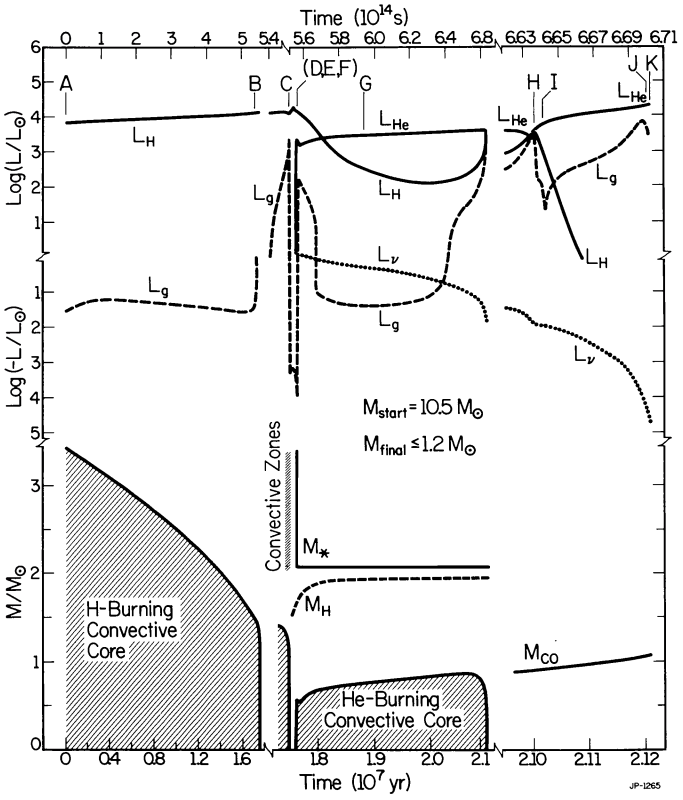

FIG. 22.—Same as Figs. 20 and 21, but for a binary component of initial mass 10.5 $M_\odot$.

TABLE 4

SOME PARAMETERS OF A MODEL OF CONSTANT MASS = 12 $M_\odot$

Stage	Age ($\times 10^{14}$ s)	log $L/L_\odot$	log $R/R_\odot$	log T_e	log T_c	log ρ_c	M_{He}
A.....	0.0	4.02	0.62	4.46	7.52	0.90	...
B.....	4.376222	4.13	0.93	4.37	7.61	1.08	1.86
C.....	4.462281	4.36	0.87	4.41	7.74	1.61	1.91
D	4.497299	4.37	2.13	3.79	8.18	3.34	2.18
E.....	4.532118	4.45	1.56	4.10	8.19	3.32	2.35
F.....	5.072288	4.41	2.61	3.56	8.32	3.39	3.21
G	5.249012	4.74	2.85	3.52	8.88	5.42	3.36

TABLE 5

SOME PARAMETERS OF A CLOSE BINARY COMPONENT WITH INITIAL MASS 11 $M_\odot$

Stage	Age ($\times 10^{14}$ s)	$M_*/M_\odot$	log $L/L_\odot$	log $R/R_\odot$	log T_e	log T_c	log ρ_c	$M_{He}/M_\odot$	$M_{CO}/M_\odot$	X	Y	X_{12} ($\times 10^{-3}$)	X_{14} ($\times 10^{-3}$)	X_{16} ($\times 10^{-3}$)
A	0.0	11.0	3.91	0.60	4.44	7.52	0.95	...	...	0.70	0.28	2.82	0.92	8.40
B	4.912258	11.0	4.18	0.90	4.36	7.60	1.10	...	...	...	...	2.82	0.92	8.40
C	5.050609	11.0	4.24	0.85	4.40	7.71	1.58	1.575	...	...	...	2.82	0.92	8.40
D ...	5.090844	11.0	3.96	2.32	3.59	8.17	3.40	1.838	...	...	...	...	...	...
E	5.093921	11.0	4.15	2.50	3.55	8.17	3.41	1.858	...	0.67	0.31	1.75	3.16	7.27
F	5.098367	2.31	4.13	2.46	3.57	8.18	3.52	1.875	...	0.56	0.42	0.74	6.79	4.55
G ...	5.580491	2.31	3.71	0.27	4.55	8.23	3.42	2.092	...	0.56	0.42	0.74	6.79	4.55
H ...	6.033501	2.31	4.07	0.74	4.41	8.44	4.08	2.125	1.017	0.56	0.42	0.74	6.79	4.55
I	6.040771	2.31	3.98	0.59	4.46	8.45	4.32	2.125	1.018	0.56	0.42	0.74	6.79	4.55
J	6.087507	2.18	4.31	2.49	3.59	8.65	6.73	2.125	1.119	0.50	0.48	0.11	9.32	2.59

TABLE 6

SOME PARAMETERS OF A CLOSE BINARY COMPONENT WITH INITIAL MASS 10.5 $M_\odot$

Stage	Age ($\times 10^{14}$ s)	$M_*/M_\odot$	log $L/L_\odot$	log $R/R_\odot$	log T_e	log T_c	log ρ_c	$M_{He}/M_\odot$	$M_{CO}/M_\odot$	X	Y	X_{12} ($\times 10^{-3}$)	X_{14} ($\times 10^{-3}$)	X_{16} ($\times 10^{-3}$)
A	0.0	10.5	3.84	0.59	4.43	7.51	0.96	...	...	0.70	0.28	2.82	0.92	8.40
B	5.372758	10.5	4.11	0.89	4.35	7.59	1.11	...	...	0.70	0.28	2.82	0.92	8.40
C	5.520028	10.5	4.17	0.83	4.39	7.71	1.56	~1.260	...	0.70	0.28	2.82	0.92	8.40
D ...	5.564288	10.5	3.85	2.25	3.60	8.17	3.51	1.662	...	0.68	0.30	2.60	1.63	7.90
E	5.564828	10.5	4.06	2.43	3.56	8.17	3.50	1.684	...	0.67	0.31	1.73	3.13	7.33
F	5.565661	2.18	4.16	2.28	3.66	8.16	3.48	1.692	...	0.48	0.50	0.12	9.81	2.03
G ...	5.941649	2.18	3.50	−0.06	4.67	8.21	3.43	1.936	...	0.48	0.50	0.12	9.81	2.03
H ...	6.636929	2.18	3.93	0.18	4.65	8.43	4.11	1.960	0.900	0.48	0.50	0.12	9.81	2.03
I	6.641856	2.18	3.85	0.13	4.66	8.43	4.24	1.964	0.904	0.48	0.50	0.12	9.81	2.03
J	6.700824	2.18	4.23	2.14	3.75	8.63	6.67	1.964	1.068	0.48	0.50	0.12	9.81	2.03
K ...	6.702026	1.24	4.36	2.05	3.83	8.59	6.82	1.239	1.073	0.00	0.98	0.309	11.2	0.11

becomes as large as 1 $M_\odot$ for initial mass in the neighborhood of 10 $M_\odot$, and then declines rapidly as initial mass rises above 10.5 $M_\odot$. In the intermediate initial mass range, the magnitude of ΔM_2 may be related to the propensity of matter in helium-rich layers to expand after the exhaustion of central helium. The sharp dropoff in ΔM_2 for initial masses larger than 10.5 M_0 is due to the ignition of carbon almost immediately after the exhaustion of central helium. In the 5 $M_\odot$ initial mass case, ΔM_2 is small because only matter in hydrogen-rich layers expands during shell helium burning and the total mass in these layers is small.

One might expect ΔM_2 simply to decrease continuously as initial mass is decreased below 5 $M_\odot$. By examining the evolution of models of initial mass 3 $M_\odot$ and 4 $M_\odot$, we find that, in fact, ΔM_2 must actually vanish at some point, simply because, below some critical initial mass, even hydrogen-rich layers do not expand following core helium exhaustion. Evolutionary tracks of the 3 $M_\odot$ and 4 $M_\odot$ models in the H-R diagram are shown in Figure 24, and the variation with time of internal characteristics is shown in Figures 25 and 26. Evolution in the ρ-T plane is given in Figure 23. Tables 7–8 given information about the models at points labeled in the figures.

In both instances, mass loss is instituted just before the onset of core helium burning and is adjusted in such a way as to maintain nearly constant stellar radius. In the 3 $M_\odot$ case, this means $\dot{M} \sim -3\times10^{-3}$ $M_\odot$ yr^{-1} at $R \sim 18$ $R_\odot$, and, in the 4 $M_\odot$ case, it means $\dot{M} \sim -4\times10^{-3}$ $M_\odot$ yr^{-1} at $R \sim 20$ $R_\odot$. Roche-lobe detachment is assumed to occur when remnant mass decreases to $M_{R1} = 0.378$ $M_\odot$ in the 3 $M_\odot$ case and to $M_{R1} = 0.523$ $M_\odot$ in the 4 $M_\odot$ case. The lifetime of the core helium-burning phase is, in both instances, in excess of the main-sequence lifetime, with τ_{He}/τ_H being 2.14 for the remnant of the 3 $M_\odot$ model and 1.08 for the remnant of the 4 $M_\odot$

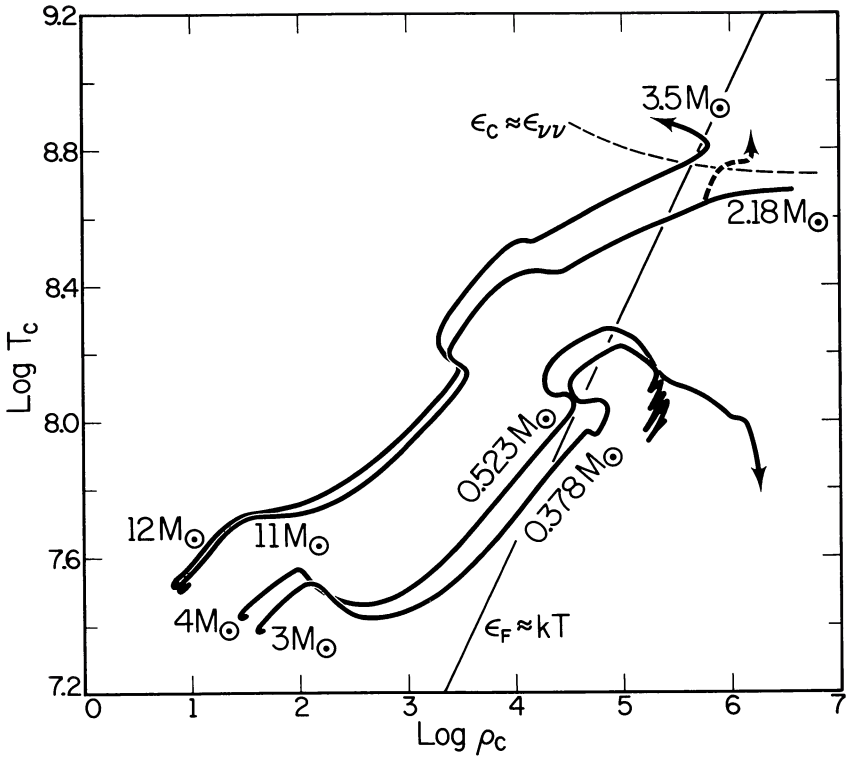

FIG. 23.—Evolution in the temperature-density plane of models of binary components of initial masses 12, 11, 4, and 3 $M_\odot$

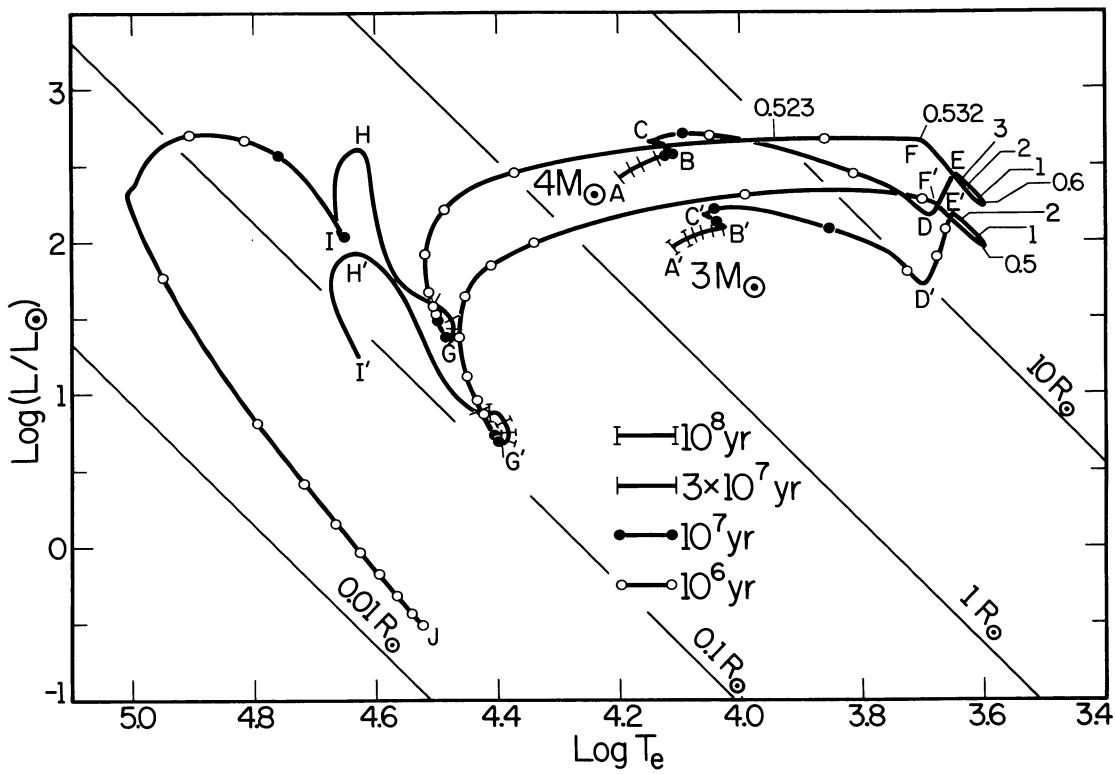

FIG. 24.—Evolution in the H-R diagram of binary components of initial mass 3 $M_\odot$ and 4 $M_\odot$. The track of the 0.378 $M_\odot$ remnant of the model of initial mass 3 $M_\odot$ is terminated at the point where oscillations begin. During the mass-loss phases, between points E and F, remnant mass in solar units is marked at several positions.

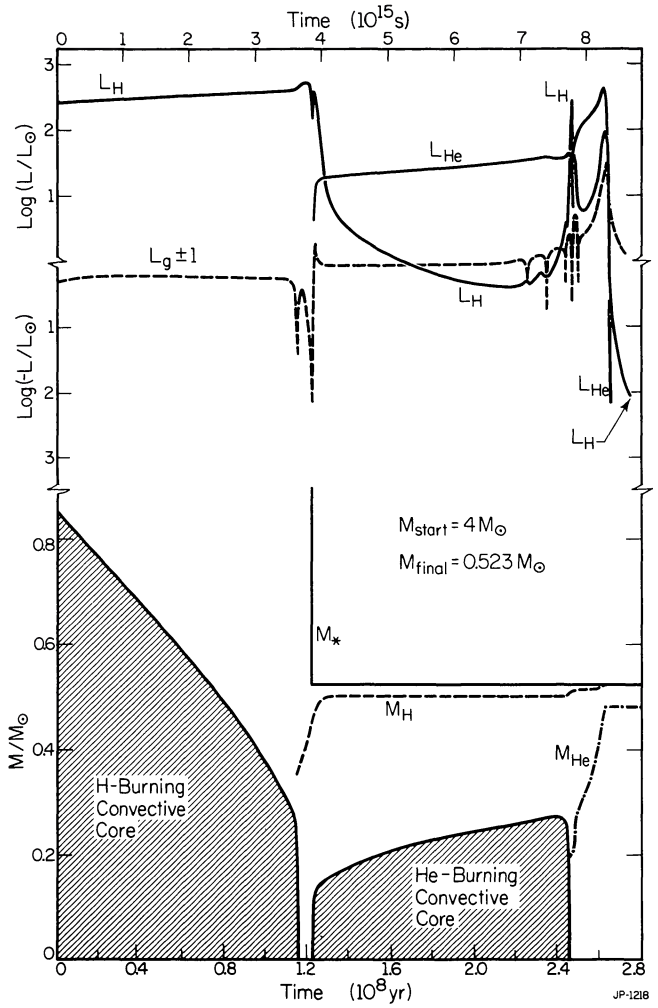

FIG. 25.—The variation with time of interior characteristics of a binary component of initial mass 4 $M_\odot$. Notation is the same as in Figs. 20–22.

model. In contrast with the behavior of remnants of models of initial mass as large as 5 $M_\odot$, the 0.378 $M_\odot$ and 0.523 $M_\odot$ remnants do not expand to giant dimensions after the exhaustion of central helium. Both remnants remain compact and continue to burn both hydrogen and helium in shells.

After several small hydrogen shell flashes and one large final flash, the total mass in the hydrogen-rich layers of the 0.523 $M_\odot$ remnant is reduced to about 10^{-5} $M_\odot$. The distribution of elements in the final model is shown in Figure 27. Note that the mass of the helium-rich layer remaining below the surface is substantially larger than in the case of the more massive remnants studied earlier. The mass below the surface at which $Y \sim 0.9$ is $\Delta M_{Y=0.9} \sim 0.033$ $M_\odot$, and the mass below the surface at which $Y = 0.1$ is $\Delta M_{Y=0.1} = 0.052$ $M_\odot$.

The evolution of the 0.378 $M_\odot$ remnant becomes quite complicated, as helium burns in a series of thermal pulses that affect the entire star. Not only do large oscillations in the H-R diagram occur (these are *not* shown in Fig. 24), but large oscillations also occur in central density and temperature (see Fig. 23). The thermal pulses are not a consequence of the accumulation of a critical mass of helium due to quiescent hydrogen burning, as in thermally pulsing AGB stars, but are an example of a true self-excited relaxation oscillation (see Iben, Fujimoto, and Sugimoto 1985, for a complete discussion). After all nuclear-burning phases are completed, the total mass of carbon and oxygen in the remnant is 0.263 $M_\odot$, the mass of the hydrogen-rich surface layer is 0.00018 $M_\odot$, and ^{4}He and ^{14}N make up the remaining 0.115 $M_\odot$. The distribution of elements in the final model is shown in Figure 28.

In real counterparts of both model stars, it is quite possible that a stellar wind will abstract much (and possibly all) of the hydrogen remaining in surface layers during shell helium burning or even after all burning has effectively ceased. For example, a mass-loss rate of only 3×10^{-12} $M_\odot$ yr^{-1} operating over the most luminous ($L_* > 100$ $L_\odot$) portion of the 0.523 $M_\odot$ track between points I and J would remove the hydrogen-rich layers from the 0.523 $M_\odot$ remnant. That this is a relatively modest wind follows from estimates of wind mass-loss rates from central stars of planetary nebulae, for which values of 10^{-8} to 10^{-7} $M_\odot$ yr^{-1} are not uncommonly found (e.g., Heap 1982, 1983; Perinotto 1983). An examination of the energetics reinforces the perception of moderateness. A lower limit to the rate at which energy must be supplied to produce a wind of velocity v and mass-loss rate $\dot{M}$ is $\dot{E}_{\rm min} = \max(v^2\dot{M}/2, v_{\rm esc}^2\dot{M}/2)$, where $v_{\rm esc}$ is the escape

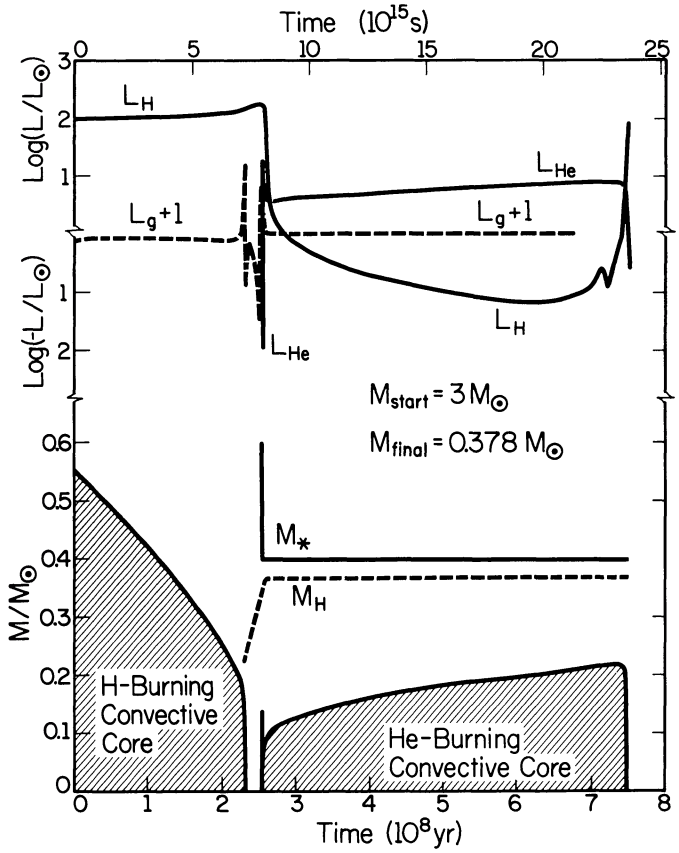

FIG. 26.—Same as Fig. 25 for a binary component of initial mass 3 $M_\odot$. Oscillatory behavior which appears after helium is exhausted at the center is not shown.

TABLE 7

SOME PARAMETERS OF A CLOSE BINARY COMPONENT WITH INITIAL MASS 3 $M_\odot$

Stage	Age (10^{13} s)	$M_*/M_\odot$	log $L/L_\odot$	log $R/R_\odot$	log T_e	log T_c	log ρ_c	M_{He}	M_{CO}	X	Y	X_{12} ($\times10^{-3}$)	X_{14} ($\times10^{-3}$)	X_{16} ($\times10^{-3}$)
A′ ...	0.0	3.0	1.96	0.27	4.11	8.39	1.65	...	...	0.70	0.28	2.84	0.92	8.40
B′ ...	7.047207	3.0	2.09	0.52	4.02	8.45	1.80	...	...	0.70	0.28	2.84	0.92	8.40
C′ ...	7.316155	3.0	2.17	0.48	4.06	8.52	2.17	0.226	...	0.70	0.28	2.84	0.92	8.40
D′ ...	7.941284	3.0	1.72	0.98	3.70	8.82	4.26	0.324	...	0.70	0.28	2.84	0.92	8.40
E′ ...	8.015462	3.0	2.17	1.31	3.65	8.94	4.67	0.338	...	0.69	0.29	1.74	2.31	8.35
F′ ...	8.035903	0.39	2.22	1.29	3.67	8.97	4.80	0.344	...	0.37	0.62	0.07	10.8	1.00
G′ ...	9.937170	0.38	0.65	−0.93	4.39	8.05	4.58	0.365	...	0.37	0.62	0.07	10.8	1.00
H′ ...	23.696696	0.38	1.93	−0.77	4.63	8.22	5.16	0.372	0.144	0.37	0.62	0.07	10.8	1.00
I″ ...	23.93822	0.38	1.10	−1.09	4.58	8.01	5.36	0.374	0.173	0.37	0.62	0.07	10.8	1.00

TABLE 8

SOME PARAMETERS OF A CLOSE BINARY COMPONENT WITH INITIAL MASS 4 $M_\odot$

Stage	Age (10^{13} s)	$M_*/M_\odot$	log $L/L_\odot$	log $R/R_\odot$	log T_e	log T_c	log ρ_c	M_{He}	M_{CO}	X	Y	X_{12} ($\times10^{-3}$)	X_{14} ($\times10^{-3}$)	X_{16} ($\times10^{-3}$)
A	0.0	4.0	2.51	0.39	4.20	7.40	1.49	...	...	0.70	0.28	2.84	0.92	8.40
B	3.556887	4.0	2.59	0.60	4.11	7.49	1.66	...	...	0.70	0.28	2.84	0.92	8.40
C	3.646515	4.0	2.65	0.56	4.14	7.55	2.05	0.330	...	0.70	0.28	2.84	0.92	8.40
D ...	3.862158	4.0	2.16	1.23	3.69	7.90	2.16	0.445	...	0.70	0.28	2.84	0.92	8.40
E	3.867218	4.0	2.40	1.43	3.65	7.94	4.27	0.446	...	0.70	0.28	2.84	0.92	8.40
F	3.877437	0.53	2.54	1.51	3.64	8.00	4.45	0.458	...	0.29	0.70	0.07	11.2	0.55
G ...	4.290993	0.52	1.39	−0.75	4.48	8.08	4.29	0.500	...	0.29	0.70	0.07	11.2	0.55
H ...	7.784543	0.52	2.60	−0.43	4.63	8.27	4.97	0.509	0.186	0.29	0.70	0.07	11.2	0.55
I	7.814677	0.52	1.96	−0.79	4.65	8.19	5.12	0.512	0.204	0.29	0.70	0.07	11.2	0.55
J	8.576363	0.52	0.55	−1.77	4.51	7.73	6.28	0.523	0.477	0.29	0.70	0.07	11.2	0.55

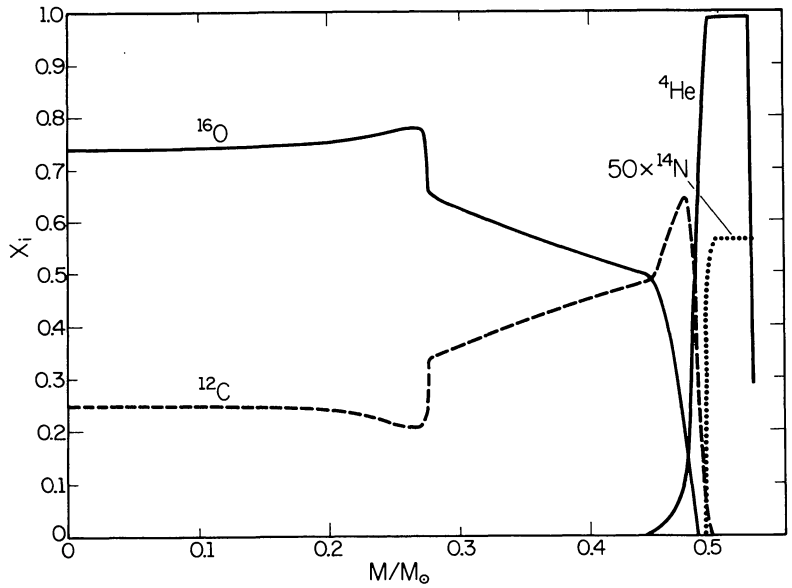

FIG. 27.—Abundances by mass of ^{4}He, ^{12}C, ^{14}N, and ^{16}O as a function of mass within the 0.523 $M_\odot$ remnant of the model of initial mass 4 $M_\odot$. The mass of the surface layer containing hydrogen is about 2.6×10^{-4}, and the average abundance of hydrogen in this layer is $\bar{X}_H \sim 0.291$. Further, $\bar{X}_4 \sim 0.70$, $\bar{X}_{12} \sim 6.9\times10^{-5}$, $\bar{X}_{14} \sim 1.12\times10^{-2}$, and $\bar{X}_{16} \sim 5.5\times10^{-4}$.

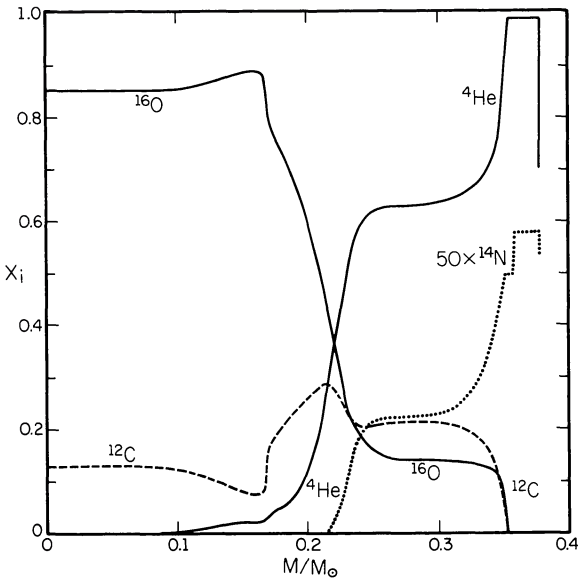

FIG. 28.—Abundances by mass of ^{4}He, ^{12}C, ^{14}N, and ^{16}O as a function of mass within the 0.378 remnant of the model of initial mass 3 $M_\odot$. Hydrogen occurs in a thin surface layer of mass about 8.5×10^{-4} $M_\odot$ at an abundance by mass of $\bar{X}_H \sim 0.2$. In this layer, $\bar{X}_4 \sim 0.78$, $\bar{X}_{12} \sim 4\times10^{-4}$, $\bar{X}_{14} \sim 1.06\times10^{-2}$, and $\bar{X}_{16} \sim 6\times10^{-4}$.

velocity at the surface of the star. We have

$$\dot{E}_{\rm min} \approx 0.82\times10^{-3}\, L_\odot \left(\dot{M}/10^{-11}\, M_\odot\ {\rm yr}^{-1}\right) \times\left\{\max\left[\left(v/10^3\ {\rm km\ s^{-1}}\right)^2, 0.38 M_*/R_*\right]\right\}, \quad (11)$$

where M_* and R_* are the mass and radius of the star in solar units. Between points I and J along the track of the 0.523 $M_\odot$ remnant in Figure 24, $R_* > 0.03$. Hence, for $\dot{M} \sim 3\times10^{-12}$ $M_\odot$ yr^{-1} and $v < 6000$ km s^{-1}, $\dot{E}_{\rm min} < 10^{-2}$ $L_\odot$, and, for the 2.3×10^7 yr that the star is more luminous than 10^2 $L_\odot$ following point I, $\dot{E}_{\rm min}/L_* < 10^{-4}$. Under the same conditions, the momentum density of the wind relative to the momentum density in the radiation field surrounding the star is less than 10^{-2}. Whether this ratio is considered to be an indicator of a "strong" or of a "weak" wind is, to some extent, a matter of taste. Judging from those ratios characterizing winds from planetary nebula nuclei, the wind required to strip all of the hydrogen from the 0.523 $M_\odot$ remnant would seem to be a relatively weak one.

It has come as something of a surprise to us that a remnant of mass as small as 0.4 $M_\odot$ can convert 70% of its initial helium into carbon and oxygen. The surprise stems from the fact that a single low-mass star does not ignite and burn helium until the mass of its electron-degenerate core reaches about 0.5 $M_\odot$. The answer to the apparent conundrum is very simply that, in the 0.4 $M_\odot$ remnant of a model which, as a single star, would not experience a helium core flash, helium is ignited under relatively nondegenerate conditions.

In an earlier communication (Iben and Tutukov 1984*b*), we assumed that all remnants less massive than 0.5 $M_\odot$ would become nearly pure helium degenerate dwarfs and derived a Galactic frequency of about 0.005 yr^{-1} for the rate at which double degenerates composed of helium and of total mass larger than 0.65 $M_\odot$ would merge to possibly produce type I supernovae; the primordial masses of potentially explosive systems ranged from 3.2 $M_\odot$ to 3.8 $M_\odot$. Our current finding that a 3 $M_\odot$ progenitor produces a degenerate remnant containing only 0.115 $M_\odot$ of helium demonstrates that our earlier estimates are erroneous. The composition of remnants changes rapidly as progenitor mass decreases from 4 $M_\odot$ to 3 $M_\odot$, and it will be interesting to see if any remnant deriving from progenitors in the mass range 2.3–3.0 $M_\odot$ is composed only of helium.

It is also important to determine the sensitivity of the final remnant mass to the point in the evolutionary track when Roche-lobe filling is assumed to first occur. A comparison of our results for a 4 $M_\odot$ progenitor with those obtained by Harmanec (1970) suggests that the sensitivity is minimal. Assuming the conservation of total system mass and angular momentum, Harmanec follows the evolution of systems consisting initially of two main-sequence stars, one of mass 4 $M_\odot$ and the other of mass 3.2 $M_\odot$ or of mass 1.6 $M_\odot$. Initial separations are chosen in such a way that the primary fills its Roche lobe just after leaving the main sequence. In both instances, the 4 $M_\odot$ progenitor leaves a remnant of mass 0.52 $M_\odot$. We find exactly the same remnant mass, even though Roche-lobe filling does not occur until the primary becomes a giant. We note that, in the Harmanec systems, once the secondary becomes more massive than the primary, the orbital separation increases and the Roche lobe of the primary increases as mass transfer continues. In order to fill its Roche lobe and drive this continued mass transfer, the primary must develop a larger and larger hydrogen-exhausted core. The primary swells to become a giant and does not detach from its Roche lobe until helium is ignited at the center. We infer that the basic reason for the detachment is the same as in our experiments: the mass of the hydrogen-rich surface layers decreases below some critical value. Since initial masses are the same, since initial compositions are essentially the same, and since final detachment occurs during the giant phase (despite the widely divergent assumptions regarding the fate of system mass and angular momentum), it is understandable that remnant masses turn out to be the same. It will be important to determine for other primary masses as well whether or not remnant mass resulting from "case B" Roche-lobe overflow is independent of where Roche-lobe filling first begins. In closing this section, we note that the core helium-burning lifetimes of the lowest-mass remnants considered here are several times larger than given by equation (8). A better approximation for these remnant masses is

$$\tau_{\rm He} = 5.0\times10^{10}\, M_{\rm MS}^{-4.3}\ {\rm yr}. \quad (12)$$

V. FINAL REMNANT MASSES

We are now in a position to estimate the ranges in the main-sequence masses of binary components that can potentially become bare degenerate dwarfs composed primarily of He, of C and O, or of O and Ne. The analysis is summarized in Figures 29 and 30. The curve $M_H(R1)$ in Figure 29 gives the mass at the center of the hydrogen-burning shell when a model first achieves (or is about to achieve) giant dimensions

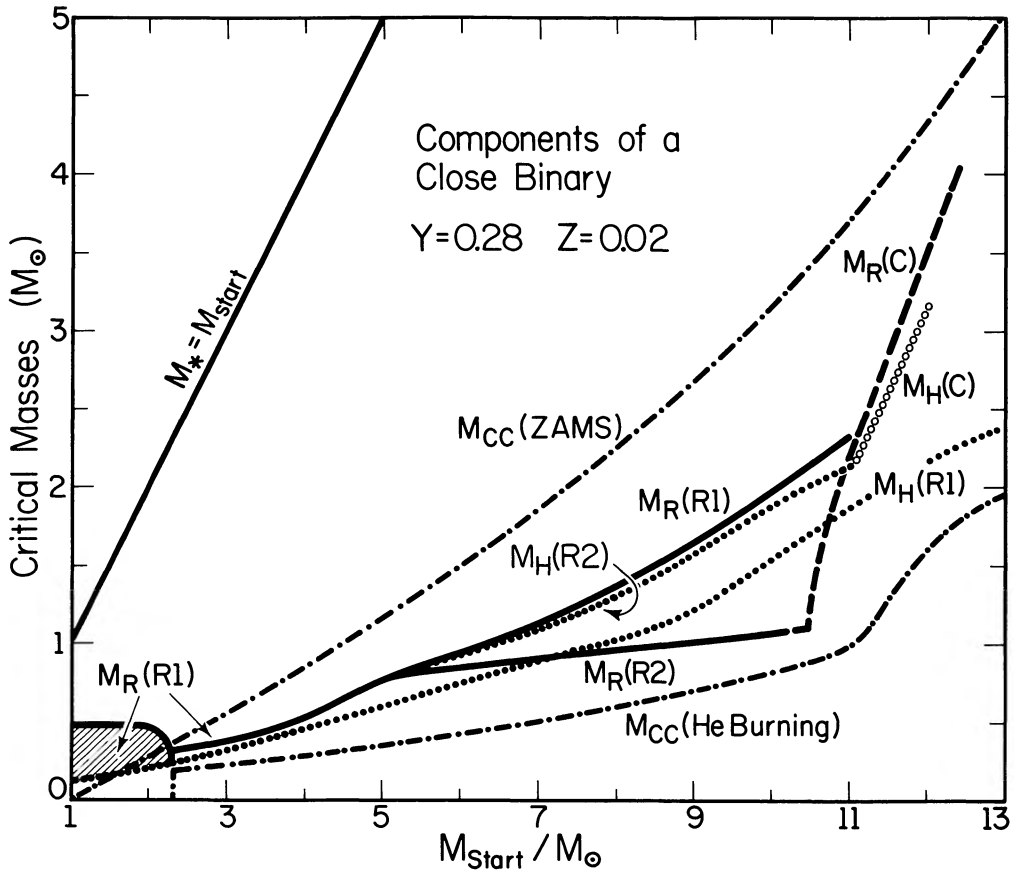

FIG. 29.—Critical masses as a function of initial stellar mass: M_{cc}(ZAMS) = maximum mass in the hydrogen-burning convective core during the main-sequence phase; $M_H(R1)$ = mass at the center of the hydrogen-burning shell (HBS) at the start of the first mass-loss phase; $M_H(R2)$ = mass at the center of the HBS at the start of the second mass-loss phase; M_H(C) = mass at the HBS when carbon burning begins; M_R(R) = remnant mass after the first mass-loss event; and $M_R(R2)$ = remnant mass after the second mass-loss event.

and, we assume, begins to lose mass by Roche-lobe overflow. The curve $M_R(R1)$ gives the model mass at the end of the first Roche-lobe–filling stage, as obtained in our experiments. The relationship between $M_R(R1)$ and M_{MS} is given in good approximation by

$$M_R(R1) \approx 0.08 M_{MS}^{1.4}. \quad (13)$$

Since we have adopted somewhat arbitrary criteria for beginning and ending mass loss, the curve for $M_R(R1)$ should actually be a band, the lower limit of which corresponds to the situation when Roche-lobe overflow begins immediately after a model leaves the main sequence and continues until very little mass is left above the hydrogen-burning shell. Since the center of the hydrogen-burning shell moves outward in mass very rapidly as a model moves toward the giant branch, the lower limit corresponds to a position somewhere between the curves for $M_H(R1)$ and $M_R(R1)$. The upper limit should not be too different from the curve $M_R(R1)$ which our experiments define, provided Roche-lobe overflow begins when stellar radius is smaller than the maximum achieved by the single-star counterpart at the onset of core helium burning. The comparison given in the previous section between our results and those of Harmanec for a 4 $M_\odot$ primary suggests that the lower limit is also very close to $M_R(R1)$.

The curve $M_H(R2)$ in Figure 29 gives the mass at the center of the hydrogen-burning shell when the second phase of mass loss begins (defined as occurring after the exhaustion of central helium and during shell helium burning), and the curve $M_R(R2)$ gives the remnant mass at the termination of this phase, as defined by our experiments. Again, the curve $M_R(R2)$ should really be a band, whose upper limit is given by our experiments. For initial masses between about 7 $M_\odot$ and 10.3 $M_\odot$ the band is quite narrow, since the values of $M_R(R2)$ which we find are smaller than $M_H(R1)$ for initial masses in this range. The maximum value of $M_R(R2)$ is 1.08 $M_\odot$ and occurs for an initial mass of about 10.3 $M_\odot$. For initial masses in the range 2.3–7 $M_\odot$, the lower limit to the band of final CO degenerate remnants lies between the curves $M_R(R2)$ and $M_H(R1)$. Although a proper definition of this lower limit requires detailed calculations, we anticipate that it lies much closer to the curve $M_R(R2)$ than to $M_H(R1)$. The expectation relies on the fact that a rapid mass-loss rate during the first phase of Roche-lobe overflow can be maintained only if the mass in hydrogen-rich layers is large enough that these layers attempt to expand in response to the growth in mass of the helium core. The solid curve in Figure 30 between initial masses of 2.3 $M_\odot$ and 10.3 $M_\odot$ is therefore our best estimate of typical masses of CO degenerate dwarfs produced by components of close binaries.

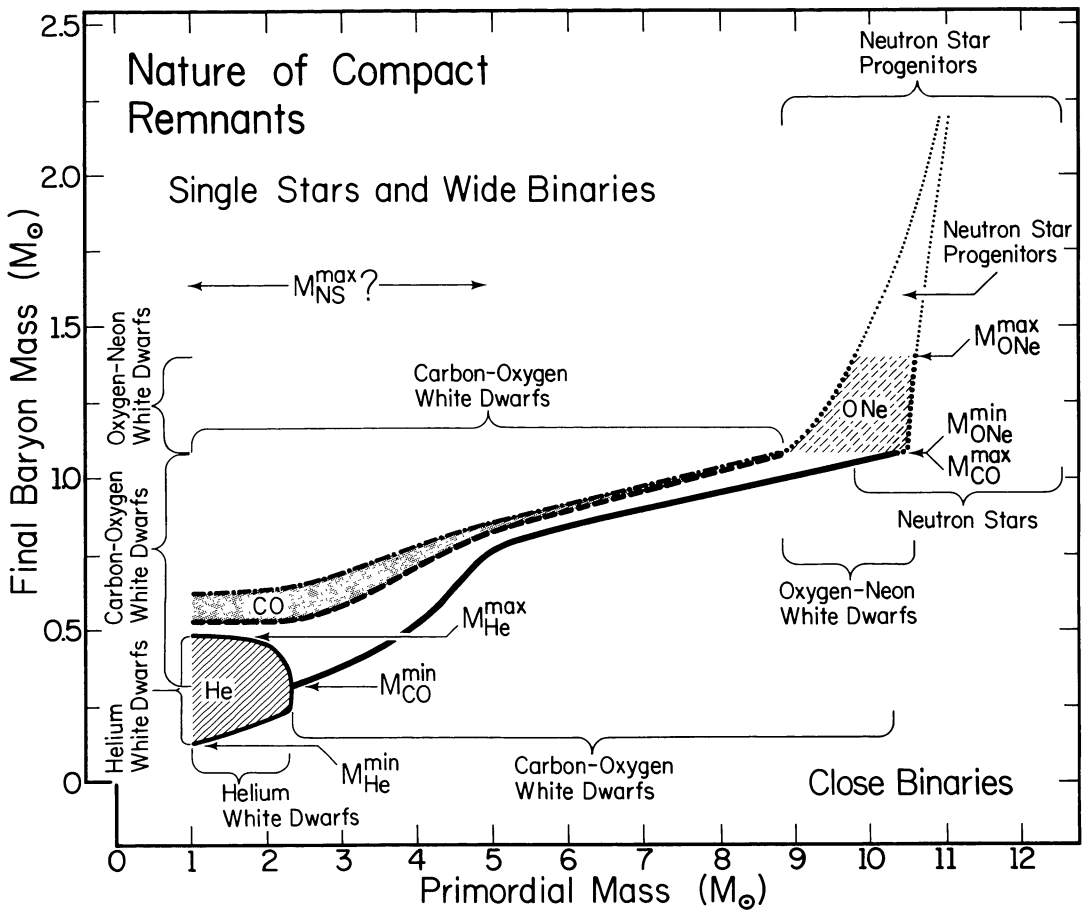

FIG. 30.—The masses and compositions of degenerate dwarfs formed by single stars and by components of interacting binaries. The solid curve extending from 2.3 $M_\odot$ to 10.3 $M_\odot$ is the upper bound on the masses of CO degenerate dwarfs formed in close binaries (first Roche-lobe overflow just before or just after the ignition of central helium). The lower solid curve extending from 1 $M_\odot$ to 2.3 $M_\odot$ is the lower bound on masses of helium degenerate dwarfs formed by stars in close binaries which experience Roche-lobe overflow immediately after forming an electron-degenerate core composed of helium. The upper solid curve extending from 1 $M_\odot$ to 2.3 $M_\odot$ is the upper bound on masses of helium degenerate dwarfs formed in close binaries. The unshaded region gives the possible range in masses of CO degenerate dwarfs formed in wide binaries by components which experience Roche-lobe overflow for the first time during the early AGB phase. The shaded region between the dash and dash-dot curves gives the range in masses of CO degenerate dwarfs formed in wide binaries by components that first experience Roche-lobe overflow during the thermally pulsing AGB (TP-AGB) phase. The dash-dot curve is an estimate of the masses of CO degenerate dwarfs formed by single stars in consequence of mass loss during the TP-AGB phase. Single stars and components of wide binaries cannot form helium degenerate dwarfs or oxygen-neon degenerate dwarfs. In close binaries of appropriate initial configuration, components of initial mass in the range 8.8–10.6 $M_\odot$ may form ONe degenerate dwarfs, with a preponderance being formed by components of initial mass in the range 10.3–10.6 $M_\odot$.

Components initially less massive than about 2.3 $M_\odot$ develop an electron degenerate core after exhausting central hydrogen and depart from the main sequence in an attempt to become red giants when the mass of this core exceeds some fraction of the total stellar mass. This fraction is known as the Schönberg-Chandrasekhar (1942) limit. For the composition we have chosen, the critical core mass varies from about 0.13 $M_\odot$ when total mass is 1 $M_\odot$ to about 0.23 $M_\odot$ when total mass is 2.3 $M_\odot$. The lower solid curve bordering the hatched region in Figure 30 gives the critical core mass necessary for expansion away from the main sequence. The upper solid curve bordering the hatched region gives the mass of the helium core within a single star when helium is ignited in this core to terminate further expansion. Since the radius of a single star increases as its core mass increases, and since the initial orbital separations of components in real binary systems can vary from a few solar radii to many astronomical units, there will be systems in which a component first fills its Roche lobe when its core mass lies at any given point within the hatched region and produces a degenerate helium dwarf whose mass is nearly equal to the mass at this given point.

The situation with regard to degenerate dwarf formation near the upper end of the initial mass spectrum requires much additional work to define satisfactorily. At this point we can say with some assurance only that, for the composition chosen, close binary components of initial mass larger than 11 $M_\odot$ cannot produce degenerate dwarfs, and that components less massive than 8.8 $M_\odot$ will produce CO degenerate dwarfs. This latter statement follows from the following facts: (1) even a single model star less massive than 8.8 $M_\odot$ will produce an

electron-degenerate CO core of initial mass less than 1.08 $M_\odot$, and (2) real single stars that develop CO cores larger than about 0.85 $M_\odot$ lose their hydrogen-rich envelopes via a "superwind" on a time scale short compared with the time scale for core growth (see, e.g., Iben 1984*b*, 1985*a*, for discussion and references).

What happens for initial masses in the range 8.8–11 $M_\odot$ is highly sensitive to the primordial binary characteristics, even if we were to understand quantitatively the physics of mass transfer. We therefore content ourselves with the construction of a speculative band (the two dotted curves in Fig. 30). The points on the band given by $M_R(R2) \sim 1.08\ M_\odot$ at $M_{\rm start} = 8.8\ M_\odot$ and $M_{\rm start} \approx 10.3\ M_\odot$ and the points given by our experiments with the models of initial mass 10.5 $M_\odot$ and 11 $M_\odot$ are reasonably well defined. Recognizing the dangers of interpolating between these points, we may still make reasonable qualitative inferences. For example, there is an overlap in initial masses such that the mass-losing star may wind up as either a CO degenerate dwarf or an ONe degenerate dwarf. Those stars which ignite carbon with $M_R(R2)$ in the range 1.08–1.4 $M_\odot$ will become ONe white dwarfs, and those with $M_R(R2) \lesssim 1.08\ M_\odot$ will become CO degenerate dwarfs. The upper limit on initial mass for stars which can produce a CO degenerate dwarf is about 10.3 $M_\odot$. For our specific guess at band boundaries, potential progenitors of ONe white dwarfs have initial masses in the range 8.8–10.6 $M_\odot$, with only a narrow range of initial masses 10.3–10.6 $M_\odot$ established as likely progenitors. Remnants more massive than 1.4 $M_\odot$ will presumably go on to become supernovae.

Up to this point we have focused on binary components which fill their Roche lobes for the first time just before or just after helium ignites in the core. It is worthwhile to compare masses and composition types of degenerate dwarfs formed in this way with masses and types formed by single stars and components of wider binaries in which Roche-lobe overflow does not occur for the first time until after the development of an electron-degenerate CO core.

The dashed curve that forms the lower boundary of the shaded region in Figure 30 defines the mass of the CO core that a single star developes as it enters the thermally pulsing AGB (TP–AGB) phase (see, e.g., Becker and Iben 1979, 1980; Iben 1982), and the dash-dot curve that forms the upper boundary of the shaded region is an estimate of the final stellar mass when the AGB phase is terminated. For initial masses less than about 4 $M_\odot$ and corresponding minimum CO core masses on the TP–AGB of about 0.7 $M_\odot$, the lifetime in the TP–AGB phase is assumed to be on the order of 10^6 yr; for initial masses between 5 $M_\odot$ and 8.8 $M_\odot$ and corresponding CO core masses larger than about 0.8 $M_\odot$, the lifetime in the TP–AGB phase is assumed to be on the order of only 10^5 yr. Thus, during the TP–AGB phase, CO core mass grows by something on the order of 0.1 $M_\odot$ in low-mass progenitors, but only by something on the order of 0.01 $M_\odot$ in higher-mass progenitors. These estimates are based on the distributions of AGB stars in fields and clusters in the Magellanic Clouds (see, e.g., Frogel and Blanco 1984; Aaronson and Mould 1985; Iben 1984*b*). We see that the only type of degenerate dwarf which a single star (of mass large enough to complete all nuclear burning in a Hubble time) can produce is composed of carbon and oxygen, and the mass of this degenerate dwarf increases monotonically with progenitor mass from about 0.55 $M_\odot$ to about 1.1 $M_\odot$.

We may use the results of single star evolution to estimate the masses of degenerate dwarfs formed by components of wide binaries defined as those in which the first phase of Roche-lobe overflow does not occur until after helium is exhausted in the core. If a component does not fill its Roche lobe until it has entered the TP–AGB phase, then this component will produce a CO degenerate dwarf whose mass lies within the shaded region in Figure 30 defined by single stars. Almost all of the hydrogen-rich matter in a TP–AGB star lies within a deep convective envelope. Further, during a thermal pulse, stellar radius increases by typically 30% over that obtaining during the quiescent hydrogen-burning phase between pulses. Therefore, when the Roche lobe is filled for the first time during the peak of a thermal pulse, mass loss will occur on a nearly dynamical time scale and a common envelope will be formed. Drag forces will bring the components closer together, accelerating the rate of mass loss, and one may expect that all of the mass outside the CO core will be lost in the course of a single pulse, or at least in a very few pulses. Thus, the mass of the CO degenerate remnant produced in a wide binary by a component which fills its Roche lobe for the first time during the TP–AGB phase will be almost exactly the mass of the CO core when Roche-lobe filling begins.

Components that fill their Roche lobes for the first time during the early AGB (E–AGB) phase (the star contains an electron-degenerate CO core which grows in mass in consequence of shell helium burning, hydrogen does not burn, and stellar radius increases with increasing CO core mass) will produce a CO degenerate dwarf whose mass might be expected to lie in the unshaded region in Figure 30 between the solid and dashed curves at a point which should depend on the initial binary configuration. However, Lauterborn (1970) shows that, in the approximation which conserves system mass and angular momentum in the mass loss/transfer process, the mass of the final remnant of a 5 $M_\odot$ primary undergoing case C mass transfer will be at least as large as the minimum mass of the CO core of a TP–AGB model of a single star of the same initial mass. Calculation of case C mass loss based on algorithms similar to those used in this paper (Iben 1985*a*) show that this is actually a general result: the final remnant mass may be as large as or somewhat larger than the minimum CO core mass achieved by single stars at the beginning of the TP–AGB phase, and this final mass is not terribly sensitive to initial orbital conditions. Thus, for any given initial primary mass, the mass of the remnant produced as a result of case C mass loss is distinctly larger than the mass produced by case B mass loss.

One final possible channel for producing degenerate dwarfs involves mass transfer during the main-sequence phase (Paczyński 1966; Kippenhahn and Weigert 1967; Plavec, Kriz, and Horn 1969). The mass of the primary is reduced to from about one-half to one-fifth of its primordial value, the precise value being a function of the initial conditions which determine the abundance of hydrogen at the center of the primary when Roche-lobe contact is first established. The

reduction in mass of the primary leads to a corresponding reduction in interior temperatures and to a strong decrease in the rate of evolution (and consequently) of mass transfer. The reversal of mass ratio between the primary and secondary leads to an increase in orbital separation, and the secondary can evolve completely through the main-sequence phase before filling its Roche lobe. When it does fill its Roche lobe, an early "case B" mass loss/transfer event takes place, and the end result may be either a He, a HeCO, or a CO degenerate dwarf. Since only very few real systems are expected to be formed with small enough separations (Kraicheva *et al.* 1978) for this scenario to be played out, we have chosen not to consider further its contribution to the pool of degenerate dwarfs.

An important motivation for pursuing the calculations reported in this paper has been the hope of contributing to an understanding of the precursors of Type I supernovae, especially with regard to their formation frequency. In several earlier papers (Iben and Tutukov 1984*a*, *b*, 1985), we have been led to conclude that the most likely Type I supernova scenario is one which leads to a system of two CO degenerate dwarfs which have a combined mass larger than 1.4 $M_\odot$ and which can be brought into Roche-lobe contact by the emission of gravitational-wave radiation in less than a Hubble time. An additional motivation has been to contribute to an estimation of the formation frequency of helium degenerate dwarfs relative to the formation frequency of CO degenerate dwarfs, a ratio which may have bearing on the number versus age distribution of degenerate dwarfs in the solar vicinity (Iben and Tutukov 1984*c*). Finally, we have wished to discover more precisely the nature of progenitor systems which may lead to the formation of ONe degenerate dwarfs, both as the most massive of accretors in cataclysmic systems and as precursors of electron-capture supernovae in close double degenerate systems.

We suppose that, in zeroth approximation, the formation frequency of binaries of various types is given by the expression (Iben and Tutukov 1984*a*, *b*)

$$dN(\mathrm{yr}^{-1}) = 0.2\frac{dM}{M^{2.5}}d\log A, \qquad (14)$$

where dN is the rate of formation of stars with M and A (both in solar units) in the intervals of dM and dA. When integrated over all stars of sufficient mass to evolve to the degenerate dwarf state or to the neutron star state in less than a Hubble time, equation (14) implies a binary formation rate in our Galaxy of $\nu_{\mathrm{binary}} \sim 0.67\ \mathrm{yr}^{-1}$. Since our aim is to estimate only the relative formation frequency of degenerate dwarfs of various types, we do not attempt to justify this as an absolute rate. Further, and as a step toward completeness, we suppose that the frequency with which single stars are formed is roughly one-half of the rate at which binaries (defined as systems with an initial orbital separation less than about 10^6 $R_\odot$) are formed, so that $\nu_{\mathrm{single}} \sim 0.33\ \mathrm{yr}^{-1}$.

In order to employ equation (14) further, we require not only some idea of the mass ranges which lead to the various possible final states but also some idea of the appropriate ranges in primordial orbital separations. We shall assume here that appropriate Roche-lobe radii, stellar radii, and primordial separations are related simply by $R_{\mathrm{Roche}} \sim R_{\mathrm{star}} \sim A/2$. Radii of single stars during various phases of evolution are sketched in Figure 31 as a function of initial stellar mass. We first address single stars and wide binaries in which Roche-lobe contact is not made until a component enters the TP–AGB phase. To first order, stellar radius at the beginning of the TP–AGB phase varies from about 100 $R_\odot$ to about 700 $R_\odot$ as initial stellar mass varies from 1 $M_\odot$ to 8.8 $M_\odot$. The appropriate "phase space" for stars in binaries that establish Roche-lobe contact during the TP–AGB phase is given by the region between the curves labeled "start" and "end" of TP–AGB phase. Using this phase space, we estimate from equation (14) that the frequency with which CO degenerate dwarfs are produced in wide binaries in which Roche-lobe contact is made during the TP–AGB phase is $\nu_{\mathrm{CO}}^{\mathrm{TP}} \sim 0.04\ \mathrm{yr}^{-1}$. In a similar fashion, we have that the frequency with which CO degenerate dwarfs are produced in wide binaries which do not establish contact plus the frequency with which single stars produce CO degenerate dwarfs is $\nu_{\mathrm{CO}}^{\mathrm{wide+single}} \sim 0.2\times 3.2/1.5+0.33 \sim 0.74\ \mathrm{yr}^{-1}$. Note that we count a degenerate pair as a single degenerate dwarf, recognizing the (factor of 2) logical inconsistency, but relying on the well-known selection effect against detecting close double degenerates of disparate masses and cooling ages.

The stellar radius at central helium ignition (see the curve in Fig. 31 labeled "End of First Red Giant Branch Phase") varies from about 12 $R_\odot$ to about 200 $R_\odot$ as initial stellar mass increases from 2.3 $M_\odot$ to 8.8 $M_\odot$. Using the phase space defined by the region between the curves "End of First Red Giant Branch Phase" and "Start of TP–AGB Phase," we estimate that the formation frequency of CO degenerate dwarfs in binary systems in which Roche-lobe contact is first established during the E–AGB phase is about $\nu_{\mathrm{CO}}^{\mathrm{E}} \sim 0.013\ \mathrm{yr}^{-1}$.

At the end of the main-sequence phase, stellar radius varies from about 3 $R_\odot$ to about 8 $R_\odot$ as initial mass varies from 2.3 $M_\odot$ to 10.3 $M_\odot$, and, using the phase space defined by the region between the curves "End of Main Sequence Phase" and "End of First Red Giant Branch Phase," we have that the frequency with which helium stars and therefrom CO or HeCO degenerate dwarfs are formed in binaries is about $\nu_{\mathrm{CO}}^{\mathrm{He}\rightarrow\mathrm{CO}} \sim 0.035\ \mathrm{yr}^{-1}$.

Assuming that stellar radius is about 200 $R_\odot$ for all stars that develop electron-degenerate helium cores and ultimately experience a core helium flash (if permitted), we have

$$\nu_{\mathrm{He}} \sim 0.2\times 1.8\int_1^{2.3} dM/M^{2.5} \sim 0.17\ \mathrm{yr}^{-1}.$$

We note that, contrary to the assertion in Iben and Tutukov (1984*a*, *b*), binary components of main-sequence mass in the 2.3–3.8 $M_\odot$ range do not produce pure helium degenerate dwarfs. Had we assumed that they did, ν_{He} would be larger than our current estimate by about 0.02 yr^{-1}.

The best we can do at this stage for ONe degenerate dwarfs is to suggest limits on formation frequency. Our experiments suggest that stars of primordial mass between 10.3 $M_\odot$ and 10.6 $M_\odot$ will not become CO degenerate dwarfs under any circumstances, but that, in binaries, they have a good chance

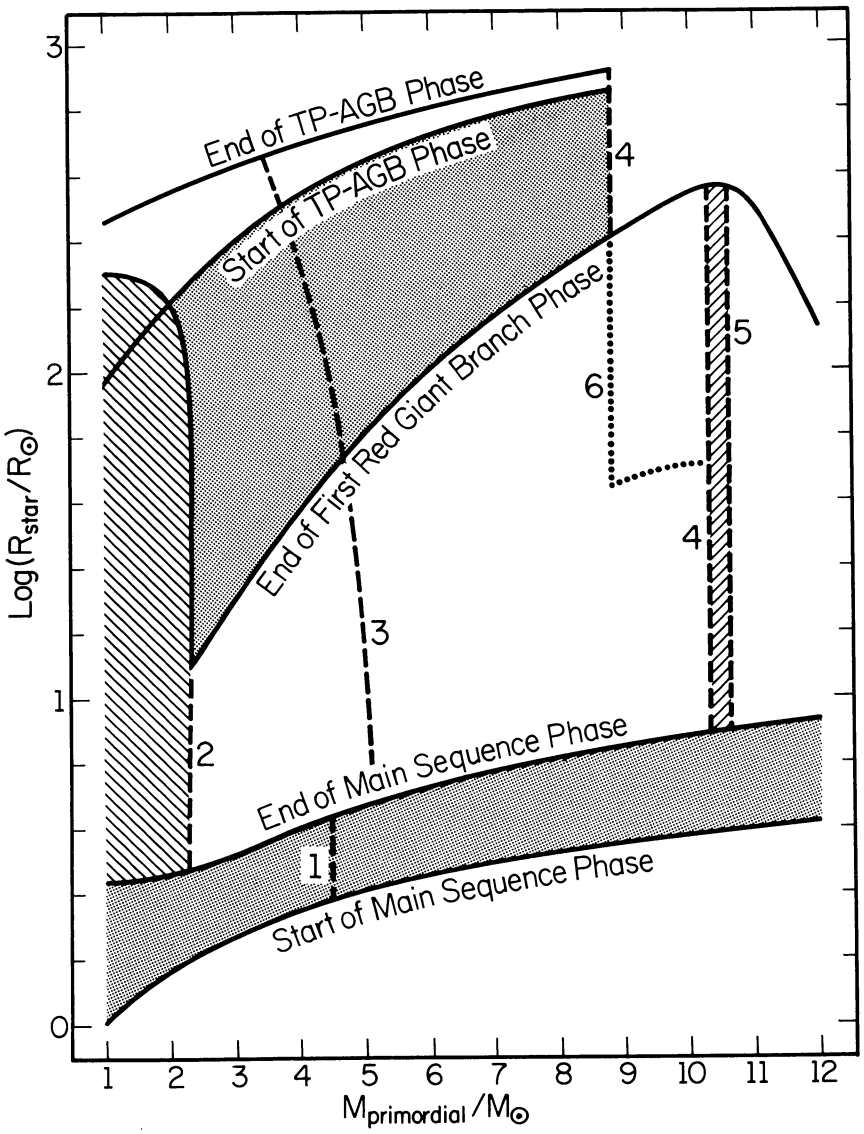

FIG. 31.—Stellar radius at the beginning and end of various phases as a function of the initial mass of a Roche-lobe filling star. The dashed line gives the minimum primordial mass of a primary required for the eventual production of a Type I supernova due to the merging of two CO degenerate dwarfs; along this line, the secondary must also be initially, or become eventually, as massive as the primary, and common-envelope action must force the separation of the two degenerate components to be less than about 3 $R_\odot$ when the second dwarf is first formed. In practice, the "average minimum" primary mass for Type I supernova formation will lie along a line to the right of the dashed curve. If Roche-lobe overflow first occurs when primary radius is in the main-sequence range, one expects the ultimate formation of a single star with a mass comparable to the sum of the initial masses of the individual components before merging. If the sum of these masses is less than about 9 $M_\odot$, the net result is a CO dwarf; if the sum is between about 9 $M_\odot$ and 12 $M_\odot$, the net result is an electron-capture supernova leaving a neutron star; and if the sum exceeds about 12 $M_\odot$, the net result is a Type II supernova leaving a neutron star.

of becoming ONe degenerate dwarfs if Roche-lobe overflow occurs prior to or just at the moment of helium ignition in the core. Choosing R_{star} between 8 $R_\odot$ and 300 $R_\odot$, equation (14) gives $\nu_{ONe} \gtrsim 10^{-4}$ yr^{-1}. We have seen that stars initially as massive as 10.3 $M_\odot$ may become CO degenerate dwarfs if common-envelope action action can bring components close enough together, but we expect that the larger A is to begin with, the less likely this will be to happen. Let us suppose, extravagantly, that all those binaries with component masses initially between 8.8 $M_\odot$ and 10.3 $M_\odot$ and with primary stellar radius entering the region bordered by the dotted curve and the curve labeled "End of First Red Giant Branch" in Figure 31 produce ONe degenerate dwarfs. Then, $\nu_{ONe} \lesssim 9 \times 10^{-4} + 10^{-4} \sim 10^{-3}$ yr $^{-1}$ (we must at the same time reduce $\nu_{CO}^{He \rightarrow CO}$ by 10^{-3} yr^{-1}). Adding up all of the frequencies, we obtain a degenerate dwarf formation frequency of about 1 yr^{-1}.

It is easy also to estimate the formation frequency of the various types of supernovae that are anticipated.The formation frequency of electron-capture supernovae ($M_{star} \sim 9$–12 $M_\odot$, and $A \gtrsim 600$ $R_\odot$ for stars in binaries) is on the order of $\nu_{ec} \sim 10^{-2}$ yr^{-1}, and the formation frequency of Type II

supernovae (all binaries and single stars with $M_{\rm star} \gtrsim 12\ M_\odot$) is $\nu_{\rm II} \sim 10^{-2}$ yr^{-1} also. The dashed curve in Figure 31 labeled 3 marks the minimum mass which a primary must have if it is to produce a CO degenerate dwarf of mass at least as large as 0.7 $M_\odot$. In order to prevent common-envelope action from bringing the binary components so close as to prevent the secondary from developing a helium core before filling its Roche lobe, we require that the primordial binary separation be larger than a critical value of order 70 $R_\odot$ (Iben and Tutukov 1984*b*). Then, from equation (14) and the phase space in Figure 31 defined by curves 3 and 4, a line given by $M_{\rm primordial} = 8.8\ M_\odot$, a line given by $R_{\rm star} > 35\ R_\odot$, and the curve labeled "End of TP–AGB Phase," we have that the formation frequency of Type I supernovae (merging CO degenerate dwarfs of total mass larger than 1.4 $M_\odot$) is about 10^{-2} yr^{-1}.

The rate at which binaries merge while on the main sequence is on the order of $\nu_{\rm merge} \sim 0.2 \times 0.3/1.5 \sim 0.04$ yr^{-1}. If the sum of the initial masses of the merging components is less than 8.8 $M_\odot$, the merged single star will eject most of its hydrogen-rich envelope and evolve into a CO degenerate dwarf of mass less than 1.08 $M_\odot$. If the sum exceeds 8.8 $M_\odot$, the final remnant will be a neutron star. We emphasize once again that these estimates are extremely rough, no one frequency estimate being believable to better than a factor of 2, at best.

It is of interest to know the formation frequency of planetary nebulae with central stars which are short-period binaries. It is likely that all single stars and those components of wide binaries which are of initial mass less than about 8.8 $M_\odot$ pass through a planetary nebula phase. One might anticipate also that many close binaries which undergo a common-envelope phase, after which the mass donor becomes a luminous subdwarf (hot OB star), would also appear as planetary nebulae. We might guess a rate $\nu_{\rm PN}^{\rm common\ envelope} \sim \nu_{\rm CO}^{\rm close} + \nu_{\rm CO}^{\rm E} + \nu_{\rm CO}^{\rm TP} \sim 0.1$ yr^{-1} as the formation frequency of bright planetary nebulae with luminous and close binary central stars. However, in these cases, the mass donor does not become hot enough to ionize the ejected nebula until it has entered the core helium-burning phase, and, by then, it has become much dimmer than a typical PN central star (see Figs. 1–3, 17, and 24). By the time the central star exhausts helium at its center and grows large enough to eject material into a second common envelope, the matter in the first-formed nebula has long since dispersed. The second nebular shell (consisting predominantly of helium, if it is of substantial mass) will fluoresce when the central star achieves a surface temperature of the order of or larger than $T_e \sim 5 \times 10^4$ K, but, because the rate of evolution to such a high T_e typically requires of the order of a few $\times 10^4$ yr (see Figs. 1–3), this second nebular shell may have also dispersed to such an extent that its emission measure is below the limit of detectability. Thus, among observed nebulae, those which owe their existence to common-envelope action and which contain a bright, close binary may be much fewer in number than our formation frequency estimate would lead us to believe.

Our result that stars which develop into nondegenerate helium stars of mass less than 0.5 $M_\odot$ go on to burn helium and ultimately become degenerate dwarfs with large CO cores could have been anticipated from results of single-star calculations (e.g., Iben 1965*b*). The result requires major modifications in the estimates of the formation frequency of potential Type I supernova precursors for several scenarios considered by Iben and Tutukov (1984*b*, *c*, hereinafter IT). For example, the frequency $\nu_{\rm HeHe} \sim 5 \times 10^{-3}$ yr^{-1} estimated by IT for the production of double helium degenerates of total mass larger than 0.8 $M_\odot$ is based on the assumption that components of initial mass in the range 3.2–3.8 $M_\odot$ become helium degenerate dwarfs of mass 0.4–0.5 $M_\odot$. We now have that $\nu_{\rm HeHe} \sim 0$ and can eliminate merging helium dwarfs originating in this fashion from the list of Type I supernova precursors.

Similarly, the IT estimate of the rate at which two helium dwarfs of any mass merge is too large. Only close binary components of main-sequence mass less than 2.3 $M_\odot$ are sure to become "pure" helium degenerate dwarfs. From equation (2) we may estimate that only for initial binary separations less than about 27 $R_\odot$ will the final double helium degenerates be close enough ($\lesssim 3\ R_\odot$) to merge on a Hubble time. From the helium core mass–radius relationship used by IT (see also Giannone and Giannuzzi 1970, 1972), this implies for the primary a maximum helium core mass at Roche-lobe overflow of $M_{\rm He} \sim 0.26$–$0.28\ M_\odot$. The helium dwarf formed by the secondary will be even smaller than this. The formation frequency of double helium degenerates (now of total mass $\lesssim 0.6\ M_\odot$) becomes $\nu_{\rm HeHe}^{\rm merge} \sim 0.08$ yr^{-1} instead of the 0.15 yr^{-1} given by IT.

Finally, the formation frequency of CO and helium degenerate dwarf combinations which are close enough to merge within a Hubble time is reduced to $\nu_{\rm COHe}^{\rm merge} \sim 6 \times 10^{-4}$ yr^{-1}, and, since the maximum mass of the helium dwarf is likely to be smaller than 0.27 $M_\odot$ and the mass of the CO dwarf is smaller than 1.1 $M_\odot$, merging will almost surely lead to the R CrB phenomenon rather than to a Type I supernova explosion, regardless of the rate at which matter is accreted by the central dwarf from the thick disk (see § VIII*c*).

VI. THE EFFECTS OF MASS TRANSFER ON THE EVOLUTIONARY BEHAVIOR OF SYSTEMS IN WHICH COMPONENTS ARE OF COMPARABLE PRIMORDIAL MASS

In the foregoing experiments, we have assumed tacitly that no mass is transferred from one component to the other, so that mass lost from either component is lost also from the binary system. During the first phase of mass loss from the primary, this assumption is likely to be valid only as long as the primary possesses a deep convective envelope and as long as the primary mass is larger than about three-fifths of the mass of the secondary. Then, the time scale for mass loss from the primary will be much smaller than the thermal time scale of the secondary. The secondary will swell to fill its Roche lobe, a common envelope will be formed, and the orbital separation will decrease. However, when the mass ratio of primary to secondary drops below the critical value of 0.6 and/or when the fraction of mass in the convective envelope of the primary becomes too small, the rate of mass loss from the primary drops sharply, and, therefore, the secondary may accrete much of the mass transferred. Assuming that no

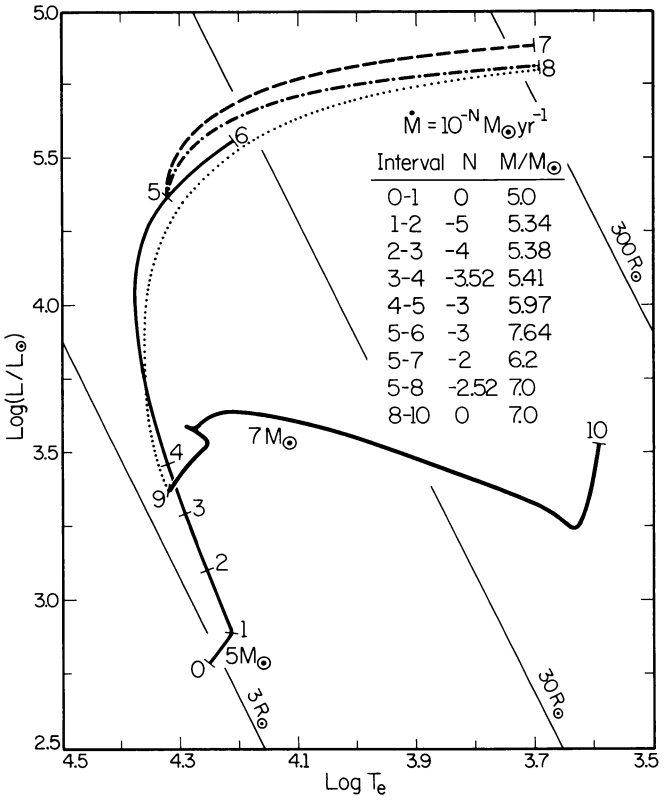

FIG. 32.—Response of an evolved main-sequence star to accretion. The direct liberation of the kinetic energy of infalling matter is ignored, and only energy liberated in response to internal readjustment due to increasing interior mass is included. Accretion rates (in $M_\odot$ yr^{-1}) between adjacent labeled points and stellar masses at these points are given. At the onset of accretion, the abundance by mass of hydrogen at the center of the 5 $M_\odot$ model is 0.44.

further mass is lost from the system, and assuming that also no orbital angular momentum is lost, the orbital separation will increase with continued mass transfer. Even though the radius of the Roche lobe surrounding the donor will shrink *relative* to the system semimajor axis, the donor will detach from this lobe, and mass flow will cease "earlier" (larger primary mass) than would have been the case had the secondary continued to reject matter offered by the primary.

Relevant computations include those reported by Benson (1970), Yungelson (1973*a*, *b*), de Loore and De Greve (1975), Ulrich and Burger (1976), Flannery and Ulrich (1977), Kippenhahn and Meyer-Hofmeister (1977), Neo *et al.* (1977), Packet and De Greve (1979), and Fujimoto, Iben, and Becker (1981). These and similar computations may be summarized by saying that, if $\dot{M}_{\rm accrete} \gg \dot{M}_{\rm KH}$, the accreting model expands and evolves through a series of thermal equilibrium states.

An example of how a secondary of primordial mass in the 5–6 $M_\odot$ range might respond to mass transfer from a companion of comparable mass is shown in Figure 32. A 5 $M_\odot$ model is evolved through the first portion of its main-sequence phase until its central hydrogen abundance by mass is reduced to $X_c \sim 0.44$ (from an initial value of 0.71). Then, accretion is begun, first at a rate of 10^{-5} $M_\odot$ yr^{-1}, and then at successively larger rates imposed at arbitrary times. We assume that matter flowing from the companion dissipates most of its directed kinetic energy into heat on forming an accretion disk, and that the only effect of accretion from the disk onto the secondary is the release of entropy internally as a consequence of internal structural changes.

It is clear from Figure 32 that, for mass-transfer rates larger than several times 10^{-3} $M_\odot$ yr^{-1}, an evolved main-sequence star of initial mass in the 5–6 $M_\odot$ range will rapidly grow in radius and fill its Roche lobe before having accreted very much mass. We envision, then, that during the first phase of mass loss from the primary, a common envelope will form and prevent the 5–6 $M_\odot$ secondary from increasing in mass by, say, more than about 10%, while the mass of the primary drops to about three-fifths of the mass of the secondary, or to about 3–4 $M_\odot$. Thereupon, the mass-loss rate from the primary will adopt values more like those we have assumed in our experiments (e.g., $\lesssim 10^{-5}$ $M_\odot$ yr^{-1} from the giant progeny of a model of initial mass ~ 5 $M_\odot$). Figure 32 shows that, for accretion rates much less than 10^{-3} $M_\odot$ yr^{-1}, the radius of the secondary remains smaller than a few times its main-sequence radius. Hence, during the final portion of the first mass-transfer event, the secondary will grow in mass at the same rate as the primary is losing mass. In the case at hand, we might guess that the secondary grows to a mass of 7–8 $M_\odot$ while the primary drops in mass to ~ 0.75 $M_\odot$.

Once the first episode of mass transfer ceases, the primary shrinks to become a core helium-burning star, evolving much like the model remnants in our experiments, and the secondary finishes out its main-sequence phase on a time scale appropriate to its new mass. In Figure 32 we show the further evolution of a model which, midway in its main-sequence phase, has grown suddenly in mass from 5 $M_\odot$ to 7 $M_\odot$. Remarkably, the remaining main-sequence lifetime of the model of suddenly increased mass is nearly the same as if no mass had been added. This is due to the fact that the increased mass leads to an enlarged convective core and to a consequent injection of fresh hydrogen fuel.

The relatively long lifetime of the core helium-burning phase of the primary remnant has a profound implication for the future evolution of the binary system when the two components are primordially of similar mass. Since the main-sequence lifetime of the secondary is nearly the same as that of the primary, the remainder of its main-sequence lifetime after the first mass-transfer episode has been completed may be shorter than the core helium-burning lifetime of the primary remnant. Therefore, the secondary will develop a hydrogen-exhausted helium core and swell to giant dimensions *before* the primary remnant has a chance to swell again because of internal restructuring after it exhausts helium at its center. This means that the secondary will fill its Roche lobe and attempt to transfer mass to the compact, helium-burning primary remnant. What must happen then is that the remnant swells in consequence of the burning of freshly added hydrogen-rich material. One might anticipate that the hydrogen-burning rate $L_{\rm H}$ will reach a steady state value of about 5–$10 L_{\rm He}$, as is the case for single core helium-burning stars of intermediate mass, and that hydrogen will be processed at a

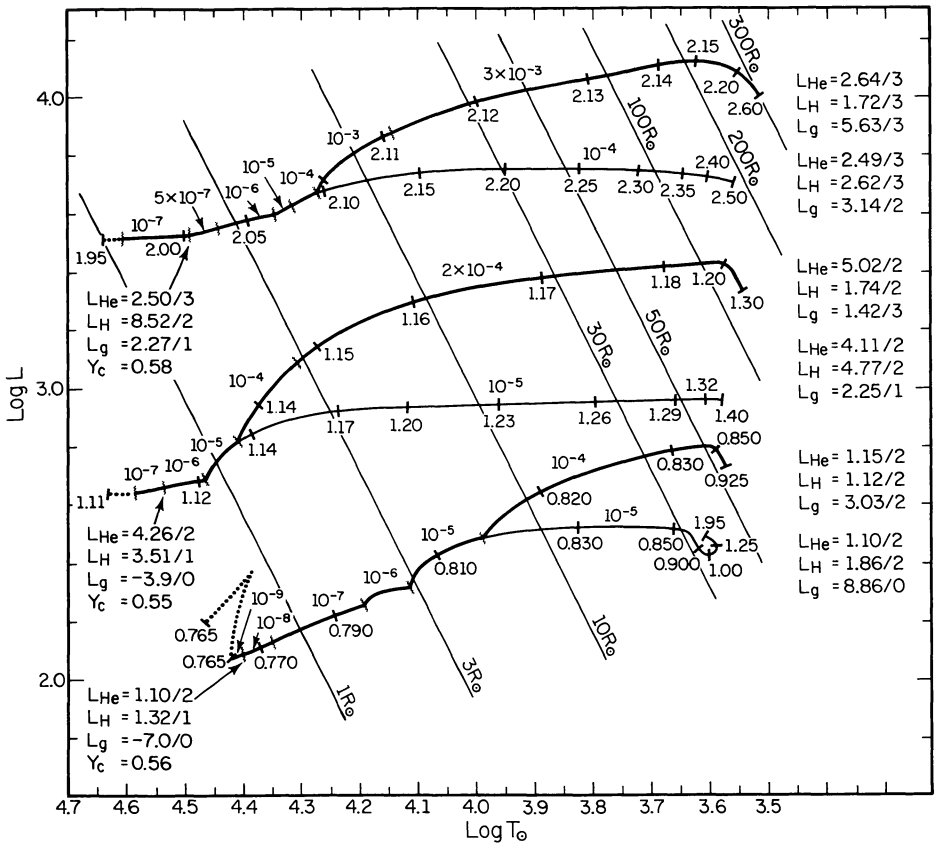

FIG. 33.—Response of core helium-burning remnants to accretion. Accretion rates (in $M_\odot$ yr^{-1}) are indicated by integers with exponents and refer to intervals between hatched bars. Stellar mass (in $M_\odot$) is indicated beside solid bars. The rates of energy generation by helium-burning reactions ($L_{\rm He}$), by hydrogen-burning reactions ($L_{\rm H}$), and by the release of "gravitational" energy [$L_g = -\int(T\,dS/dt)\,dM$] near the beginning of each track and at the end of each track are given in solar units ($L_\odot$).

rate $\dot{M}_{\rm crit}(M_\odot\ {\rm yr}^{-1}) \approx 10^{-11} L_{\rm H} \sim 10^{-10} L_{\rm He}$, or, for typical remnants, at the rate $\dot{M}_{\rm crit} \sim 10^{-8}\ M_\odot\ {\rm yr}^{-1}$. Since the secondary transfers mass at a much larger rate than this (larger than $10^{-5}\ M_\odot\ {\rm yr}^{-1}$ in the experiments we have performed), we expect the primary remnant to grow in mass and in size until it reaches the dimensions of a single isolated star of the same hydrogen-exhausted core mass residing in the core helium-burning band. Since the radius of such an isolated star can be quite large (e.g., 30–70 $R_\odot$ for a 5 $M_\odot$ star with a core mass ~ 0.75–$1.1\ M_\odot$, see Iben 1965*b*), it is probable in many instances that the primary remnant will again fill its Roche lobe.

That the core helium-burning remnant of the primary will swell to giant dimensions in response to mass accretion at rates comparable to or smaller than those at which the secondary is expected to lose mass is demonstrated in Figure 33. In each case, mass accretion at the indicated rates is begun after the remnant has consumed approximately half of the helium it will eventually consume in its central convective region. The most interesting aspect of the structures which result is that the rate of hydrogen burning is comparable to the rate of helium burning rather than, as expected from the behavior of single core helium-burning stars, almost an order of magnitude larger. Even so, each model "remnant" approaches the Hayashi border, i.e., develops a radius as large as or larger than did its companion during the first mass-loss phase. Since, by assumption, the first mass-transfer event ceased when the primary shrank within its Roche lobe, it will fill this lobe again and attempt to drive mass back onto the secondary. Inevitably, a common envelope will be formed, the two components will be drawn together by drag forces, and most of the matter outside the hydrogen-burning shells of *both* components will be lost from the system. The mass-loss process will cease once both components shrink within their respective Roche lobes. We thus anticipate the formation of systems consisting of two close, compact core helium-burning remnants, of masses M_{1R} and $M_{2R} \sim M_{1R}$, which ultimately evolve into two CO degenerate dwarfs. Whether M_{2R} is larger or smaller than M_{1R} depends on (1) whether the first episode of mass transfer/loss produces a secondary mass which is larger or smaller than the primordial mass of the primary, (2) the degree to which the components are drawn closer together or spread further apart during the first mass-transfer event, and (3) the effect of a common envelope during the second mass-transfer episode. In any event, when both components are primordially of comparable mass and if both eventually evolve into degenerate dwarfs, it is quite likely that the primordially lighter star will become the heavier dwarf in the final double degenerate system.

The scenario we have just described will in most instances not be followed if the masses of the components are primordially close to the upper end of the intermediate-mass range.

For example, if the two components begin with masses of, say, 8 $M_\odot$ and 9 $M_\odot$, the core helium-burning lifetime of the primary remnant of the first mass transfer/loss stage may be smaller than the remaining main-sequence lifetime of the secondary, even if the secondary grows to a mass of, say, ~ 11–13 $M_\odot$ during the first mass-transfer stage. A further difference is then that the secondary may not fill its Roche lobe for the first time until after it has nearly completed the core helium-burning phase. This means that the remnant of the secondary will experience carbon burning and may evolve into a degenerate ONe dwarf of mass larger than the primary remnant or, more probably, be massive enough ($M_{2R} > M_{\rm Chandrasekhar}$) that it experiences a supernova explosion triggered by electron capture on ^{24}Mg (Miyaji *et al.* 1980; Nomoto 1982) or on ^{23}Na, leaving a neutron star remnant. If the two components remain bound and at a separation less than ~ 3 $R_\odot$, orbital angular momentum loss due to gravitational-wave radiation (GWR) will force them closer together until the primary remnant, a CO dwarf, becomes a thick disk about its compact companion. If this companion is an ONe degenerate dwarf, accretion of disk material onto the central star will continue until the mass of the central star approaches 1.4 $M_\odot$, whereupon electron capture on ^{24}Mg and/or on ^{23}Na will lead to core collapse; the final result will be a single neutron star. If the central star is already a neutron star, accretion of disk material may result in a central star more massive than a stable neutron star. In this event, a single black hole may be the final result.

A still different scenario arises if the first mass-transfer event converts the secondary into an evolved main-sequence star of mass greater than ~ 12–15 $M_\odot$, in which case the secondary may ultimately develop an FeNi core and experience a collapse triggered by a phase transition (heavy elements dissociate into alpha-particles) and explode as a supernova, leaving a neutron star remnant. Prior to this, the primary remnant may have been converted into a massive CO or ONe degenerate dwarf. Since the Type II SN explosion of the secondary may eject most of the mass of the system, this system will not in most instances survive as a binary but will result in two unbound, rapidly moving compact objects, one a neutron star and the other a degenerate dwarf.

VII. THE INITIAL RESPONSE OF A CO DWARF REMNANT TO A FINAL SLOW ACCRETION EVENT

If the mass of the secondary is primordially much less than that of the primary, then it is probable that the CO dwarf remnant of the primary will have evolved to very low luminosity before its companion leaves the main sequence. The rate of dimming is given approximately by $L \sim 10^9\ L_\odot [t({\rm yr})]^{-7/5}$ (e.g., Iben and Tutukov 1984*c*). The cooling process will continue uninterrupted until, and if, the secondary fills its Roche lobe. If the primordial secondary is of very low mass (say, $\lesssim M_\odot$), it may not fill its Roche lobe at all in a Hubble time unless the first two common-envelope stages bring it close enough to the primary that angular momentum loss by a magnetic stellar wind (MSW) or GWR can establish Roche-lobe contact over a period of 10^9–10^{10} yr (e.g., Iben and Tutukov 1984*d*). The luminosity of the dwarf at this time will have decreased to $L \sim 10^{-3}$ to 10^{-4} $L_\odot$. Thus, in many systems in which the mass of the secondary is initially of mass less than ~ 2 $M_\odot$, the CO dwarf remnant of the primary will have dimmed to very low luminosities. Interior temperatures will have dropped to only a few $\times 10^6$ K, and matter will have crystallized. The opacity in the main body of the dwarf will be very small because of the high conductivity of degenerate electrons.

It is natural to expect that the accretion by a cold dwarf of fresh matter with a large hydrogen abundance will lead to hydrogen shell flashes which are much stronger than those experienced by "hot" accreting dwarfs (Nomoto, Nariai, and Sugimoto 1980; Iben 1982). The effects of the accumulation of a cold, temporarily inert, hydrogen shell have been analyzed many times (e.g., Gurevich and Lebedinskij 1947; Schatzman 1965; Starrfield, Sparks, and Truran 1974; Starrfield, Truran, and Sparks 1972; Tutukov and Yungelson 1972). The main properties of the accumulation process can be viewed in the following way. The hydrogen-rich shell formed by accreted matter is heated by compression but cooled by radiative diffusion of energy both inward and outward from the temperature maximum in the shell. Heating at first only slightly outweighs cooling. However, as the mass of the hydrogen-rich shell increases, the extent of the disparity between heating and cooling grows since the optical depth above the temperature maximum increases and this increase lengthens the time scale for outward diffusion. As a consequence, the net rate of heating increases until the steady accumulation of hydrogen-rich matter is interrupted by a thermonuclear runaway.

We have computed the evolution of an initially very cold (central temperature $T \approx 1.23 \times 10^6$ K) and dim ($L_0 \approx 10^{-4.5}$ $L_\odot$) CO dwarf of initial mass 0.599 $M_\odot$ (see Iben 1984*a*; Iben and Tutukov 1984*c*) influenced by the accretion of cold, low-entropy matter at rates 10^{-11}, 10^{-10}, 10^{-9}, and 10^{-8} $M_\odot$ yr^{-1}. The last three accretion rates are interesting because they can occur in a low-mass binary consisting of a CO dwarf and a secondary of initial mass $\lesssim M_\odot$ in which mass transfer is driven at first by a MSW and then by GWR. Thus, the computed evolution is applicable, for example, to early stages in the evolution of cataclysmic binaries.

The thermal evolution of matter in the accreting dwarf is shown in Figure 34 for the case of accretion at the rate $\dot{M} = 10^{-10}$ $M_\odot$ yr^{-1}. It is evident that the maximum in the interior temperature occurs in the region containing freshly accreted matter. The opacity of the low-temperature matter in the deep interior is so small that most of the gravitational potential energy released by the accreted matter is transferred into the inner parts of the dwarf. For most of the evolution, the flux of energy inward exceeds the rate of radiative losses from the surface by several factors of 10. This circumstance influences strongly the thermal evolution of the shell, which remains relatively cool, not because of surface losses, but because of an influx of radiation into the interior. The inner part of the dwarf is crystallized and has a very low thermal capacity; consequently, matter there is heated significantly before a thermonuclear runaway occurs in the shell.

^{3}He burns in that portion of the envelope which is below freshly accreted matter. The abundance by mass of ^{3}He in this portion initially exceeds $\sim 10^{-2}$. Almost all of the energy released by ^{3}He burning goes into heating the main body of the CO dwarf.

As time progresses, the location of the maximum in the nuclear energy generation rate (ϵ_n) is shifted outward, ever closer to the location of the temperature maximum in the shell. A thermonuclear runaway begins after about 7×10^7 yr of accretion, when the mass of the hydrogen-rich surface layer of the CO dwarf reaches about 0.007 $M_\odot$ and the maximum temperature of the shell reaches about 3.5×10^6 K. The thermal time scale at this moment becomes less than the accretion time scale, and the mass of the hydrogen-rich envelope will not change before the onset of an explosion.

Similar calculations with accretion rates of 10^{-9} and 10^{-11} $M_\odot$ yr^{-1} show that the critical mass leading to a thermonuclear runaway varies from ~ 0.003 $M_\odot$ to ~ 0.01 $M_\odot$. Such large masses considerably exceed masses usually quoted for nova envelopes. The small mass of the CO core (0.6 $M_\odot$) possibly prevents a nova explosion in this case (Fujimoto 1980), and the thermal flash may form a giant envelope, transforming the dwarf into a "born-again" AGB star (Iben 1982). The shift in the location of the maximum temperature point toward the surface, as shown in Figure 34, also acts to mitigate the violence of the explosion. Formally, the lifetime of the resulting AGB star can be rather long ($\sim 10^5$ yr). However, since, by assumption, the dwarf has a close companion, the newly established giant envelope will be lost rather quickly by the binary core friction process. A planetary nebula–like envelope will be formed. This process will be repeated several times before the interior temperature of the CO dwarf has been raised to a sufficiently large value that the character of recurrent flashes reaches a limit cycle. The critical envelope mass for an outburst will decrease with each flash until the limit cycle is attained.

The consequences of accretion of cold matter onto a cold, massive (1–1.4 $M_\odot$) dwarf may be more dramatic. The inward transfer of energy liberated by accreted matter will lead to an accumulation in this case also of hydrogen-rich envelope mass which is several times larger than the normal critical value for an outburst. The thermonuclear explosion initiated by hydrogen burning in this case could lead to a helium-burning runaway. This will make the shell burst a more violent one than normal.

As a final comment, we remark that the nature of the response of a cold dwarf to accretion will alter somewhat the analysis of the limits on core mass and accretion rates that lead to supernova outbursts triggered by a carbon-burning thermonuclear runaway.

VIII. POSSIBLE APPLICATIONS TO REAL SYSTEMS

We stress once again the fact that the results of our experiments can be viewed only as plausible outcomes of close binary star evolution. Not only have we employed mass loss/transfer algorithms that are based on intuition rather than on first principles, but our approximations to the physics of the deep interior (for example, with regard to mixing near convective-radiative boundaries or mixing through marginally convectively unstable regions) may be grossly in error. We believe, nevertheless, that our results may be used as qualitative guides toward understanding properties of real systems. In fact, the primary justification for performing our experiments has been the establishment of a numerical framework for discussing the outcome of the evolution of real binary systems. We admit that the scenarios which we are about to propose are possibly even more speculative than are the results of our experiments, but we are convinced of the importance of engaging in speculation of this sort.

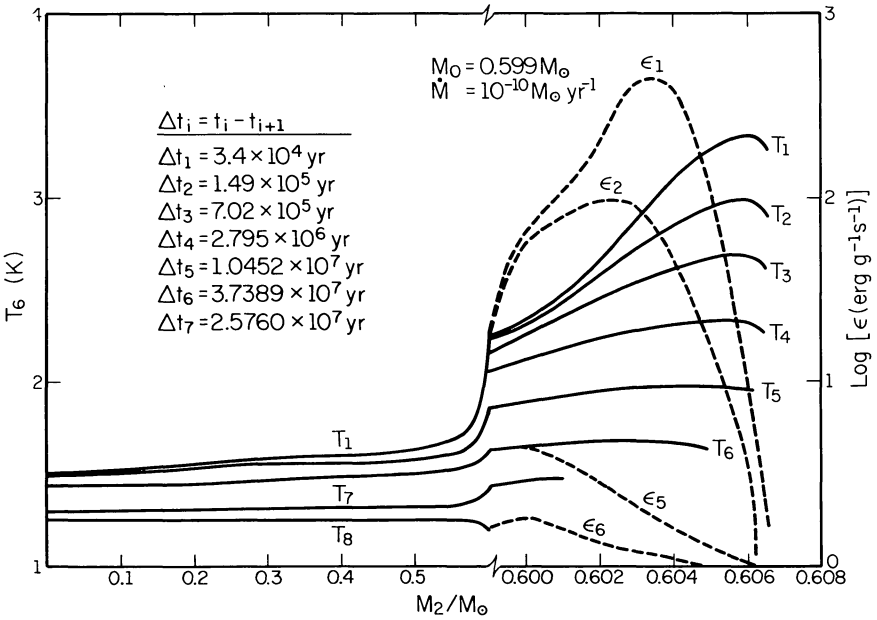

FIG. 34.—Response of a cold CO degenerate dwarf of mass 0.599 $M_\odot$ to accretion of hydrogen-rich matter at the rate 10^{-10} $M_\odot$ yr^{-1}. Both local nuclear energy generation rates and temperature (units of 10^6 K) are given as a function of position (in mass from the center) within the model star. The time interval between the establishment of the various profiles is given by the Δt's.

a) *The Formation of Binary and Millisecond Pulsars*

Our experiments have relevance for questions as to the origin and the low frequency of occurrence of (1) pulsars (spinning, magnetized neutron stars) in binaries and (2) rapidly rotating ("millisecond") pulsars. We suggest that (1) the companion of a pulsar in a binary is most likely to be (or to eventually evolve into) a degenerate dwarf, and (2) a rapidly rotating pulsar retains memory of a spin-up phase that occurs as a consequence of mass transfer onto a degenerate dwarf progenitor of the neutron star before it implodes to neutron star dimensions.

Let us first concentrate on the origin of pulsars in binaries. It is an unusual binary system that can evolve into a bound system consisting of two neutron stars. After a first neutron star is formed, the companion, if it is itself to ultimately evolve into a neutron star, will in general be much more massive (by perhaps a factor of 5–10) than the already-formed neutron star; ejection by this companion of all but a neutron star core in a supernova event will therefore lead to a disruption of the system, and the net result will be two freely moving neutron stars (see, e.g., Tutukov and Yungelson 1973*a*, *b*, *c*; Flannery and van den Heuvel 1975; de Loore, De Greve, and De Cuyper 1975; Hills 1978; De Cuyper 1981; Cordes and Wasserman 1984).

There is a small but finite "window" which may lead to a bound double neutron star system (see, also, Flannery and van den Heuvel 1975; Smarr and Blandford 1976). The basic criterion for retaining duplicity in the wake of a final explosion is a simple one. If its orbital eccentricity is initially small, then a binary system will remain bound following the explosion of one of its components if the mass lost from the system in consequence of the explosion is less than the sum of the masses of the surviving components. For nonzero initial eccentricity, the criterion is of course slightly more complicated (see, e.g., Tutukov 1980). Suppose that we begin with a close binary containing a star of mass 11–12 $M_\odot$ and a companion of mass 7–10 $M_\odot$. Suppose further that the initially more massive primary component loses all but about 2–4 $M_\odot$ before experiencing core collapse triggered by electron capture and that the initially less massive secondary component grows to a mass in the 11–12 $M_\odot$ range. Then the secondary will also lose all but about 2–4 $M_\odot$ before it undergoes a supernova explosion. In the second supernova explosion, the secondary loses 0.6–2.6 $M_\odot$, but this is less than the combined mass of the two remnant neutron stars, and the system may remain bound, although the orbit will be highly eccentric. This scenario may possibly account for PSR 1913+16, which has a total mass of about 2.8 $M_\odot$ and a high eccentricity (Taylor *et al.* 1976). The rapid rotation rate of the pulsar component (60 ms) may be accounted for by supposing that the compact ONe core of the immediate supernova progenitor is spun up by interaction with matter in the common envelope formed just prior to each explosion. Another way of describing the criterion for retaining duplicity in a system of initially small eccentricity is that the mass of the secondary just prior to the neutron star–producing explosion must be less than about $3 \times 1.4\ M_\odot = 4.2\ M_\odot$. But this means that the secondary may have a mass anywhere in the range 10–15 $M_\odot$ prior to losing mass by Roche-lobe overflow. Thus, there is a finite possibility of forming a double neutron star system in which the secondary experiences a core collapse and a supernova explosion in consequence of the photodisintegration of iron-peak nuclei.

Other scenarios lead to the formation of systems containing a pulsar and a degenerate dwarf. In order to ensure that the original binary system survives as a bound system containing just one pulsar, we may insist that the immediate progenitor of the neutron star be less massive than its companion at the moment of the supernova explosion. This can be accomplished in two ways: (1) the masses and the separation of the primordial components may be chosen in such a way that, before it implodes-explodes, the primary loses mass to become less massive than its companion, while the companion remains less massive than about 10 $M_\odot$ prior to the implosion-explosion of the primary; (2) primordial masses and separation may be chosen in such a way that the primary loses enough matter during early evolutionary phases that its remnant must ultimately evolve into a degenerate dwarf, whereas the companion gains enough mass that it can undergo an implosion-explosion event before the primary experiences a second mass-loss event and becomes a degenerate dwarf. Both scenarios require the primary to lose considerable mass, and this is most easily accomplished by Roche-lobe overflow. The first scenario requires that the primordial mass ratio be far from unity—otherwise the secondary will gain too much mass and itself evolve into a neutron star; it requires further that the primary lose enough mass by Roche-lobe overflow and (if it is initially of mass $M_{MS} > 25\ M_\odot$) also by wind mass loss, until it is less massive than its companion at the moment of supernova outburst. The second scenario requires that the primordial mass ratio be on the order of unity and that the sum of the component masses be less than $\sim 15\ M_\odot$ but larger than $\sim 12\ M_\odot$—Roche-lobe overflow will then ensure that the mass of the primary is reduced sufficiently that the remnant evolves into a degenerate dwarf, while the secondary gains just enough mass to develop an ONe core of mass larger than 1.4 $M_\odot$ but not enough mass to keep from expanding and losing most of the matter outside its core before an implosion-explosion event occurs.

At this stage, it is best to focus on specific cases. Out of the four currently known systems containing pulsars, we choose those containing PSR 0655+64 ($P_{orb} \sim 24.7$ hr, $P_{rot} \sim 0.196$ s, eccentricity $e \sim 10^{-5}$) and PSR 1913+16 ($P_{orb} \sim 8$ hr, $P_{rot} \sim 60$ ms, $e \sim 0.6$). Making use of the scintillation properties of PSR 0655+64, Lyne (1984) determines a relationship between secondary and primary mass such that, if the primary (neutron star) is of mass 1.4 $M_\odot$, then the secondary is of mass ~ 0.7–$0.8\ M_\odot$. This system therefore provides a perfect illustration of the scenarios we are advocating: the companion of the pulsar is either now or will evolve into a degenerate dwarf. Of course, there is no absolute guarantee that the 0.7 $M_\odot$ companion is not a main-sequence star which is bound to the pulsar by virtue of an exchange capture or a tidal capture which occurred after the formation of the pulsar. However, the very small number (~ 20) of analogous, low-mass, X-ray binary systems which are detected because of mass transfer from a main-sequence companion and which are therefore probably detectable for perhaps 10^8–10^9 yr, coupled with the probability that a pulsar is detectable for not much more than a few times 10^7 yr, makes this latter interpretation unlikely,

and we prefer to think that the companion of PSR 0655+64 is a degenerate dwarf. Since its mass is ~ 0.7–$0.8\ M_\odot$, its progenitor must have at some time (either primordially or in consequence of accretion from the progenitor of the neutron star) been of mass $\sim 5\ M_\odot$ or larger. There are undoubtedly many ways to achieve an appropriate primordial system. We will choose only one. Let the primordial primary be of mass ~ 12–$15\ M_\odot$ and the secondary be of mass ~ 5–$6\ M_\odot$. Choose the primordial separation in such a way that a common envelope is formed when the primary expands during the shell helium-burning stage, with most of the mass lost from the primary also lost from the system. The mass-loss phase ends when the primary is reduced to $\lesssim 4\ M_\odot$ and the remnant goes on to implode in consequence of electron capture on ^{24}Mg and/or ^{23}Na in an electron-degenerate ONe core. The accompanying explosion undoubtedly perturbs the orbit into a state of high eccentricity, but, if the first common-envelope phase has brought the binary components close enough together, the tidal action of the neutron star on the main-sequence secondary may be enough to circularize the orbit. If not, then circularization will surely occur during one or both of the common-envelope phases which eventuate when the secondary expands, first after exhausting central hydrogen and again after exhausting central helium. A common envelope is ensured since mass loss from the secondary will proceed at a rate far in excess of the Eddington limit for accretion onto a neutron star.

The case of PSR 1913+16 is more difficult to understand as a neutron star—degenerate dwarf system since the sum of the component masses is equal to $2.8\ M_\odot$ within $\sim 3\%$ (Taylor 1981; Taylor and Weisberg 1982). For example, if the pulsar mass is really about $1.4\ M_\odot$, then the mass of the secondary must be at least $1.3\ M_\odot$, and this implies that, if it is a degenerate dwarf, the secondary must be composed of oxygen and neon. This being the case, its progenitor must at some point early in its main-sequence phase have had a mass in a fairly narrow range, say, $10 \pm 0.5\ M_\odot$. Let us suppose that both components were primordially of mass in this range. The slightly more massive primary fills its Roche lobe during the shell hydrogen-burning stage and shrinks within this lobe when its mass is reduced to about 3–$4\ M_\odot$. The evolution of the secondary, which is already nearly at the end of its main-sequence phase when the first mass-transfer event occurs, may accelerate somewhat in response to mass accretion (having increased in mass to, say, 12–$15\ M_\odot$), possibly overtaking its companion in an evolutionary sense. When it expands during shell helium burning, a common envelope is formed, and its mass is reduced to something on the order of 4–$5\ M_\odot$. Note that, since the secondary is much more massive than its companion when Roche-lobe overflow begins (say, $14\ M_\odot$ as opposed to $4\ M_\odot$), orbital shrinkage may be much more pronounced than in the first instance of mass transfer from primary to secondary, and the remnant of the secondary may therefore be smaller than that of the primary even though its core is more evolved. The secondary now experiences a supernova explosion triggered by electron capture, and the primary, after undergoing a second phase of mass loss during shell helium burning, evolves into a degenerate ONe dwarf. The high (60 ms) rotation rate of the remnant pulsar is again attributed to a spin-up which occurs either during the first mass-transfer event, while the neutron star progenitor is near the end of its main-sequence phase, or during a common-envelope phase formed when the secondary expands for the last time.

A possible explanation of how an isolated neutron star can achieve a spin rate as large as that exhibited by PSR 1937+214 ($P_{\rm rot} = 1.6$ ms, Backer *et al.* 1982) is given by a scenario which produces the neutron star by the merging of two degenerate dwarfs, at least one of which is an ONe degenerate dwarf. In this scenario, all we require is that the two degenerate dwarfs are close enough to be drawn into Roche-lobe contact within a Hubble time. The spin-up occurs when the lighter degenerate dwarf fills its Roche lobe and forms a thick disk about the central ONe degenerate dwarf, which ultimately transforms itself into an even more rapidly spinning neutron star after growing to the Chandrasekhar mass by accretion from the disk (Iben and Tutukov 1984*b*). Of course, there are ways in which a neutron star may be spun up after it is already formed. For example, one may consider spin-up in a low-mass X-ray binary formed by tidal capture. Because of the low gyration radius of a neutron star relative to that of a white dwarf, the amount of mass which must be accreted directly by the neutron star in order to achieve a given spin frequency is larger than that which must be accreted by a degenerate dwarf precursor by a factor of $(R_{\rm DD}/R_{\rm NS})^{1/2} \sim 30$, where $R_{\rm DD}$ is the radius of the degenerate dwarf and $R_{\rm NS}$ is the radius of the neutron star.

b) Core Helium-Burning Remnants, sdB and sdO Stars, and Non-DA Degenerate Dwarfs

Helium stars of mass less than $10\ M_\odot$ can probably form only in close binaries since the wind emitted by a single low- or intermediate-mass star is not strong enough to abstract the surface hydrogen-rich layer until the star has developed a CO core and become an AGB star (see, e.g., Iben and Renzini 1983). Following the prescriptions in § V, we may estimate that about 10% of all main-sequence stars with primordial masses in the range $2.3 \lesssim M_1 \lesssim 10$ have close helium components in the core helium-burning stage. However, the bolometric luminosity of the helium-burning component is only about 20% of the luminosity of the primary B star, and the fact that the bolometric correction is much greater for the helium-burning star than for its main-sequence companion considerably reduces the likelihood of discovery by standard optical techniques. Detection in the far-ultraviolet is perhaps more promising.

The estimate we have just given is for systems in which primordial masses of the components are roughly equal, assuming that the secondary does not change its mass during the first Roche-lobe–filling phase. If we assume that the secondary accretes *all* of the matter lost by the primary, then the mass of the former almost doubles. Thus, the secondaries in evolved binaries with initial primary masses in the range 2.3–$10\ M_\odot$ will become stars with masses in the range 4–$20\ M_\odot$. But, since the number of primary stars born with masses in the 4–$20\ M_\odot$ range is (according to the Salpeter mass function) about $2^{1.5} \approx 2.8$ times smaller than the number of stars born with half such masses, the relative number of OB stars in the 4–$20\ M_\odot$ range with compact components in the core

helium-burning stage increases to at least 30%; and, since the hydrogen-burning lifetime of the secondary is $\sim 2^2 \sim 4$ times smaller than before, making the lifetime of the compact primary comparable to that of its companion, the frequency increases to perhaps 50%. Thus, combined optical and UV searches for OB stars with close satellites in the helium-burning stage might conceivably allow one to determine observationally the outcome of the first common-envelope stage experienced by binaries consisting primordially of two intermediate-mass stars of comparable mass.

The low luminosity and high surface temperature of the core helium-burning component explains one more peculiarity of intermediate-mass binary star evolution relative to that of higher-mass systems. The evolution of massive ($M_1 \gtrsim 20\ M_\odot$) close binaries leads to the formation of massive helium stars of the Wolf-Rayet type with luminosities comparable to the luminosities of their main-sequence companions (e.g., Tutukov and Yungelson 1973*a*, *b*, *c*). Massive helium stars with luminosities close to the Eddington limit typically emit an intense stellar wind, and the "effective" temperature T_e actually is set in the wind, far above the stellar "surface," making the star masquerade as an OB main-sequence star of the same luminosity. Thus, the optical luminosities of both components in a massive binary are comparable. In contrast, the bolometric luminosity of a low-mass remnant ($M_{\rm He} \approx 0.3$–$2.5\ M_\odot$) is either only $\sim 20\%$ of the luminosity of its main-sequence companion (if the companion accretes very little mass during the common-envelope stage) or on the order of 5% of its companion's luminosity (if the secondary accretes most of the mass lost by the original primary), and the factor of 2 difference in effective temperatures between the low-mass helium remnant and its main-sequence companion leads to an additional difference of about 5 mag in the visual. Thus, in the visual, the helium-burning component in a moderate-mass close binary is from 7 to 8 mag dimmer than its main-sequence companion, and this huge disparity makes discovery in the visual highly unlikely.

Ultimately, the primordial secondary may swell to fill its Roche lobe. If the mass ratio of the components of the primordial system is large, then the primary remnant will by this time have already expanded a second time to fill its Roche lobe and evolved into a CO degenerate dwarf. After a common-envelope stage, the secondary becomes a compact helium-burning star in orbit around a previously constructed degenerate dwarf. But, once more, the low luminosity and the large bolometric correction of both the helium-burning remnant and the degenerate dwarf make the probability of discovering such systems very small. If the mass ratio of the components of the primordial system is near unity, the secondary will swell to fill its Roche lobe before the primary remnant has completed its phase of core helium burning. The resulting pair of compact, but nondegenerate, remnants will also be very difficult to detect.

On the other hand, degenerate dwarfs are also difficult to detect and yet observers have succeeded in finding several thousand of them in the solar vicinity. There are two classes of compact objects of similar, low luminosity—the sdB stars (showing surface hydrogen) and the sdO stars (hotter than the sdB stars but showing no surface hydrogen)—which have long eluded satisfactory explanation. We note that the helium-burning remnants of the 3 and 4 $M_\odot$ precursors in our experiments (see § IV) have luminosities and surface tempertures in the ranges exhibited by sdB and sdO stars. They also spend enough time as core helium-burning stars that a hot wind may well abstract all of the surface hydrogen from many of them during this phase. In this picture, then, an sdB star is a core helium-burning remnant that may, in many instances, evolve into an sdO star which is either in the final phase of core helium burning or in the shell helium-burning stage.

Using equations (13) and (14), we can estimate the total number of low-mass (0.3–2.5 $M_\odot$) helium stars in our Galaxy that are in the core helium-burning stage, assuming that all of them are products of close binaries with $2.3 \lesssim M_1 \lesssim 10$ and $10 \lesssim A \lesssim 250$. We find this number to be about 2×10^7, corresponding to an average distance from one to another of about 15 pc. The frequency of formation of such objects is about 0.06 $\rm yr^{-1}$, and the average lifetime is about $\langle \tau_{\rm He} \rangle \sim 3 \times 10^8$ yr. Perhaps 10% of these lose their surface hydrogen layers by wind mass loss and become sdO stars and then non-DA white dwarfs.

We can estimate the fraction of non-DA degenerate dwarfs formed by mass transfer in binaries with an initial primary of mass in the range $6 \lesssim M_1 \lesssim 10$ and semimajor axis in the range $10 \lesssim A \lesssim 500$ by assuming that the binary components lose all of their surface hydrogen during their second mass-loss phase. Using equation (1), we obtain a frequency of formation of about 10^{-2} $\rm yr^{-1}$, whereas the total frequency of CO dwarf formation is about 0.5 $\rm yr^{-1}$ (e.g., Weidemann 1979; Iben and Tutukov 1984*c*). Since about 10%–15% of all hot white dwarfs are non-DA (e.g., Weidemann 1979; Liebert 1980), we see that this binary scenario may produce perhaps 15%–20% of all hot non-DA white dwarfs.

c) Extreme Helium Stars, R Coronae Borealis Stars, Hydrogen-deficient Stars, and the Like

Thus far, about 30 stars have been discovered that appear to be giants with hydrogen-deficient envelopes and exhibit, from time to time, large decreases in surface temperature and in visual brightness (see Payne-Gaposchkin 1963; Warner 1967; Feast 1975). The temporary dimming is usually attributed to the formation, in or above the helium- and carbon-rich envelope, of an optically thick dust shell. These stars are known as R CrB stars. Approximately half of them have been examined spectroscopically (see Warner 1967), with particular attention being paid to R CrB, RY Sgr, and XX Cam (Schönberner 1975, 1977; Cottrell and Lambert 1982). The most striking compositional characteristic of these stars is the almost complete absence of hydrogen (Bidelman 1953), with abundances by mass of less than 10^{-5} to 10^{-4} being established. The abundances of CNO elements relative to Fe are larger than solar by factors of 10–30 (Schönberner 1975; Cottrell and Lambert 1982; Heber 1983).

Several R CrB stars, such as RY Sgr, pulsate periodically with amplitudes of about 1 minute (Mazzaco and Milesi 1982). The pulsational periods vary from ~ 38 days for RY Sgr (Mazzaco and Milesi 1982) and ~ 42.8 days for UW Cen to ~ 139 days for S Aps (Kilkenny and Flanagan 1983). These periods are known to vary systematically. The pulsation period

of S Aps is thought to decrease on a time scale of ~ 300 yr, that of RY Sgr to decrease on a time scale of ~ 8200 yr, and that of UW Cen to increase on a time scale of ~ 1500 yr.

Bolometric magnitudes of R CrB stars have been estimated to be in the range $M_{\rm bol} = -4$ to -6 (e.g., Warner 1967; Drilling *et al.* 1984), corresponding to $\log L = 3.5$–4.3. Warner (1967) estimates that there may be approximately 100 of them in the Galaxy. Using data from Zhilyaev *et al.* (1978), Webbink (1984*b*) estimates their total number in the Galaxy to be $(123 \pm 40) \times \exp_{10} [0.4(M_{\rm bol} + 5)]$ and estimates the scale height characterizing their distribution in a direction perpendicular to the Galactic plane to be $\langle |z| \rangle = (430 \pm 120) \times \exp [-0.2(M_{\rm bol} + 5)]$ pc.

Members of another class, the nonvariable hydrogen-deficient carbon stars (extreme helium stars and HdC stars), closely resemble the R CrB stars in compositional characteristics and luminosity (Warner 1967; Hunger 1975; Heber and Schönberner 1981). The more abundant members of this group exhibit larger surface temperatures than do the R CrB stars (Drilling 1980; Drilling, Landolt and Schönberner 1984; Drilling *et al.* 1984) and are sometimes known as extreme helium stars, whereas the less numerous members with surface temperatures smaller than R CrB stars are sometimes referred to as HdC stars (e.g., Warner 1967). Cottrell and Lambert (1982) point out that, in those few HdC and extreme helium stars studied spectroscopically, the abundances of CNO elements relative to Fe are somewhat smaller than in the case of R CrB stars.

Using the data quoted by Heber and Schönberner (1981), Webbink (1984*b*) derives a scale height for the extreme helium stars of $\langle |z| \rangle = (1740 \pm 700) \times \exp_{10} [-0.2(M_{\rm bol} + 5)]$ pc and estimates their numbers in the Galaxy to be $(128 \pm 50) \times \exp [0.4(M_{\rm bol} + 5)]$. Heber and Schönberner estimate $\langle |z| \rangle \sim 1100$ pc. Warner (1967) points out that most of the hot helium stars have been found by looking at faint high–Galactic latitude B stars and that there is considerable bias against finding them among normal B stars in the Galactic plane. He estimates their total number to be closer to 1000 rather than to 100 and suggests that the space distributions of both the hot and the cool nonvariable helium stars are similar and less inflated in the direction perpendicular to the plane than the formal estimates would indicate.

If it were not for the rather large apparent difference in scale height $\langle |z| \rangle$ between them, one might argue that both the variable and nonvariable helium stars belong to the same homogeneous group, sharing a common origin. The variability of the R CrB stars could be attributed to the existence of an "instability" strip, and the relative frequency of the cool HdC stars, the R CrB stars, an the hot extreme helium stars could be explained as a consequence of the width of the temperature span defining each star type and the rate of evolution of a single star which passes in turn through each phase; just as well, one could assume that the variation in some secondary parameter determines the location in temperature where a given star of the class spends most of its time and that the relative number frequencies of the various subtypes simply reflect the original distribution in this secondary parameter.

Whatever the ultimate truth, there do appear to be from several hundred to a thousand extremely hydrogen-deficient stars which are large and very luminous. Most of them also show ratios of CNO elements to Fe which are much larger than solar. Whether they have a common origin or not, we shall henceforth call them giant helium stars.

i) *Merging Degenerate Dwarfs*

One straightforward way of accounting for the extreme deficiency of hydrogen at the surfaces of giant helium stars is to suppose that these stars have been formed by the merging of two degenerate dwarfs, the lighter of which is composed primarily of helium, the other of carbon and oxygen (Tutukov and Yungelson 1979*b*; Iben and Tutukov 1984*a*, *b*; Webbink 1984*a*). The trace quantity of hydrogen in the merged product has its origin in the very thin layer of unburned hydrogen that survives at the surface of the helium dwarf. The nitrogen at the surface of the merged product has its origin in the helium dwarf, within which nearly all of the primordial ^{12}C and ^{16}O have been converted into ^{14}N. The carbon and oxygen at the surface of the merged product have their origin near the surface of the CO dwarf.

We envision that, after it fills its Roche lobe, the helium dwarf is transformed into a thick disk about the CO dwarf (Tutukov and Yungelson 1979*b*) and that "shear mixing" dredges up the requisite amount of matter from outer layers of the CO dwarf and deposits it into the thick disk. Turbulent and/or meridional currents homogenize all of the matter in the disk. The assumption of shear mixing (Durisen 1977; MacDonald 1983) is not entirely fanciful, as this process appears to be required in order to understand the overabundances of CNO elements in the ejecta of classical novae (Starrfield, Truran, and Sparks 1978). The shear forces between the CO dwarf and the thick disk, which is formed on a nearly dynamical time scale, should be much more dramatic than is the case of stable disk accretion in classical novae.

If the mass of dredged-up C-rich and O-rich material (which contains no nitrogen) is small compared with the mass of the helium dwarf, then the abundance of N and Fe at the surface of the merged product will be essentially the same as in the helium dwarf. Then, if the abundances of CNO elements and the abundance of Fe in the main-sequence precursor of the helium dwarf are in solar system proportions, the abundance of N relative to Fe in the merged product will be about 10 times larger than solar. This is precisely what is estimated to be the case for R CrB (Cottrell and Lambert 1982). In order to achieve the similarly large overabundances relative to Fe of carbon and oxygen estimated for R CrB, we require that, if the Fe abundance is solar, roughly $10^{-2}\ M_\odot$ of C and O be dredged up from the outer edge of the CO dwarf. This mass is small compared with the mass of the helium-rich envelope after merging, thus justifying our assumption that the abundances of nitrogen and iron at the surface of the merged product are essentially the same as in the precursor helium dwarf. In this picture, variations in surface abundances from one giant helium star to the next may be attributed to variations in the mass of the precursor helium dwarf and in the amount of dredged up C-rich and O-rich material, this latter amount being a function of both the mass of the helium dwarf and the mass of the CO dwarf.

Next, we estimate the formation frequency, lifetimes, and numbers predicted by the merging-dwarf scenario. Let us suppose that, in the primordial binary, the primary is of mass

in the range 2.3–10 $M_\odot$ (to produce the CO dwarf) and the secondary is of mass in the range 1–2 $M_\odot$ (to produce the helium dwarf), with separations being in the range $A \sim$ 20–1400 $R_\odot$ (see Fig. 31). Such systems are expected to produce very close double degenerate binaries ($P \lesssim 10$ hr) at a frequency of about $\nu_{\rm HeCO} \sim 0.2 \times 1.3 (\int_{2.3}^{10} M^{-2.5} dM)(1.5/6.2) \sim 0.01$ yr^{-1} (see Iben and Tutukov 1984*a*, *b*, and § V for the estimation algorithms). Gravitational-wave radiation drives the two degenerate dwarfs together until the helium dwarf of mass $M_{\rm He} = 0.2$–0.3 fills its Roche lobe. After the thick disk mixing episode is completed, the merged star consists of a CO core of very nearly the same mass $M_{\rm CO}$ as the precursor degenerate CO dwarf and a giant helium-rich envelope at the base of which helium is being converted quiescently into carbon and oxygen. The lifetime of the burning phase is about $\tau_{\rm He} = E_{\rm He} M_{\rm He} L^{-1} \approx 10^{10} M_{\rm He} L^{-1}$ yr $\sim (2.5$–$7.5) \times 10^5 M_{\rm He}$ yr $\sim (0.6$–$2) \times 10^5$ yr, where we have set $L = 6 \times 10^4 [M_{\rm CO} + (M_{\rm He}/2) - 0.5] \sim (1$–$3) \times 10^4$ and $M_{\rm He} \sim 0.25$. The predicted number of giant helium stars is thus about 1300 ± 700, which is essentially the same as the estimated number of existing giant helium stars.

The merged-degenerate dwarf picture does not necessarily connect cool helium stars, R CrB stars, and hot helium stars in an evolutionary sense. That is, the location of a shell helium-burning star in the H-R diagram is a function of CO core mass, helium envelope mass, and envelope composition. Except for very small envelopes, the track of a model in the H-R diagram is toward larger luminosities and lower surface temperatures, with the general position of the track being bluer for lower metallicities and probably also for lower CNO content. Thus, for a given Fe content, the smaller [CNO/Fe] is, the bluer the track, consistent with the indication from spectral analysis that [CNO/Fe] tends to be smaller in the hotter extreme helium stars than in the cooler R CrB stars.

If the scenario which we have sketched is appropriate for most giant helium stars, then the number ratios of C to He in R CrB and in XX Cam estimated by Cottrell and Lambert (1982), coupled with their estimates of the C to Fe and N/Fe ratios, have interesting ramifications for the absolute Fe abundance relative to solar and for the space distribution of R CrB stars. Cottrell and Lambert find C/H ~ 0.003 and 0.004 for the two stars, and, assuming that most of the surface material is helium, this implies an abundance by mass of 0.012–0.016. But this is only about 4–6 times the solar abundance and suggests that, if the abundance by mass of Fe is also solar, [C/Fe] ~ 0.6–0.8. However, Cottrell and Lambert estimate [C/Fe] ~ 1.5 and 1.2, respectively, for the two stars, and one infers that Fe must be deficient by factors of 8–2.5 relative to solar. The only way in which this inference affects our analysis of surface abundances produced by merged degenerate dwarfs is in the amount of C-rich and O-rich material which must be dredged up into the thick disk from the CO dwarf. Instead of about 0.01 $M_\odot$ of such material, we now need only 0.001–0.003 $M_\odot$. The high values of N to Fe are still a consequence of the conversion of primordial C and O into N in the precursor of the helium dwarf. The primordial ratio of all CNO elements to Fe might be expected to be less variable than is the Fe abundance alone, so that the variation in [N/Fe] from one giant helium star to another might be expected to be less dramatic than changes in [C/Fe] and [O/Fe].

The inferred low abundances of Fe suggest that the R CrB stars and, by association, the other types of giant helium stars are members of a population older than that formed by disk stars, and this is consistent with the value of $\langle |z| \rangle \sim 1000$ pc estimated directly for the hot helium stars. However, we are now presented by an additional conundrum. Since the progenitor of the CO dwarf in the merged degenerate dwarf scenario is, in most instances, initially more massive than 2.3 $M_\odot$ and therefore might be expected to belong to a young population, how are the metallicity, kinematic, and spatial characteristics of an older population developed? There are at least two effects which may contribute to an explanation. The simplest is that it takes time for the radiation of gravitational waves to bring the dwarfs close enough together to interact by mass transfer. At any moment throughout Galactic history, degenerate dwarf precursors are being formed with varying orbital separations and therefore variable time scales prior to merging. It is plausible to suppose that the precursors of most of the giant helium stars which we are now seeing were formed at a time when the scale height of the active star-forming region was several times larger and when the average metallicity of the interstellar medium was several times smaller than now. Another possibly contributing factor is that, in the merging process, some matter is lost asymmetrically from the system, which consequently achieves a larger space velocity than that with which it was initially formed. One might expect this rocket effect to be significant if the time scale for the conversion of the lighter dwarf into a thick disk is smaller than or comparable to the orbital period of the premerging system.

ii) *Bright Shell Helium-Burning Giants in Close Binaries*

Some of the properties of giant helium stars can be understood in terms of our models which, while experiencing a second phase of mass loss, develop a degenerate CO core of mass 0.894 $M_\odot$ and 1.05 $M_\odot$ and a helium-rich envelope of mass ~ 0.013 $M_\odot$. These models are appropriately bright, and there are no vestiges of hydrogen at their surfaces. However, by far the most abundant CNO element at their surfaces is nitrogen, so these models cannot account for objects such as R CrB or XX Cam. The lifetime of the 0.894 $M_\odot$ remnant at the highest "plateau" luminosity and at surface temperatures comparable to that of the cool HdC stars is about 10^4 yr, and, at surface temperatures appropriate to the hotter group of giant helium stars, the lifetime is also $\sim 10^4$ yr. The interval of "permitted" initial separations for the formation of appropriate systems is about $\Delta \log A \approx 0.6$–$1.2$, and from equation (14) we estimate the frequency of formation of giant helium stars via this route to be $\nu \sim 10^{-2}$ yr^{-1}. Thus, at any one time, the total number of nitrogen-rich, carbon-poor, and oxygen-poor giant helium stars in the Galaxy formed in this way is of the order of $\sim 10^{-2}$ yr$^{-1} \times 2 \times 10^4$ yr ~ 200, roughly 5 times less than the number of giant helium stars estimated from the observations. The cooler giant helium stars formed in this scenario evolve into hotter nonvariable helium stars in a fashion advocated by Heber and Schönberner (1981). The low relative abundance of carbon in surface layers of the models might inhibit the occurrence of pulsations and thus account for the fact that no R CrB stars analyzed spectroscopically show such underabundances. Some might pulsate, however,

and a decrease in pulsational periods such as exhibited by S Aps and RY Sgr could be interpreted as due to contraction, and our large helium-rich models can be accommodated nicely in this regard as they evolve from red to blue at constant luminosity. A secular increase in the pulsational period such as appears to occur for UW Cen could be viewed as a temporary expansion caused by some other process. In summary, this scenario could account for perhaps one out of every five giant helium stars, but only those with very large overabundances of nitrogen relative to carbon and oxygen.

Further, since the primaries of progenitor systems must have masses in the range 6–10 $M_\odot$, and since there is only a very small time lag between the cessation of the mass-loss phase and the bright helium star phase, the distribution of product giant helium stars is expected to be characterized by a rather small scale height perpendicular to the Galactic plane.

In § VIII*e* we shall discuss the possible formation of planetary nebulae with central stars which are simply hotter versions of the giant helium models on which we are here focusing. The difference between the story there and here is that, in order to achieve a planetary nebula, we must assume matter is ejected from the system, and this implies that the companion of the mass donor is a very low mass main-sequence star, a compact helium star, or degenerate dwarf. Here we can include situations in which the mass donated by the potential giant helium star is accreted by the companion. This means that the companion can be of mass comparable to that of the primary in the initial system. Thus, we might expect some giant helium stars (which are also nitrogen rich) to have companions in the mass range 5–10 $M_\odot$.

Upsilon Sagittarii with orbital period ~138 days (Plavec 1973; Schönberner and Drilling 1983), KS Per with orbital period 360 days (Wallerstein, Greene, and Tomley 1967; Plavec 1973; Drilling and Schönberner 1982), and LSS 4300 (Schönberner and Drilling 1984) may be examples of this sort of evolution. It should be noted, however, that Lauterborn (1970) interprets these stars in terms of models which have undergone case C–type mass loss. Upsilon Sagittarii is a single-lined binary consisting of a helium-rich supergiant with $T_e = 10^4$ K, $M_V = -7$, and mass ~1 $M_\odot$ and a presumably unevolved component more massive than ~5–10 $M_\odot$. The hydrogen abundance in the helium component is less than ~0.0001 by mass (Schönberner and Drilling 1983). The low mass of the supergiant together with its extremely high luminosity suggests a CO core with a helium-rich envelope of very small mass as a possible and even rather probable model. The more massive companion is not seen optically, presumably because of the huge luminosity of the supergiant. KS Per has parameters close to those of υ Sgr. The more massive component is a main-sequence star of mass ~5–6 $M_\odot$, while its companion, of mass ~1 $M_\odot$, is a helium-rich supergiant with $T_e \sim 10^4$ K, $\log g \sim 1$, $X_H \lesssim 10^{-4}$ (Wallerstein, Greene, and Tomley 1967). Both of these systems can therefore be understood in terms of our computed models.

Orbital periods provide an opportunity to estimate the primordial semimajor axes of the two systems. The semimajor axes of υ Sgr and KS Per are now approximately equal at $A_f \sim 200$–400 $R_\odot$. In accordance with formula (1), the primordial semimajor axes may have been on the order of 5 times larger than A_f, or $A \sim 10^3$–(2×10^3) $R_\odot$. But primaries in such wide systems fill their Roche lobes only after the formation of a degenerate CO core, and the experiments of Lauterborn (1970) suggest that, after the first mass-loss episode, the abundance of hydrogen at the surface of the primary may be as large as $X_H \sim 0.2$. We can circumvent the inference of large initial orbital separation by supposing that the masses of the components of the initial primary are comparable. Then, during the first common-envelope phase, a considerable fraction of the mass lost from the primordial primary is actually accreted by the primordial secondary rather than lost entirely from the system, as is assumed in deriving equation (1). Assuming the primordial masses of the components to be 5 $M_\odot$ and 5 $M_\odot$ and the final masses to be 1 $M_\odot$ and 9 $M_\odot$, we can estimate the primordial semimajor axes in the case of precise conservation of orbital angular momentum to be ~70–140 $R_\odot$, and these separations are large enough to permit the primary to develop a large helium core prior to the first episode of mass loss and then to go on to develop a surface devoid of hydrogen during a second mass-loss episode.

The Lauterborn (1970) experiment for a case C mass-transfer system assumes conservation of total system mass and angular momentum during mass loss from the primary. However, early AGB stars possess very deep convective envelopes, as do the giants studied in our experiments, and one might expect initial mass-transfer rates much larger than those obtained when conservation of total system mass and angular momentum is assumed. Experiments in progress (Iben 1985*a*) show that, if one assumes mass loss on a thermal time scale while the radius is larger than some predetermined value, case C transfer will in some instances expose at the surface layers which are essentially devoid of hydrogen. Thus, it is perhaps also possible to produce systems having the properties of υ Sgr and KS Per even from initially wide systems in which component masses are not comparable but in which common-envelope action causes pronounced orbital shrinkage and disperses from the system most of the original mass of the primary. The different results of the two sets of experiments illustrate that there are still tremendous quantitative uncertainties in our understanding of binary mass transfer and that many more concrete examples must be studied both observationally and theoretically in an effort to reduce these uncertainties.

iii) *Low-Mass Origins*

In the interest of completeness we discuss briefly an additional scenario involving helium shell flashes in single stars during the post–AGB (P–AGB) phase of evolution. Approximately 10% of all P–AGB stars are expected to undergo a final helium shell flash after they have achieved a hot white dwarf configuration (Iben 1984*a*). It has been proposed that such stars can develop a helium-rich and carbon-rich surface either as a consequence of mixing to the surface by shell convection during this flash (Iben *et al.* 1983), or as a consequence of mixing inward from the surface by envelope convection when the star expands once again to giant dimensions (Renzini 1979; Iben *et al.* 1983; Iben 1984*a*), or both.

The models are of an appropriately large luminosity, and their expected frequency of occurrence is not inconsistent with the estimated numbers of giant helium stars. To demonstrate this, we assume that $N/\tau_{He} = \nu/10$, where N is the estimated

number of quiescent helium-burning P–AGB stars, τ_{He} is their lifetime, and ν is their birthrate. Setting $\nu \sim 0.5$ yr^{-1} (Weidemann 1979) and $N \sim 1000$, we have $\tau_{He} \sim 10^4$ yr. From the models (Iben 1984*a*) we have that $\tau_{He} \sim 4 \times 10^4$ yr $(0.6\ M_\odot/M_*)^{10}$, where M_* is the mass of the P–AGB star. Combining the two estimates for τ_{He} we infer that the typical mass of a helium-burning P–AGB star may be $M_* \sim 0.64\ M_\odot$. During most of the quiescent helium-burning phase, the luminosity L_* of a model is, within a factor of 2, $L_* \sim 6 \times 10^4\ L_\odot\ (M_*/M_\odot - 0.5) = 0.84 \times 10^4\ L_\odot$, and this luminosity is not inconsistent with estimates for giant helium stars.

Unfortunately, most of the time at high luminosity is spent far to the blue of the location of the giant helium stars. Models of mass $M_* \sim 0.6$–$0.7\ M_\odot$ and with no surface hydrogen remain giants for only a few hundred years, or for a time which is comparable to the thermal time scale of a giant envelope. Thus, assuming the models to be trustworthy, the P–AGB scenario is able to account for only a percent or so of all giant helium stars.

d) *Shell and Be Stars*

We have seen that a possibly substantial fraction of the primary mass may be accreted by the secondary during the first common-envelope mass exchange phase. In wide binaries, the accreted matter carries a large angular momentum. An ordinary main-sequence star has a relatively small gyration radius ($\sim 0.1\ R_\odot$), and therefore the accretion of only a small amount of mass from the primary is enough to accelerate the rotation of a relatively unevolved secondary to the breakup rate. However, if accretion occurs on a time scale smaller than the thermal time scale of the secondary, the secondary may expand enough to avoid a potential catastrophe and accrete matter with high angular momentum per unit mass. Nevertheless, a substantial fraction of the matter transferred by the primary may wind up in a mass-losing common envelope, and, after "all of the dust has settled," one might anticipate a remnant disk of material surrounding the binary to remain bound to the system. If the final binary is close ($P_{orb} \lesssim 10$ days), then the angular momentum of the disk can be transformed into the angular momentum of orbital motion. The establishment of corotation over several thermal time scales (Zahn 1977) helps the secondary component to lose its perhaps excessive intrinsic angular momentum. But if the system is wide, then the time scale for angular momentum loss could be rather large since orbital braking in this circumstance is not as efficient. Typical stellar winds from single stars with masses less than $\sim 20\ M_\odot$ are fairly weak, and, without the amplifying influence of a magnetic field frozen into wind matter, such winds cannot help much in extracting the excessive angular momentum sufficiently rapidly. For reasons such as these, Rappaport and van den Heuvel (1982) have suggested that, in wide binaries, the component which has accreted matter from its companion may continue to rotate at rates on the verge of breakup, long after the accretion event is over. The analysis of observed properties of Be stars that are members of spectroscopic binaries provides some support for this scenario. Popova, Tutukov, and Yungelson (1982) have found about 10 Be stars in binaries characterized by $A \gtrsim 50\ R_\odot$.

Several observed Be stars may still be in the accretion stage, when the mass-exchange rate is relatively low and the common envelope is not evident (Harmanec, Koubsky, and Kzpata 1972; Kriz and Harmanec 1975; Plavec *et al.* 1982). Taking into account the possibility that shell stars and Be stars are not so much representatives of a homogeneous class as they are members of a heterogeneous group that exhibit a particular phenomenon (in this case, the presence, perhaps for diverse reasons, of a large amount of rapidly rotating gas in an envelope around a hot star), we can reasonably assume that binary interaction may be responsible for the formation of at least a few members of the group. Plavec (1973) and Plavec *et al.* (1982) present several concrete examples of Be and shell stars that are members of wide binaries experiencing mass exchange: 88 Her, 17 Lep, AX Mon, ζ Tau, etc. These systems provide evidence that at least some Be and shell stars may owe their characteristics to their presence in a close binary. Shell stars may be Be stars seen pole-on. That current duplicity is not a necessary condition for producing the Be star phenomenon seems to be established by the case of ω Ori (Abt and Levy 1978). Further, Abt and Cardona (1984) show that the frequency of Be stars with known companions is essentially the same as the frequency of B stars with known companions.

The common property of Be stars is a rapidly rotating (possibly on the verge of instability) central star surrounded for some reason by an extended dense envelope which transforms some of the stellar radiation into emission lines. The reason for the fast rotation of the central star may be in some instances the presence of a double core created in the stellar formation process during the accretion regime (Kraicheva *et al.* 1978). Such a central star could be characterized by a periodic variation in its brightness at a period shorter than that of the fundamental radial mode of the star. Possible examples of this scenario have been found, but the evidence is not yet convincing. For example, Percy (1983) has demonstrated that the Be star HR 9070 has periodic variations in its brightness at a period of 0.307 days and amplitude ≈ 0.03 mag.

e) *Massive Nuclei of Helium-rich Planetary Nebulae*

In single AGB stars, which are thought to be the precursors of most planetary nebula nuclei (PNNi), the mass of the helium-rich layer between the CO core and the hydrogen-rich envelope is a strong function of the mass of the CO core. Just before each thermal pulse, the mass ΔM_{He} of this layer is related to the core mass M_{CO} by $\Delta M_{He} \sim 2\ \Delta M_H \sim 0.02\ M_\odot\ (0.6\ M_\odot/M_{CO})^8$, where ΔM_H is the mass of matter processed by the hydrogen-burning shell between pulses (Iben 1984*a*). During a pulse and during the subsequent quiescent helium-burning phase, ΔM_{He} is decreased by roughly a factor of 2 to $\Delta M_{He} \sim \Delta M_H$. A single star will not depart from the AGB until it has ejected (presumably in the form of a planetary nebula) all but a mass of about $\Delta M_H/10$ of hydrogen-rich matter above the helium-rich layer. During the subsequent PNN stages, the remnant star can burn either hydrogen or helium or both, depending on precisely when in the thermal pulse cycle departure from the AGB occurs (Iben 1984*a*), and it does so at luminosities close to that given by the core mass–luminosity relationship for AGB stars: $L \sim 6 \times 10^4\ L_\odot\ (M_{CO}/M_\odot - 0.5)$. The net result is that the lifetime of the PNN stage is a very strong function of M_{CO} or, through the

core mass–luminosity relation, of the luminosity. In first approximation this lifetime may be written $\tau_{\rm PNN} \sim (1.6\text{–}4)\times 10^4$ yr $(0.6\ M_\odot/M_{\rm CO})^{10} \sim (1.6\text{–}4)\times 10^4$ yr $(6000\ L_\odot/L)^3$, where the smaller figure is appropriate for hydrogen-burning PNNi and the larger figure for helium-burning PNNi (Iben 1984*a*).

A quite different behavior is predicted by our models for the evolution of a PNN produced by a close binary. There are many parts to the story, but we shall focus on only one. As we have seen, components of initial mass in the range 5–10 $M_\odot$ experience a second phase of mass loss. When the amount of mass lost is substantial, it consists primarily of helium, and the stellar remnant evolves to the blue at high luminosity, eventually achieving surface temperatures large enough for the ejected nebular material to be excited into fluorescence.

Apart from the fact that the nebular matter consists essentially of pure helium, the most remarkable feature that distinguishes this situation from the single-star case is that the lifetime of the remnant at high luminosity and high surface temperature is only weakly dependent upon the mass of the remnant. In all three relevant cases ($M_{\rm remnant} = 0.752$, 0.894, and 1.06), this lifetime is on the order of $\tau_{\rm PNN} \sim (2\text{–}3)\times 10^4$ yr (see Figs. 1–3). The reason for this is that, although the luminosity is still given to good approximation by the core mass–luminosity relation for single hydrogen-burning AGB stars, the mass of helium fuel with which the remnant in a close binary leaves the region of giants is nearly independent of remnant mass, being $\Delta M_{\rm He} \sim 0.013$ in all three cases, and most of this fuel is used up during the PNN phase. Thus, $\tau_{\rm PNN}$ varies from one case to the next only because the plateau luminosity varies among the cases. At maximum brightness along the plateau portion of each track, our models are characterized by $M_{\rm bol} \sim -5.6$ ($M_{\rm remnant} = 0.752$), $M_{\rm bol} \sim -6.2$ ($M_{\rm remnant} = 0.894$), and $M_{\rm bol} \sim -6.8$ ($M_{\rm remnant} = 1.06$). At these same magnitudes, the lifetime of a PNN derived from a single AGB star would be $\tau_{\rm PNN} \sim$ 2000–5000 yr, 250–600 yr, and 16–40 yr, respectively.

Since the rate of mass transfer during the second phase of mass loss from a given component is several orders of magnitude smaller than during the first phase, whether or not a common envelope (and hence a potential planetary nebula) is formed depends upon the mass and compactness of the companion of the mass donor. The most favorable situation occurs when the companion is a compact helium star or degenerate dwarf.

The final characteristic to be emphasized is the composition of the ejected nebula. This nebula will consist primarily of helium, and the CNO elements will be in a distribution formed during hydrogen burning at high temperatures; namely, $N \gg C > O$.

In summary, in a close binary which initially contains components of mass in the range 5–10 $M_\odot$, a fourth episode of mass transfer may produce a helium-rich and nitrogen-rich planetary nebula which fluoresces for $(1\text{–}2)\times 10^4$ yr and at the center of which is a binary system consisting of a very hot ($T_e \gtrsim 10^5$ K) star of magnitude $M_{\rm bol} \sim -6 \pm 0.5$ and a fairly massive degenerate dwarf or compact helium star. The nebular mass may vary from $\lesssim 0.1\ M_\odot$ to $\gtrsim 1\ M_\odot$. The formation probability of such a system in our Galaxy should be very similar to the rate of formation of giant helium stars via the scenario described in § VIII*c*(ii), and there should therefore be on the order of 100 of them at any one time in the Galaxy.

One should also expect to find about 10 such planetary nebulae in the Magellanic Clouds at any one time. In fact, a recent UV search (Maran *et al.* 1982; Stecher *et al.* 1982) has revealed three PNN which appear to be intrinsically uncommonly bright, with $M_{\rm bol} \sim -6.5$. Given that the theoretical lifetime of such a bright PNN deriving from a single AGB star is less than or about 100 yr, the presence of so many bright PNNi in the Clouds is perhaps more easily understood in terms of the scenario we are proposing here.

f) *Cooling Curves for Degenerate Dwarfs in Close Binaries*

Close binary components with initial masses in the range 2.3–10 $M_\odot$ will evolve into compact helium stars and then become degenerate CO (or HeCO) dwarfs if the initial semimajor axis of the binary is in the approximate range 6–700 $R_\odot$, with the lower limit increasing from about 6 $R_\odot$ to 16 $R_\odot$ and the upper limit increasing from about 25 $R_\odot$ to 700 $R_\odot$ as component mass increases from 2.3 $M_\odot$ to 10 $M_\odot$ (see Fig. 31). Degenerate CO dwarfs form also during the evolution of binaries with initial component masses in the range 1–9 $M_\odot$ if the semimajor axis of the binary is initially in the range 25–1600 $R_\odot$, again with both lower and upper limits being a function of component mass. From § V, we have that the frequency of formation of CO dwarfs in close binaries is about $\nu_{\rm CO}^{\rm close} = \nu_{\rm CO}^{\rm TP} + \nu_{\rm CO}^{\rm E} + \nu_{\rm CO}^{\rm He\rightarrow CO} \sim 0.09$ yr^{-1}. Since the total frequency of CO dwarf formation in our Galaxy is about 0.5–1 yr^{-1} (Iben and Tutukov 1984*b*), roughly 10%–20% of all CO dwarfs are formed in close binaries and formed in a mass distribution somewhat different from that of single stars. Thus, the close binary star contribution to CO dwarf statistics is not negligible, and it is of interest to study the cooling curves and the related space density–stellar magnitude curves of the CO dwarfs which are the products of close binary star evolution (e.g., the models we have obtained for this paper) and to compare several of them with those of CO dwarfs of mass 0.6 $M_\odot$ studied in an earlier paper (Iben and Tutukov 1984*c*).

Each cooling curve for the models we have selected has been transformed by standard procedures into a relationship between the space density of dwarfs and their absolute bolometric magnitude, assuming the same formation frequency in each case. The results are shown in Figure 35, along with results taken from Iben and Tutukov (1984*c*) for dwarfs of mass 0.6 $M_\odot$. For the latter CO dwarfs we have presented two curves, one for those whose progenitors depart from the AGB during the shell hydrogen-burning stage and do not experience another shell helium flash before becoming cool white dwarfs (case A) and another for those whose progenitors do experience a P–AGB helium shell flash (case B). Case A dwarfs have a hydrogen-rich envelope of mass $M_e \sim (1\text{–}3)\times 10^{-4}\ M_\odot$ and continue to burn hydrogen via the *p-p* chains during much of their lifetime, whereas case B dwarfs have no hydrogen at the surface and are therefore generically related to those CO dwarfs formed in close binaries in which hydrogen burning does not influence the evolution. In all cases, we set $t = 0$ at the moment when the progenitor of the dwarf first reaches an effective temperature $T_e = 30{,}000$ K in evolving from the red to the blue.

At low luminosities, the differences between curves for different masses are minor, and we can conclude that cooling

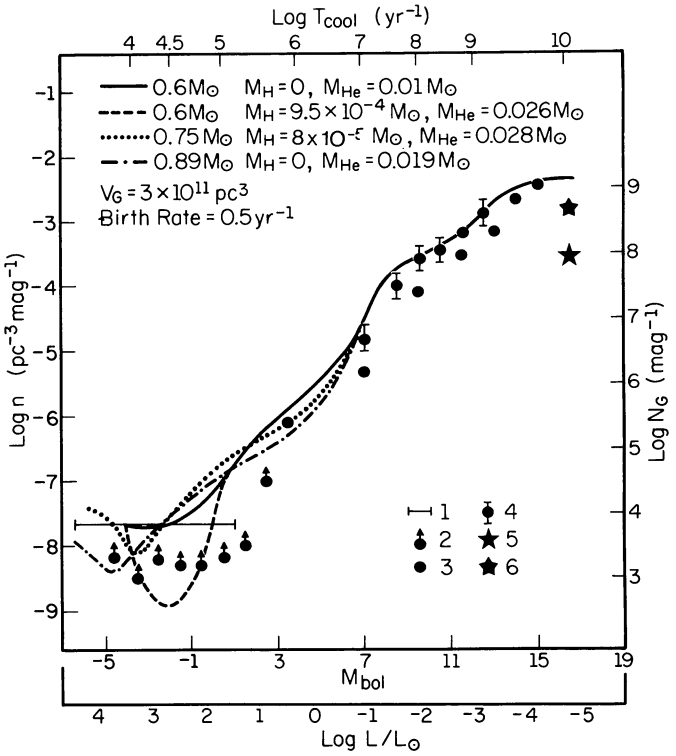

FIG. 35.—Theoretical luminosity functions for CO degenerate dwarfs of different masses. The dwarf formation rate is in each case assumed to be 0.5 yr^{-1}, and the galactic volume $\sim 3\times10^{11}$ pc^3 (Iben and Tutukov 1984*b*). Data taken from (1) Cahn (1983), (2) Kaler (1983), (3) Sion and Liebert (1977) and Liebert (1980), (4) Green (1977), (5) Liebert (1979) and Liebert *et al.* (1979), and (6) Iben and Tutukov (1984*c*).

curves for dwarfs with masses between 0.6 $M_\odot$ and 1.0 $M_\odot$ do not depend significantly on the dwarf mass. Only for the brightest white dwarf precursors ($M_{bol}<1$) do distribution functions for different masses and origins differ from one another to any great extent. For single stars, derived distribution functions for $M_{bol}<1$ differ from one another not primarily because of differences in progenitor masses, but because of differences in the phase in the thermal pulse cycle at which a precursor star leaves the AGB to become a PNN. Case B progenitors of white dwarfs burn helium on a long time scale at high luminosities, whereas case A progenitors experience a phase of rapid dimming when the rate of hydrogen burning via the CN cycle abruptly becomes insignificant. We see from Figure 35 that, to achieve agreement with the observed distribution of PNNi in the magnitude range $-4<M_{bol}<0$, a considerable fraction of all PNNi must be in the helium-burning stage.

In computing the evolution of the CO dwarfs derived from close binaries, we have assumed that no further mass is lost following the second detachment from the Roche lobe. However, we know from the observations that PNNi lose mass via a stellar wind (e.g., Perinotto 1983), and an understanding of the observed frequency of formation of DA and non-DA white dwarfs can be achieved by invoking such winds (Iben 1984*a*). It is interesting to know how large a wind mass-loss rate would be required to strip off all remaining vestiges of hydrogen from our 0.75 $M_\odot$ model remnant. From Figure 12 we see that approximately 10^{-4} $M_\odot$ must be lost. If a wind were to act at a constant rate over that portion of the track in Figure 1 between points M and N, a mass-loss rate of $\dot{M}\sim -2\times10^{-9}$ $M_\odot$ yr^{-1} would suffice. If the 0.89 $M_\odot$ remnant of the 6.95 $M_\odot$ model were to lose mass at the rate 2.5×10^{-7} $M_\odot$ yr^{-1} between points K and Ω, one might expect it to lose its helium-rich envelope. However, since it is helium burning that controls the rate of evolution across the H-R diagram at nearly constant luminosity, the actual effect of such a high rate of mass loss would not be to divest the star of its entire helium-rich envelope but rather to speed up the evolution along the track until the mass of the helium-rich envelope decreases below a critical limit. The model would then dim and cool rapidly, and the rate of mass loss would presumably drop at least as rapidly.

Although, in most instances, the formation of one degenerate CO dwarf in a close binary will be followed ultimately by the formation of a second degenerate CO dwarf, the probability of detecting such double degenerate dwarf systems is considerably reduced by the fact that the first-formed dwarf may have dimmed considerably before the second one is formed. The heating inside the final common envelope which is instigated by the secondary during shell helium burning (Taam 1979) is not enough to restore the interior of the cold remnant of the primary to its original high temperature. Therefore, after the final common-envelope stage, the first-formed remnant cools rapidly until it achieves the low interior temperature and low luminosity which it had attained prior to the final common-envelope episode. The cooling time is so short that the dwarf will dim by many magnitudes before the ejected matter expands enough to become transparent to the optical radiation from the double core. At this point, the ejected matter will appear as a "classical" planetary nebula excited by the last-formed degenerate remnant. The first-formed remnant will escape ready detection because of its low luminosity.

g) *Barium Stars and* CH *Stars*

Barium stars are Population I stars which exhibit overabundances, relative to Fe, of barium and of other *s*-process elements (Bidelman and Keenan 1951; Boyarchuk 1974; Tomkin and Lambert 1979; Cowley and Downs 1980). Carbon appears to be nearly normal (Pilachowski 1977; Sneden, Lambert, and Pilachowski 1981), but Tomkin and Lambert (1979) and Lambert (1984) demonstrate a correlation between carbon and *s*-process element abundances. CH stars are the Population II counterparts of the Ba stars.

Ba stars were identified first among red giants, and it is estimated that about 1% of all red giants are Ba stars (see McClure 1983, 1984*a*, *b*). However, it is also known that the Ba or CH star abundance syndrome is not limited to giants (e.g., Bond 1974; Sneden and Bond 1976; Luck and Bond 1982; Lambert 1984). For example, two main-sequence stars —the K5 dwarf ε Ind (Kollatschny 1984) and the G8 dwarf ξ Boo A (Boyarchuk and Eglitis 1984)—display overabundances of Ba, La, Ce, Nd, Eu, and Zr relative to Fe by factors of 2–10. Lambert (1984) reviews the overall situation, showing that the Ba and CH abundance syndromes occur in stars of nearly all types, from main-sequence stars of near-solar luminosity to stars at all levels along the giant branch with luminosities up to several thousand times solar.

The origin of the spectral characteristics of Ba stars and of CH stars has in recent years often been attributed to some phenomenon which can occur only in a close binary (Böhm-Vitense 1980; McClure 1980, 1983, 1984*a*, *b*; McClure, Fletcher, and Nemec 1980; Dominy and Lambert 1983; Böhm-Vitense, Nemec, and Proffitt 1984; Lambert 1984). The argument goes as follows. The luminosities and radii of the giant Ba stars imply that they have degenerate helium cores, primordial masses less than about 2.3 $M_\odot$, and deep convective envelopes. Models of such stars do not form *s*-process elements themselves, and, as suggested by McClure, Fletcher, and Nemec (1980) and by D'Antona and Mazzitelli (1980), they may owe their peculiar surface compositions to the one-time presence of a primordially more massive companion which passed through the AGB phase with a degenerate CO core. During the thermally pulsing AGB phase, the companion presumably generated *s*-process elements in its convective helium-burning shell, dredged this material to its surface, and transferred the enriched material (presumably by Roche-lobe overflow) to the star which is now called a Ba or CH star. The idea of pollution by a companion has, of course, been broached in many other contexts (e.g., van den Heuvel 1968*a*, *b*).

Overabundances of Ba and other *s*-process elements typically reach factors of ~ 3–10 (Boyarchuk 1974). The theoretical overabundances of these elements in bright AGB stars which lose mass at the Reimers rate and live for about 10^6 yr may become as large as a factor of 20 (Iben and Truran 1978), but real AGB stars with large enough CO cores to permit the production of *s*-process isotopes by the capture of neutrons due to the $^{22}\mathrm{Ne}(\alpha, n)^{25}\mathrm{Mg}$ reaction probably live for only $\sim 10^5$ yr (see Frogel and Blanco 1984; Aaronson and Mould 1985; Iben 1984*b*) and therefore can generate only a factor of 2 or so overabundance in the eventually accreted matter. Since this enriched matter will be diluted further by convective mixing with unprocessed material in the star which has accreted it, we infer that the companion which produced the *s*-process isotopes at overabundances greater than the factor of 3–10 found in Ba stars must be of fairly low mass and generate *s*-process elements by tapping some neutron source other than the $^{22}\mathrm{Ne}(\alpha, n)^{25}\mathrm{Mg}$ reaction. The most likely reaction has long been suspected to be $^{13}\mathrm{C}(\alpha, n)^{16}\mathrm{O}$, and recent observational evidence (e.g., Tomkin and Lambert 1983; Lambert 1984) and theoretical evidence (e.g., Iben and Renzini 1982, 1983; Iben 1983) support this suspicion.

Since by now it has been rather convincingly established that Ba and CH stars are all probably members of binaries (Böhm-Vitense 1980; McClure 1980; McClure, Fletcher, and Nemec 1980; Dominy and Lambert 1983; McClure 1983, 1984*a*, *b*) with orbital periods typically in the range 100–1000 days, and since the typical mass of the current (red giant) secondary is perhaps 2–3 times smaller than the mass of the progenitor of the degenerate dwarf companion (McClure 1983, 1984*a*, *b*), the inference of a causal connection between the high duplicity rate and the surface composition anomalies is quite attractive. The relatively short orbital period, coupled with the high probability that the massive component is a CO dwarf, suggest strongly that the system must have passed through a common-envelope stage during which the transfer of enriched material could have occurred.

It is possible to quantify this argument. From Figure 31 we have that, if mass loss from the primary is not to occur prior to the TP–AGB phase, then the orbital separation must be sufficiently large to permit the primary to achieve a radius given approximately by $R_1 \sim 10^{2.25}(M_1/2.3)^{0.545S}$, where $S = 0$ when $M_1 < 2.3$ and $S = 1$ when $M_1 \geq 2.3$. We may relate the semimajor axis to the Roche-lobe radius of the primary by $R_\mathrm{R} \approx 0.52A(M_1/M_t)^{0.44}$ (Tutukov and Yungelson 1979*b*) and set $P_\mathrm{orb} = (0.1 \text{ days})A^{3/2}/M_t^{1/2}$, where $M_t = M_1 + M_2$ is the total mass of the system. Setting $M_2 = 1$ and $R_1 = R_\mathrm{R}$, we find that the minimum orbital period is about 750 days at $M_1 \sim 2$ and varies from about 1000 days at $M_1 = 1$ to about 2000 days at $M_1 = 9$. It follows that considerable orbital shrinkage, presumably because of common-envelope action, must have occurred in those binaries containing Ba stars for which the orbital period is much less than 750 days.

We next ask, at what stage in its evolution is it most likely that the proto-Ba or proto-CH star intercepts some enriched matter from its companion? Suppose that mass transfer from the AGB primary begins when the secondary is still on the main sequence. We might suppose that the main-sequence secondary becomes inflated to giant dimensions in response to accretion at a rate larger than M_2/τ_KH. But since the companion of the Ba star is now presumably a white dwarf, the mass-transfer event must have been already completed. The thermal time scale of a red giant envelope is only about 10^{-4} of the nuclear time scale of an isolated giant, so that the "bloated" stage of the main-sequence core could be maintained after the accretion event has been terminated for only 10^{-4} of the lifetime of a typical isolated giant. This scenario can therefore not *directly* account for the high ($\sim 10^{-2}$) frequency of Ba stars among giants. That is, even if the mass-transfer event could be maintained for 100 times longer than expected, the envelope would eventually have to contract and the Ba giant would revert to main-sequence dimensions. However, main-sequence stars eventually become giants, so this scenario could account for the known (1%) frequency of giant Ba stars if it were eventually to be established that 1% of all main-sequence stars display the Ba star abundance syndrome.

If the secondary is already a giant when it intercepts some of the matter lost by the primary while it is an AGB star, one might expect once again that a significant fraction of the mass lost by the primary may be intercepted. Giant stars with large radius and luminosity are characterized by a short thermal time scale and are therefore good accretors of the common-envelope matter enriched by *s*-process elements. Let us assume that the accreting giant has a mass M_RG and a surface abundance X_RG of some element and that it accretes from the primary an amount m ($\ll M_\mathrm{RG}$) of matter having an abundance X ($\gg X_\mathrm{RG}$) of the same element. Since the proposed accretor is a normal giant with a deep convective envelope, we assume that the accreted matter will immediately be mixed with the approximately $0.5M_\mathrm{RG}$ of the matter in this envelope. After a simple transformation, we have that the new abundance in the red giant will be

$$X'_\mathrm{RG} \approx X_\mathrm{RG} + 2\frac{m}{M_\mathrm{RG}}X. \tag{15}$$

For example, to achieve a factor of 3 overabundance of barium in the red giant when the overabundance of barium in the mass donor is, say, a factor of 10, one requires $m/M_{RG} = 0.1$. Thus, the addition of only 10% more matter to the red giant is enough to produce the Ba syndrome.

We can estimate the frequency of Ba star formation via this scenario. If we insist that the primary must fill its Roche lobe while being a TP–AGB star, then $460 \lesssim A/R_{\odot} \lesssim 2000$, or $\Delta \log A = 0.6$. About 12% of all binaries can fulfill this condition. Let us suppose that the secondary is a red giant with $L \gtrsim 10^2\ M_{\odot}$. The lifetime of such a bright giant is, depending on its mass, about 1%–10% of its main-sequence lifetime, and this percentage is a measure of the probability that the primary becomes a TP–AGB star while the secondary is a giant. Thus, 10^{-3} to 10^{-2} of all giants could become Ba stars by accreting matter from a TP–AGB companion. Taking into account the tendency of binary components to be of comparable mass, the upper limit of this estimate is most likely, in agreement with the observed frequency of Ba stars among giants. The ease with which one can predict a frequency of occurrence close to that observed suggests that the frequency of Ba and CH stars among main-sequence stars may be considerably less than 1%.

We caution, however, that we have assumed that the efficiency with which matter is transferred between the AGB star and the red giant is large, and this assumption may not be justified. The complexity arises because in the course of mass transfer a common envelope which is in a convective state is likely to arise. Both the accretor and the donor have deep convective envelopes. Since the donor is initially more massive than the accretor, mass transfer will lead to a decrease in the semimajor axis, and the convective secondary eventually also fills its Roche lobe and a convective common envelope is formed. If the matter of both envelopes were completely adiabatic, and if the entropy of the common envelope were smaller than the entropy of the red giant convective envelope, mass exchange between the two envelopes would proceed on the convective-envelope mixing time scale, or on only several dynamical time scales. If the ordering of entropies is the reverse, then the thermal time scale seems more relevant for the accretion time scale. Despite the many interesting details of the ensuing physics, the final result of such a process is undoubtedly still a usual pair of degenerate dwarfs, but the mass exchange could lead to unusual surface abundances.

Thus, ending our discussion of the Ba syndrome, we conclude that the most promising scenario for their origin is mass exchange between components of a binary in which, during the mass-transfer episode, the primary is a thermally pulsing AGB star with a CO core and the secondary is a giant with a degenerate helium core. An outstanding problem which must be addressed is the nature of mixing between matter of two giants immersed in a common envelope.

IX. SUMMARY

Binary components that fill their Roche lobes after central hydrogen exhaustion, but before or near the onset of core helium burning, experience one or two phases of mass loss, depending upon their initial main-sequence mass. If they are initially of mass in the range $M_{MS} \sim 2.3$–$4.8\ M_{\odot}$, they fill their Roche lobes only once, not expanding again to giant dimensions following the exhaustion of helium at the center. They become degenerate dwarfs of mass between 0.3 and 0.7 and consist of a carbon-oxygen core surrounded by a helium-nitrogen envelope. The mass of the HeN layer relative to the mass of the CO core increases rapidly with decreasing remnant mass. If their main-sequence mass is in the range $M_{MS} \sim 4.8$–$10.3\ M_{\odot}$, they experience two episodes of mass loss. The second Roche-lobe–filling episode occurs after central helium exhaustion. During the first mass-loss episode, most of the hydrogen-rich envelope is lost. If, during the second episode, the mass of the helium core is in a narrow interval corresponding to a main-sequence mass between $4.8\ M_{\odot}$ and $5.2\ M_{\odot}$, the second mass-loss episode removes only a hydrogen-rich envelope, as the pure helium portion of the envelope above the helium-burning shell remains very compact. If the main-sequence mass is larger than $5.2\ M_{\odot}$, then the second mass-loss episode also removes helium-rich material, and this can be of substantial mass for the most massive stars in the range. Such stars may become giant stars with nearly pure helium envelopes, produce planetary nebulae consisting of helium and nitrogen, and evolve into DB white dwarfs. Components with main-sequence mass in the range 10.3–$10.6\ M_{\odot}$ and also some with mass in the range 8.8–$10.3\ M_{\odot}$ may evolve into "bare" oxygen-neon degenerate dwarfs of mass between $1.08\ M_{\odot}$ and $1.4\ M_{\odot}$. Components more massive than $10.6\ M_{\odot}$ cannot lose enough mass before igniting carbon to avoid a core collapse and a supernova explosion, which results in the ejection of all matter above the core, leaving a neutron star remnant. Close binary components of main-sequence mass less than $2.3\ M_{\odot}$ become helium degenerate dwarfs; those in the mass range 4.8–$8.8\ M_{\odot}$ and many of main-sequence mass in the 8.8–$10.3\ M_{\odot}$ range become CO degenerate dwarfs.

A very rough estimate of the frequencies with which degenerate dwarfs of all types are produced by both binary stars and single stars gives $\nu_{He} \sim 0.17\ \mathrm{yr}^{-1}$, $\nu_{CO} \sim 0.83\ \mathrm{yr}^{-1}$, and $\nu_{ONe} \sim (1\text{–}10)\times 10^{-4}\ \mathrm{yr}^{-1}$. About 10% of the double CO degenerate pairs formed in close binaries (total formation rate $\nu_{CO}^{close} \sim 0.09\ \mathrm{yr}^{-1}$) are massive enough (the maximum mass of a CO degenerate dwarf is $1.08\ M_{\odot}$) and, in a Hubble time, can be brought close enough together by gravitational-wave radiation to merge and evolve into Type I supernovae. Most binaries which produce at least one ONe degenerate dwarf also produce a CO dwarf at a sufficiently small separation from the ONe dwarf that merging will occur within a Hubble time; a core collapse initiated by electron capture and the formation of a rapidly spinning neutron star pulsar follow.

Double helium degenerate dwarfs arise from binary components of initial main-sequence mass less than about $2.3\ M_{\odot}$, and the total mass of a double helium-degenerate binary is expected to be less than about $0.5\ M_{\odot}$. For these reasons, double helium-degenerate binaries are not likely precursors of Type I supernovae, contrary to earlier estimates (Iben and Tutukov 1984*a*, *b*). A probable outcome of systems which form a CO dwarf and a He dwarf close enough to merge in a Hubble time is a giant helium star at the surface of which both carbon and nitrogen are overabundant and hydrogen is extremely underabundant relative to both helium and iron.

As many as four mass-transfer events may punctuate the transformation of an intermediate-mass binary system into a

close double degenerate pair. If the component masses are primordially comparable, it is likely that the components will alternate as mass donors, with most of the orbital shrinkage occurring during the last three mass-transfer phases when a common envelope forms. If the mass ratio is primordially small, then the primary will attempt to donate mass twice before the secondary has evolved appreciably.

Cooling curves for CO dwarfs with different masses may be divided into two segments: a shell helium-burning stage whose lifetime decreases with increasing dwarf mass in accordance with $\tau_{He} = E_{He} M_{He}/L_{CO}$ (where M_{He} is the minimum mass of a giant helium envelope that sits atop a CO core) and at the base of which a helium burning produces energy at the rate L_{CO}; and a second stage driven by neutrino cooling at a rate which essentially does not depend on the mass of the CO dwarf. Theoretical luminosity functions agree with those which can be estimated from the observations of nuclei of planetary nebulae.

It is a pleasure to thank the US National Science Foundation, the USSR Academy of Sciences, and the Research Board of the University of Illinois for their support. We sincerely thank Sandra Moy, Robert Penka, and Michael Randall for expediting the calculations required in the preparation of this paper. The patience and excellent draftsmanship of Robert MacFarlane, Joe Hartrich, and Susan Lefferts are gratefully acknowledged. Deana Griffin's cheerful mien and word-processing skill have been much appreciated. A. V. T. thanks Lev Yungelson and Ena Ergma for useful discussions, and I. I., Jr., thanks Professors Mustel and Massevich for making possible a visit to the Astronomical Council of the USSR Academy of Sciences, where much of the revision of the paper took place. Finally, thanks to Edward Olson, David L. Lambert, Detlef Schönberner, George Wallerstein, Ronald Webbink, and a very knowledgeable referee for enlightening comments which have helped us to excise errors and clarify arguments.

REFERENCES

Aaronson, M., and Mould, J. 1985, *Ap. J.*, **288**, 551.
Abt, H. A., and Cardona, O. 1984, *Ap. J.*, **285**, 190.
Abt, H. A., and Levy, S. 1978, *Ap. J. Suppl.*, **36**, 241.
Backer, D. C., Kulkarni, S. R., Heiles, C., Davis, M. M., and Goss, W. M. 1982, *Nature*, **300**, 615.
Barkat, Z. 1975, *Ann. Rev. Astr. Ap.*, **13**, 45.
Barkat, Z., Rakavy, G., Reiss, Y., and Wilson, J. R. 1975, *Ap. J.*, **196**, 633.
Barkat, Z., Reiss, Y., and Rakavy, G. 1974, *Ap. J. (Letters)*, **193**, L21.
Becker, S. A., and Iben, I., Jr. 1979, *Ap. J.*, **232**, 831.
_____. 1980, *Ap. J.*, **237**, 111.
Benson, R. S. 1970, Ph D. thesis, University of California, Berkeley.
Bidelman, W. P. 1953, *Ap. J.*, **117**, 25.
Bidelman, W. P., and Keenan, P. C. 1951, *Ap. J.*, **114**, 473.
Bodenheimer, P., and Taam, R. E. 1984, *Ap. J.*, **280**, 771.
Böhm-Vitense, E. 1980, *Ap. J. (Letters)*, **239**, L79.
Böhm-Vitense, E., Nemec, J., and Proffitt, C. 1984, *Ap. J.*, **278**, 726.
Bond, H. E. 1974, *Ap. J.*, **194**, 95.
_____. 1985, in *Cataclysmic Variables and Low Mass X-Ray Binaries*, ed. D. Q. Lamb and J. Patterson (Dordrecht: Reidel), in press.
Boyarchuk, A. A. 1974, in *IAU Symposium 66, Late Stages of Stellar Evolution*, ed. R. J. Tayler and J. E. Hesser (Dordrecht: Reidel), p. 188.
Boyarchuk, A. A., and Eglitis, I. 1984, *Bull. Crimean Ap. Obs.*, **64**, 1.
Cahn, J. 1983, private communication.
Cordes, J. M., and Wasserman, I. 1984, *Ap. J.*, **279**, 798.
Cottrell, P. L., and Lambert, D. L. 1982, *Ap. J.*, **261**, 595.
Cowley, Ch. R., and Downs, P. L. 1980, *Ap. J.*, **236**, 648.
D'Antona, F., and Mazzitelli, I. 1980, *Ap. J.*, **238**, 229.
De Cuyper, J. P. 1981, in *Pulsars*, ed. W. Sieber and R. Wielebinski (Dordrecht: Reidel), p. 399.
Delgado, A. J., and Thomas, H.-C. 1981, *Astr. Ap.*, **96**, 142.
de Loore, C., and De Greve, J. P. 1975, *Ap. Space Sci.*, **35**, 241.
de Loore, C., De Greve, J. P., and De Cuyper, J. C. 1975, *Ap. Space Sci.*, **36**, 219.
Divine, N. 1965, *Ap. J.*, **142**, 824.
Dominy, J. F., and Lambert, D. L. 1983, *Ap. J.*, **270**, 180.
Drilling, J. S. 1980, *Ap. J. (Letters)*, **242**, L43.
Drilling, J. S., Landolt, A. U., and Schönberner, D. 1984, *Ap. J.*, **279**, 748.
Drilling, J. S., and Schönberner, D. 1982, *Astr. Ap.*, **113**, L22.
Drilling, J. S., Schönberner, D., Heber, U., and Lynas-Gray, A. E. 1984, *Ap. J.*, **278**, 224.
Durisen, R. H. 1977, *Ap. J.*, **213**, 145.
Feast, H. W. 1975, in *IAU Symposium 67, Variable Stars and Stellar Evolution*, ed. V. E. Sherwood and L. Plaut (Dordrecht: Reidel), p. 123.
Flannery, B. P., and Ulrich, R. K. 1977, *Ap. J.*, **212**, 533.
Flannery, B. P., and van den Heuvel, E. P. J. 1975, *Astr. Ap.*, **39**, 61.
Fowler, W. F., Caughlan, G. R., and Zimmerman, B. A. 1975, *Ann. Rev. Astr. Ap.*, **13**, 69.
Frogel, J., and Blanco, V. M. 1984, in *IAU Symposium 105, Observational Tests of the Stellar Evolution Theory*, ed. A. Maeder and A. Renzini (Dordrecht: Reidel).
Fujimoto, M. Y. 1980, in *Type I Supernovae*, ed. J. C. Wheeler (Austin: University of Texas Press), p. 155.
Fujimoto, M. Y., Iben, I., Jr., and Becker, S. A. 1981, in *IAU Colloquium 59, Effects of Mass Loss on Stellar Evolution*, ed. C. Chiosi and R. Stalio (Dordrecht: Reidel), p. 401.
Giannone, P., and Giannuzzi, M. A. 1970, *Astr. Ap.*, **6**, 317.
_____. 1972, *Astr. Ap.*, **19**, 298.
Grauer, A. D., and Bond, H. E. 1982, *IAU Circ.*, No. 3714.
_____. 1983, *Ap. J.*, **271**, 259.
_____. 1984, *Ap. J.*, **277**, 211.
Green, R. F. 1977, Ph.D. thesis, California Institute of Technology.
Gurevich, A. L., and Lebedinskij, M. A. 1947, *Zh. Eksper. Teoret. Fiz.*, **17**, 792.
Harmanec, P. 1970, *Bull. Astr. Inst. Czechoslovakia*, **21**, 113.
Harmanec, P., Koubsky, D., and Kzpata, J. 1972, *Ap. Letters*, **11**, 119.
Hazard, C., Terlevich, B., Morton, D. C., Sargent, W. L. W., and Ferland, G. 1980, *Nature*, **285**, 463.
Heap, S. R. 1982, in *IAU Symposium 99, Wolf-Rayet Stars*, ed. C. W. H. de Loore and A. J. Willis (Dordrecht: Reidel), p. 423.
_____. 1983, in *IAU Symposium 103, Planetary Nebulae*, ed. D. R. Flower (Dordrecht: Reidel), p. 375.
Heber, U. 1983, *Astr. Ap.*, **118**, 39.
Heber, U., and Schönberner, D. 1981, *Astr. Ap.*, **102**, 73.
Hills, J. G. 1978, *A.J.*, **221**, 973.
Hunger, K. 1975, in *Problems in Stellar Atmospheres and Envelopes*, ed. B. Baschek, W. H. Kegel, and G. Traving (New York: Springer), p. 57.
Iben, I., Jr. 1965*a*, *Ap. J.*, **141**, 993.
_____. 1965*b*, *Ap. J.*, **142**, 1447.
_____. 1966*a*, *Ap. J.*, **143**, 483.
_____. 1966*b*, *Ap. J.*, **143**, 505.
_____. 1966*c*, *Ap. J.*, **143**, 516.
_____. 1967, *Ann. Rev. Astr. Ap.*, **5**, 571.
_____. 1972, *Ap. J.*, **178**, 433.
_____. 1975, *Ap. J.*, **196**, 525.
_____. 1976, *Ap. J.*, **208**, 165.
_____. 1982, *Ap. J.*, **259**, 244.
_____. 1983, *Ap. J. (Letters)*, **275**, L65.
_____. 1984*a*, *Ap. J.*, **277**, 333.
_____. 1984*b*, in *IAU Symposium 105, Observational Tests of the Stellar Evolution Theory*, ed. A. Maeder and A. Renzini (Dordrecht: Reidel), p. 3.
_____. 1985*a*, in preparation.
_____. 1985*b*, *Quart. J.R.A.S.*, **26**, 1.
Iben, I., Jr., Fujimoto, M. Y., and Sugimoto, D. 1985, in preparation.
Iben, I., Jr., Kaler, J. B., Truran, J. W., and Renzini, A. 1983, *Ap. J.*, **264**, 605.
Iben, I., Jr., and MacDonald, J. 1985, *Ap. J.*, **296**, in press.
Iben, I., Jr., and Renzini, A. 1982, *Ap. J. (Letters)* **263**, L23.
_____. 1983, *Ann. Rev. Astr. Ap.*, **21**, 271.
Iben, I., Jr., and Truran, J. W. 1978, *Ap. J.*, **220**, 980.
Iben, I., Jr., and Tutukov, A. V. 1984*a*, in *Stellar Nucleosynthesis*, ed. C. Chiosi and A. Renzini (Dordrecht: Reidel), p. 181.
_____. 1984*b*, *Ap. J. Suppl.*, **54**, 335 (IT).

Iben, I., Jr., and Tutukov, A. V., 1984*c*, *Ap. J.*, **282**, 615 (IT).
_____. 1984*d*, *Ap. J.*, **284**, 719.
_____. 1985, in *High Energy Transients*, ed. S. E. Woosley (New York: American Institute of Physics), p. 11.
Jacoby, G. H., and Ford, H. C. 1983, *Ap. J.*, **266**, 298.
Kaler, J. B. 1983, *Ap. J.*, **271**, 188.
Kaler, J. B., Iben, I., Jr., and Becker, S. A. 1978, *Ap. J.* (*Letters*), **224**, L63.
Kettner, K. U., *et al.* 1982, *Zs. Phys. A*, **308**, 73.
Kilkenny, D. K., and Flanagan, C. 1983, *M.N.R.A.S.*, **203**, 19.
Kippenhahn, R., and Meyer-Hofmeister, E. 1977, *Astr. Ap.*, **54**, 539.
Kippenhahn, R., and Weigert, A. 1967, *Zs. Ap.*, **65**, 251.
Kollatschny, W. 1984, *Astr. Ap.*, **86**, 308.
Kraicheva, Z. T., Popova, E. T., Tutukov, A. V., and Yungelson, L. R. 1978, *Astr. Zh.*, **56**, 1118.
Kriz, S., and Harmanec, P. 1975, *Bull. Astr. Inst. Czechoslovakia*, **26**, 65.
Kumar, C. K. 1978, *Ap. J.* (*Letters*), **219**, L13.
Lamb, S. A., Iben, I., Jr., and Howard, W. M. 1976, *Ap. J.*, **207**, 209.
Lambert, D. L. 1984, in *Cool Stars with Excesses of Heavy Elements*, ed. C. Jashek and P. C. Keenan (Dordrecht: Reidel).
Lauterborn, D. 1970, *Astr. Ap.*, **7**, 150.
Law, W. Y. 1982, *Astr. Ap.*, **108**, 118.
Law, W. Y., and Ritter, H. 1983, *Astr. Ap.*, **123**, 33.
Liebert, J. 1979, in *White Dwarfs and Variable Degenerate Stars*, ed. H. M. Van Horn and V. Weidemann (Rochester: University of Rochester), p. 146.
_____. 1980, *Ann. Rev. Astr. Ap.*, **18**, 363.
Liebert, J., Dahn, C. C., Gresharn, M., and Strittmatter, P. A. 1979, *Ap. J.*, **223**, 226.
Luck, E. R., and Bond, H. E. 1982, *Ap. J.*, **259**, 792.
Lyne, A. G. 1984, paper presented at Supernovae and Pulsars meeting, Rutherford Laboratory, Abingdon, March 22–23.
MacDonald, J. 1983, *Ap. J.*, **267**, 732.
Maran, S. P., Aller, L. H., Gull, T. R., and Stecher, T. P. 1982, *Ap. J.* (*Letters*), **253**, L43.
Mazzaco, H. G., and Milesi, G. E. 1982, *A.J.*, **87**, 1775.
McClure, R. D. 1980, *Ap. J.* (*Letters*), **235**, L35.
_____. 1983, *Ap. J.*, **268**, 264.
_____. 1984*a*, *Pub. A.S.P.*, **96**, 117.
_____. 1984*b*, in *Cool Stars with Excesses of Heavy Elements*, ed. C. Jashek and P. C. Keenan (Dordrecht: Reidel).
McClure, R. D., Fletcher, J. M., and Nemec, J. M. 1980, *Ap. J.* (*Letters*), **238**, L35.
Meyer, F., and Meyer-Hofmeister, E. 1979, *Astr. Ap.*, **78**, 167.
Miyaji, S., Nomoto, K., Yokoi, K., and Sugimoto, D. 1980, *Pub. Astr. Soc. Japan*, **32**, 303.
Neo, S., Miyaji, S., Nomoto, K., and Sugimoto, D. 1977, *Pub. Astr. Soc. Japan*, **29**, 249.
Nomoto, K. 1980, in *Type I Supernovae*, ed. J. C. Wheeler (Austin: University of Texas Press), p. 164.
_____. 1982, in *Supernovae: A Survey of Current Research*, ed. M. J. Rees and R. J. Stoneham (Dordrecht: Reidel), p. 205.
_____. 1984*a*, *Ap. J.*, **277**, 791.
_____. 1984*b*, in *Stellar Nucleosynthesis*, ed. C. Chiosi and A. Renzini (Dordrecht: Reidel), p. 205.
Nomoto, K., Nariai, K., and Sugimoto, D. 1980, in *IAU Symposium 88, Close Binary Stars: Observations and Interpretation*, ed. M. J. Plavec, D. M. Popper, and R. K. Ulrich (Dordrecht: Reidel), p. 139.
Packet, W., and De Greve, J. P. 1979, *Astr. Ap.*, **75**, 255.
Paczyński, B. 1966, *Acta Astr.*, **16**, 23.
_____. 1970*a*, *Acta Astr.*, **20**, 47.
_____. 1970*b*, *Acta Astr.*, **20**, 195.
_____. 1971, *Acta Astr.*, **21**, 1.
_____. 1976, in *IAU Symposium 73, The Structure and Evolution of Close Binary Systems*, eds. P. Eggleton, S. Mitton, and J. Whelan (Dordrecht: Reidel), p. 75.
Payne-Gaposchkin, C. 1963, *Ap. J.*, **138**, 320.
Percy, J. P. 1983, *A.J.*, **88**, 427.
Perinotto, M. 1983, in *IAU Symposium 103, Planetary Nebulae*, ed. D. R. Flower (Dordrecht: Reidel), p. 323.
Pilachowski, C. A. 1977, *Astr. Ap.*, **54**, 465.
Plavec, M. J. 1973, in *IAU Symposium 51, Extended Atmospheres and Circumstellar Matter in Spectroscopic Binary Systems*, ed. A. H. Batten (Dordrecht: Reidel), pp. 216, 249.
_____. 1983*a*, *Ap. J.*, **275**, 251.
_____. 1983*b*, *J.R.A.S. Canada*, **77**, 283.
Plavec, M. J., Dobias, J. J., Weiland, J. L., and Stone, P. S. 1982, in *IAU Symposium 98, Be Stars*, ed. M. Jaschek and H.-G. Groth (Dordrecht: Reidel), p. 485.
Plavec, M. J., Kriz, S., and Horn, J. 1969, *Bull. Astr. Inst. Czechoslovakia*, **20**, 41.
Plavec, M. J., Ulrich, R. K., and Polidan, R. S. 1973, *Pub. A.S.P.*, **85**, 769.
Popova, E. I., Tutukov, A. V., and Yungelson, L. R. 1982, *Ap. Space Sci.*, **88**, 155.
Rappaport, S., and van den Heuvel, E. P. J. 1982, in *IAU Symposium 98, Be Stars*, ed. M. Jaschek and H.-G. Groth (Dordrecht: Reidel), p. 327.
Renzini, A. 1979, in *Stars and Stellar Systems*, ed. B. E. Westerlund (Dordrecht: Reidel), p. 155.
Ritter, H. 1975, *Mitt. Astr. Gesellschaft*, **36**, 93.
_____. 1976, *M.N.R.A.S.*, **175**, 279.
Schatzman, E. 1965, in *Stars and Stellar Systems*, Vol. **8**, *Stellar Structure*, ed. L. H. Aller and D. B. McLaughlin (Chicago: University of Chicago Press), p. 327.
Schönberg, M., and Chandrasekhar, S. 1942, *Ap. J.*, **96**, 161.
Schönberner, D. 1975, *Astr. Ap.*, **44**, 383.
_____. 1977, *Astr. Ap.*, **57**, 437.
Schönberner, D., and Drilling, J. S. 1983, *Ap. J.*, **268**, 225.
_____. 1984, *Ap. J.*, **276**, 229.
Simpson, E. E. 1971, *Ap. J.*, **165**, 295.
Sion, E. M., and Liebert, J. 1977, *Ap. J.*, **213**, 468.
Smarr, L. L., and Blandford, R. 1976, *Ap. J.*, **253**, 908.
Sneden, C., and Bond, H. E. 1976, *Ap. J.*, **204**, 810.
Sneden, C., Lambert, D. L., and Pilachowski, C. A. 1981, *Ap. J.*, **247**, 1052.
Sparks, W. M., and Stecher, T. P. 1974, *Ap. J.*, **188**, 149.
Starrfield, S., Sparks, W. M., and Truran, J. W. 1974, *Ap. J. Suppl.*, **28**, 247.
Starrfield, S., Truran, J. W., and Sparks, W. M. 1978, *Ap. J.*, **226**, 186.
Stecher, T. P., Maran, S. P., Gull, T. R., Aller, L. H., and Savedoff, M. P. 1982, *Ap. J.* (*Letters*), **262**, L41.
Svechnikov, M. A. 1969, *Catalog of Spectroscopic Binaries* (Sverdlovsk: University of Sverdlovsk).
Taam, R. E. 1979, *Ap. J.* (*Letters*), **20**, L29.
_____. 1984, in *High Energy Transients*, ed. S. E. Woosley (New York: American Institute of Physics), No. 115, p. 1.
Taam, R. E., Bodenheimer, P., and Ostriker, J. P. 1978, *Ap. J.*, **222**, 269.
Taylor, J. H. 1981, in *Pulsars*, ed. W. Sieber and R. Wielebinski (Dordrecht: Reidel), p. 361.
Taylor, J. H., Hulse, R. A., Fowler, L. A., Gullaborn, G. G., and Rankin, J. M. 1976, *Ap. J.* (*Letters*), **206**, L53.
Taylor, J. H., and Weisberg, J. M. 1982, *Ap. J.*, **253**, 908.
Thomas, H.-C. 1977, *Ann. Rev. Astr. Ap.*, **15**, 127.
Tomkin, J., and Lambert, D. L. 1979, *Ap. J.*, **227**, 209.
_____. 1983, *Ap. J.*, **273**, 722.
Tutukov, A. V. 1980, Doctoral dissertation, Astronomical Council of the USSR Academy of Sciences.
Tutukov, A. V., and Yungelson, L. R. 1972, *Astrofizika*, **8**, 381.
_____. 1973*a*, *Nauch. Infor.*, **27**, 3.
_____. 1973*b*, *Nauch. Infor.*, **27**, 48.
_____. 1973*c*, *Nauch. Infor.*, **27**, 57.
_____. 1979*a*, in *IAU Symposium 83, Mass Loss and Evolution of O-Type Stars*, ed. P. S. Conti and C. W. H. de Loore (Dordrecht: Reidel), p. 1.
_____. 1979*b*, *Acta Astr.*, **29**, 666.
_____. 1981, *Nauch. Infor.*, **49**, 3.
Ulrich, R. K., and Burger, H. L. 1976, *Ap. J.*, **206**, 509.
Uus, V. 1970, *Nauch. Infor.*, **17**, 3.
van den Heuvel, E. P. J. 1968*a*, *Bull. Astr. Inst. Netherlands*, **19**, 309.
_____. 1968*b*, *Bull. Astr. Inst. Netherlands*, **19**, 326.
_____. 1981*a*, in *IAU Symposium 93, Fundamental Problems in the Theory of Stellar Evolution*, ed. D. Sugimoto, D. Q. Lamb, and D. N. Schramm (Dordrecht: Reidel), p. 155.
_____. 1981*b*, in *Pulsars*, ed. W. Sieber and R. Wielebinski (Dordrecht: Reidel), p. 379.
Varshavskij, V. I., and Tutukov, A. V. 1972*a*, *Nauch. Infor.*, **26**, 35.
_____. 1972*b*, *Nauch. Infor.*, **29**, 47.
_____. 1975, *Astr. Zh.*, **52**, 227.
Wallerstein, G., Greene, T. F., and Tomley, L. J. 1967, *Ap. J.*, **150**, 245.
Warner, B. 1967, *M.N.R.A.S.*, **137**, 119.
Webbink, R. F. 1976, *Ap. J. Suppl.*, **32**, 583.
_____. 1979*a*, in *IAU Colloquium 46, Changing Trends in Variable Star Research*, ed. F. M. Bateson, J. Smak, and I. H. Urch (Hamilton: University of Waikato), p. 43.
_____. 1979*b*, in *IAU Colloquium 53, White Dwarfs and Variable Degenerate Stars*, ed. H. M. Van Horn and V. Weidemann (Rochester: University of Rochester), p. 426.
_____. 1984*a*, *Ap. J.*, **277**, 355.
_____. 1984*b*, private communication.
Weidemann, V. 1979, in *IAU Colloquium 53, White Dwarfs and Variable Degenerate Stars*, ed. H. M. Van Horn and V. Weidemann (Rochester: University of Rochester), p. 206.

Weidemann, V., 1984, *Astr. Ap.*, **134**, 61.
Yungelson, L. R. 1973*a*, *Nauch. Infor.*, **27**, 76.
_____. 1973*b*, *Nauch. Infor.*, **27**, 93.
Zahn, J.-P. 1977, *Astr. Ap.*, **57**, 383.
Zhilyaev, B. E., Orlov, M. Ya., Pugach, A. F., Rodriguez, M. G., and Totochava, A. G. 1978, in *Stars of Type R Coronae Borealis* (Kiev: Naukova dumka).

ICKO IBEN, JR.: Departments of Astronomy and Physics, University of Illinois at Urbana-Champaign, 341 Astronomy Building, 1011 W. Springfield Avenue, Urbana, IL 61801

ALEXANDER V. TUTUKOV: Astronomical Council of the USSR Academy of Sciences, 48 Pyatnitskaya, Moscow 109017, USSR